Vibration of shells with application to hollow blading

Ucmaklioglu, Mehmet

VIBRATION OF SHELLS
WITH APPLICATION TO
HOLLOW BLADING

by

MEHMET UÇMAKLIOĞLU, B.Sc.

A thesis submitted for the degree of
Doctor of Philosophy to the
Department of Engineering Science,
University of Durham.

September 1978

SEVGİLİ ANNEME VE BABAMA

(Dedicated to my Parents)

ACKNOWLEDGEMENTS

I am extremely grateful to my supervisor, Dr. P.A.T.Gill for his guidance and assistance throughout the work.

I would like to thank too Dr. J.M. Wilson, and Dr. D.L. Collins for their help and suggestions about the numerical analysis.

Thanks are also due to the Technicians in the Department of Engineering Science, to the member of staff of the Computer Unit and to the staff of the Science Site Library.

Finally, I wish to express my thanks to the Union Carbide for supplying the financial support for this work.

ABSTRACT

The finite element method was applied to the natural frequency analysis of arbitrary shell structures. A computer program based on the isoparametric thick-shell element was developed.

The program was tested against several plate and shell problems. The results were compared with the experimental and numerical results reported by other researchers with excellent agreement in most cases and fair agreement in others.

An oval cross-section hollow blade was analysed in detail both numerically and experimentally. The experimental model could not match the design geometry due to manufacturing difficulties. The numerical analysis was first performed on the nominal geometry which lead to a regular set of modes. Later, the numerical model was corrected to match the experimental model, and satisfactory agreement was obtained between the results for the lower modes of vibration.

Other topics which could be studied as an extension of this work were pointed out, and some excercises were performed on them without given any experimental verification. Finally a hollow turbine blade was analysed and very good results were obtained.

CONTENTS

CHAPTER 1

1. INTRODUCTION

As a result of the technological developments in civil, mechanical and aeronautical engineering, shell structures gained a popularity in the 20th century. Since many of such structures are subject to dynamic loading, it is important to have some indication of their vibrational characteristics.

The number of exact solutions which satisfy the governing equations and the boundary conditions of shell structures are very limited. Hence, engineers are forced to use some approximate numerical methods for their analysis. Fortunately, the present state of high speed, large storage computers provide the necessary facilities for the development of efficient numerical methods.

In the literature, different methods have been employed for the analysis of shell structures. Warburton outlines Rayleigh-Ritz, finite element, finite difference and numerical integration methods in his review of "Dynamics of Shells" (55). Petyt (48) analysed a singly curved rectangular plate using Rayleigh-Ritz, extended Rayleigh -Ritz, finite element, and Kantorovich methods. Amongst the others, finite element method occupies an outstanding position. The superiority of the method comes from its applicability to arbitrary shapes, different loading and support conditions and many other aspects of practical design.

In general, considerable work has been done on the vibrational analysis of axisymmetric shells (37), and some on the circular cylindrical shell segments. The number of publications available for more complicated shapes are very few. Kurt and Boyd (38) for instance, studied a non-circular cylindrical shell segment by using power series method. Applicability of the method is restricted by the curvature being expressed as a power series, and with the boundary conditions being simply supported at two opposite edges. McDaniel and Logan (41) studied the panels with exponential curvature using transfer matrix method. Srinivasan and Bobby(52) used a matrix method to analyse the vibrations of clamped non-circular cylindrical shell segments. Cheung and Cheung (14) applied the finite strip method to the analysis of non-circular cylindrical panels. In all these methods either the geometry or the boundary conditions impose some restrictions on their range of application.

Early application of the finite element method to the shell structures was limited to the axisymmetric shells. Finite element analysis of non-axisymmetric shells can be reviewed under three groups. Namely, flat plate elements, curved elements, and three dimensional elements.

Flat plate elements (15,21,58) have the common disadvantage of uncoupled representation of membrane and bending behaviours. Also, the representation of curved geometry using flat elements requires a fine mesh in order to achieve a reasonable degree of accuracy.

Curved shell elements, based on the assumptions of different thin-shell theories, were developed as an attempt to overcome the disadvantages of flat plate elements. Generally, it is possible to divide them into two sub-groups as cylindrical shell elements (12,43), and doubly curved shallow shells (17,39,53). Many of these elements, together with some flat ones are reviewed and compared in references (16,18,25,26).

Three dimensional brick elements were first modified and used for the analysis of thick-shell structures by Ahmad and others (1,3,4,58). The formulation of thick shell element was more attractive than the conventional shell theories because of its conceptual simplicity. Also, it was capable of reproducing shear deformations in the element, and representing any arbitrary geometry. Further modifications on the element (61,47) made it applicable to thin shell structures as well as thick shells. After these modifications it became one of the most accurate and popular element for the analysis of shells.

Most of the shell elements were initially developed for static problems. Dynamic applications of these elements are not as common as the static applications in literature. Specifically for the vibrational analysis of non-axisymmetric shells, there is very little published literature.

A valuable experimental and numerical contribution to the vibrational analysis of shells was done by Olson and Lindberg. They used a cylindrical shell element (43,44) to analyse a curved fan blade. Later, Lindberg et al. (39,45) solved the same problem using a doubly curved triangular element. Their fan blade became a popular test example for many others (2,9,11,30,40,42).

Neale developed a hybrid cylindrical shell element (42) and tested it against several problems available in the literature. His element was non-conforming. He reported that for coarse meshes it is superior to many others.

Martins and Oven (40) used the semiloof element for the analysis of thin arbitrary shells. The element gave very good results for several problems they studied. Unfortunately, the element can not accommodate lateral shear, and is applicable only to thin shell situations.

Ahmad's shell element has been applied to thick shell vibration problems by its original developers (2). The element gave good results in application to thick shell vibration problems, but they pointed out that it was overstiff for the representation of thin shells.

Hofmeister and Evensen (30) have used both the modified and unmodified elements, and the twelve-node cubic element to solve several plate and shell vibration problems. They too, reported that unmodified eight-node element was too stiff, except for simple vibration modes, or large meshes. Both modified eight-node element and the twelve-node element performed very well in most of the cases.

Bossak and Zienkiewicz (9) applied the modified version of the element to thin shell and pretwisted beam problems. They made a comparison between the results of the original and the modified elements indicating the improvement achieved by reducing the order of integration.

In the present study, a complete computer program using eight-node quadratic and ten-node cubic-quadratic elements has been developed. The program was checked against several plate and shell problems. The results were compared with the other numerical and experimental results with excellent agreement.

The study continued with the analysis of an oval cross-section shell, representing a hollow blading. Although the comparison of the experimental and numerical results were very difficult for some complicated modes which were hightly effected by the imperfect geometry of the experimental model, very good agreement was observed for simpler mode shapes. Later the program was used on pretwisted oval and aerofoil cross-section bladings and a hollow turbine blade. In general the results indicate that the method used is very efficient for the vibrational analysis of arbitrary shell structures.

CHAPTER 2

2. THEORY AND NUMERICAL FORMULATION

In this chapter the theoretical basis to the computer program which has been written for the numerical analysis in this thesis is reviewed. In addition to the general theory some points to increase the accuracy of the element, or to reduce the computational cost of the program are also mentioned.

Explanations on the program are given in Appendix 1. Appendix 2 contains a detailed explanation for the preparation of input data. A complete listing of the program is included in Appendix 5.

2.1 Theory

2.1.1. Introduction

The solution of any structural problem by finite element displacement method follows more or less the same procedure (58,19,10). First the continuum is divided into a number of "finite elements", and these elements are considered to be interconnected at a discrete number of nodes. Displacements of these nodal points are the basic unknowns of the problem. Then, the element characteristics such as the stiffness and mass matrices are evaluated. Their assembly into the system matrices is followed by a solution procedure.

2.1.2. Formulation

The displacement at any point within a typical element "e" can be defined as:

$$\{f\} = [N]\,\{\delta\}_e \qquad (2.1.1)$$

Where $[N]$ contains the shape functions which will be discussed in section 2.3 and $\{\delta\}_e$ is the vector containing the displacements of the nodes of element "e".

Strains within the element are defined as:

$$\{\varepsilon\} = [B]\,\{\delta\}_e \qquad (2.1.2)$$

Where $[B]$ can be obtained from (2.1.1) using strain-displacement relationship.

Stresses, in the elastic range, are related to the strains:

$$\{\sigma\} = [D]\,\{\varepsilon\} \qquad (2.1.3)$$

In which $[D]$ is the elasticity matrix which contains the material properties.

If $\{F\}_e$ is the vector of nodal forces equivalent to the boundary stresses and the distributed loads on the element, and $\{p\}$ is the vector of distributed loads and forces acting on a unit volume of material within the element; principle of virtual work can be applied to equate the external and internal work done due to a virtual nodal displacement $d\{\delta\}_e$. The work done by the nodal forces is:

$$(d\{\delta\}_e)^T \{F\}_e \tag{2.1.4}$$

The internal work per unit volume done by the stresses and the distributed forces is:

$$d\{\varepsilon\}^T\{\sigma\} - d\{f\}^T\{p\} \tag{2.1.5}$$

or by substituting (2.1.1) and (2.1.2)

$$(d\{\delta\}_e)^T \left([B]^T\{\sigma\} - [N]^T\{p\}\right) \tag{2.1.6}$$

Now, the external and total internal work done can be equated:

$$(d\{\delta\}_e)^T\{F\}_e = (d\{\delta\}_e)^T \left(\int [B]^T\{\sigma\}\, dV - \int [N]^T\{p\}\, dV\right) \tag{2.1.7}$$

Substitution of equation (2.1.3), followed by the substitution of (2.1.2) gives:

$$\{F\}_e = \left(\int [B]^T\ [D]\ [B]\, dV\right)\{\delta\}_e - \int [N]^T\{p\}\, dV \tag{2.1.8}$$

In which the first term contains the element stiffness matrix:

$$[k]_e = \int [B]^T\ [D]\ [B]\ dV \tag{2.1.9}$$

and the second term is the nodal forces

$$[F]_e^p = -\int [N]^T\{p\}\ dV \tag{2.1.10}$$

For dynamic problems $\{p\}$ includes inertia and damping forces in it

$$\{p\} = \{\bar{p}\} - \rho\,\frac{\partial^2}{\partial t^2}\{f\} - \mu\,\frac{\partial}{\partial t}\{f\} \tag{2.1.11}$$

where $\{\bar{p}\}$ represents the distributed loads, $-\rho\,\frac{\partial^2}{\partial t^2}\{f\}$ represents the inertia force with ρ being the mass per unit volume, and $-\mu\,\frac{\partial}{\partial t}\{f\}$ represents a linear viscous damping effect, where μ is a constant which characterizes the damping mechanism.

Substituting (2.1.11) into (2.1.10) and replacing $\{f\}$ with its equivalent in (2.1.1) gives

$$\{F\}_e^{\rho} = \{\bar{F}\}_e^{\bar{\rho}} + \int [N]^T \rho [N] \frac{\partial^2}{\partial t} \{\delta\}_e dV + \int [N]^T \mu [N] \frac{\partial}{\partial t} \{\delta\}_e dV \quad (2.1.12)$$

which contains the element mass matrix as:

$$[m]_e = \int [N]^T \rho [N] \, dV \quad (2.1.13)$$

and element damping matrix as:

$$[c]_e = \int [N]^T \mu [N] \, dV \quad (2.1.14)$$

Substituting (2.1.12) into (2.1.8) and assembling the element matrices into the system matrices, the general equation for discrete structures is obtained.

$$[K]\{\delta\} + [C] \frac{\partial}{\partial t}\{\delta\} + [M] \frac{\partial^2}{\partial t^2}\{\delta\} + [F] = 0 \quad (2.1.15)$$

Where $\{\delta\}$ lists the nodal displacements (degrees of freedoms), $[F]$ contains the external forces, specified loads and initial stresses, $[K]$, $[C]$, and $[M]$ are the system stiffness, damping and mass matrices respectively.

For the natural frequency analyses equation (2.1.15) reduces to:

$$[K]\{\delta\} + [M] \frac{\partial^2}{\partial t^2}\{\delta\} = 0 \quad (2.1.16)$$

Solution to this equation may be expressed as:

$$\{\delta\} = \{\delta_o\} e^{i\omega t} \quad (2.1.17)$$

which, when substituted into (2.1.16) leads to the eigenvalue problem

$$([K] - \omega^2 [M]) \; \{\delta_o\} = 0 \quad (2.1.18)$$

In solution, ω's will be the natural angular frequencies, and

$\{\delta_o\}$ will contain the eigenvectors describing the mode shapes of vibration.

2.2. Isoparametric Shell Element

2.2.1. Introduction

As it was stated in Chapter 1, Ahmad's isoparametric shell element was chosen for the numerical analysis of this work. This element differs from a three dimensional brick element with the assumption that the normals to the midsurface remain straight after deformation and that the strains normal to the midsurface are negligible. It also differs from the elements of thin shell theory with the assumption that the normals to the midsurface are allowed to become inclined after deformation. This assumption permits the element to experience shear deformations.

The two typical elements used in this analysis are shown in figure 2.1. The element in figure 2.1 (a) is known as 8-node isoparametric shell element which assumes a parabolic variation along the edges. The element in figure 2.1(b) is derived by combining a parabolic and a cubic element, for a better representation of sharp changes of curvature along one edge.

2.2.2. Element Formulation

The formulation of the isoparametric shell element (1,3,4, 58) follows the phases given in section 2.1.2.

The geometry of each element is prescribed by top and bottom pairs of coordinates of the nodes, and the shape functions used. ξ, η, ζ are the curvilinear coordinates of the

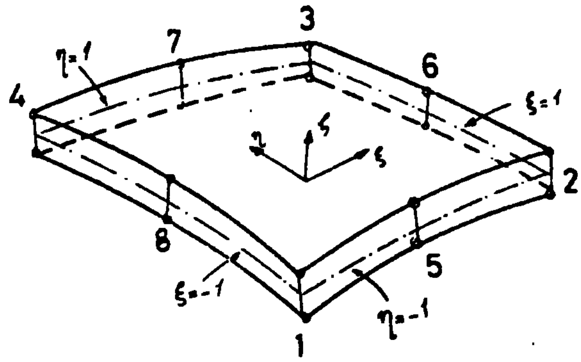

Figure 2.1 (a) : Isoparametric Shell Element with Quadratic Variation

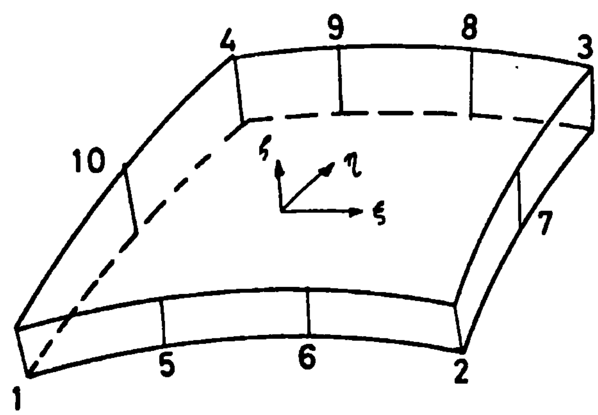

Figure 2.1 (b) : Quadratic - Cubic Shell Element

shell element, and each varies between -1 and 1 on the respective faces of the element. (See figure 2.1 (a)). Global cartesian coordinates of any point of the element are related to the curvilinear coordinates as:

$$\begin{Bmatrix} x \\ y \\ z \end{Bmatrix} = \sum N_i \begin{Bmatrix} x_i \\ y_i \\ z_i \end{Bmatrix}_{mid.} + \sum N_i \frac{\zeta}{2} \underset{\sim}{V}_{3i} \qquad (2.2.1)$$

where N_i is the shape function corresponding to node i and $\underset{\sim}{V}_{3i}$ is the thickness vector at node i.

Displacements through the element is defined in terms of the midsurface node displacements u_i, v_i, w_i, and two rotations of the $\underset{\sim}{V}_{3i}$ vector about orthogonal directions normal to it. Two such directions are given by orthonormal vectors $\underset{\sim}{v}_{1i}$ and $\underset{\sim}{v}_{2i}$ with the corresponding rotations β_i and α_i.

Displacements within the element is related to the nodal displacements as:

$$\begin{Bmatrix} u \\ v \\ w \end{Bmatrix} = \sum N_i \begin{Bmatrix} u_i \\ v_i \\ w_i \end{Bmatrix} + \sum N_i \zeta \frac{t_i}{2} \left[\underset{\sim}{v}_{1i}, -\underset{\sim}{v}_{2i} \right] \begin{Bmatrix} \alpha_i \\ \beta_i \end{Bmatrix} \qquad (2.2.2)$$

where t_i is the magnitude of the thickness vector $\underset{\sim}{V}_{3i}$.

The components of strains and stresses are defined in the local cartesian coordinates x',y',z' with z' being normal to ζ = constant surface. Three dimensional strain relationship is given as:

$$\{\varepsilon'\} = \begin{Bmatrix} \varepsilon_{x'} \\ \varepsilon_{y'} \\ \gamma_{x'y'} \\ \gamma_{x'z'} \\ \gamma_{y'z'} \end{Bmatrix} = \begin{Bmatrix} \frac{\partial u'}{\partial x'} \\ \frac{\partial v'}{\partial y'} \\ \frac{\partial u'}{\partial y'} + \frac{\partial v'}{\partial x'} \\ \frac{\partial w'}{\partial x'} + \frac{\partial u'}{\partial z'} \\ \frac{\partial w'}{\partial y'} + \frac{\partial v'}{\partial z'} \end{Bmatrix} \qquad (2.2.3)$$

The local derivatives of the local displacements are given by

$$\begin{bmatrix} \frac{\partial u'}{\partial x'} & \frac{\partial v'}{\partial x'} & \frac{\partial w'}{\partial x'} \\ \frac{\partial u'}{\partial y'} & \frac{\partial v'}{\partial y'} & \frac{\partial w'}{\partial y'} \\ \frac{\partial u'}{\partial z'} & \frac{\partial v'}{\partial z'} & \frac{\partial w'}{\partial z'} \end{bmatrix} = \theta^T J^{-1} \begin{bmatrix} \frac{\partial u}{\partial \xi} & \frac{\partial v}{\partial \xi} & \frac{\partial w}{\partial \xi} \\ \frac{\partial u}{\partial \eta} & \frac{\partial v}{\partial \eta} & \frac{\partial w}{\partial \eta} \\ \frac{\partial u}{\partial \zeta} & \frac{\partial v}{\partial \zeta} & \frac{\partial w}{\partial \zeta} \end{bmatrix} \theta \qquad (2.2.4)$$

where, θ is the orthogonal transformation matrix between the local and global system of coordinates, and J is the Jacobian matrix.

Since matrix $[B]$ can be obtained from equation (2.2.4) and matrix $[N]$ is given by the equation (2.2.2), the stiffness and mass matrices of equation (2.1.9) and (2.1.13) can now be evaluated.

2.3. Shape Functions

2.3.1. Introduction

As was mentioned previously, displacements throughout the element are defined as a function of the nodal displacements. In the isoparametric formulation the same functions, namely the shape functions, are used to describe both the geometry and the displacements (58). Conveniently, these functions can be chosen as polynomials.

For the convergence of finite element analysis, there are two criteria to be satisfied (58,19,60):

a) Continuity of the displacements between the elements should exist.

b) Elements should be able to reproduce any required state of constant strain. This criteria includes the rigid body displacements as a special case.

In selecting the polynomials for the shape functions, these two criteria must be taken into account. An additional desirable property of the shape functions is the geometric invariance (22,23,19).

To satisfy the first condition the displacement function along the boundary of the two adjacent elements must only be influenced by the nodes on this boundary, and the order of the polynomial must be uniquely determined by the number of these nodes (60,24). Second criteria is automatically satisfied for the isoparametric shape functions (24). To achieve the geometric invariance it is necessary to choose symmetric polynomials as the shape functions (19).

By definition, shape functions take a unit value at a preferred node and zero at all other nodes. Suitable shape functions, satisfying all the conditions mentioned above are available in the literature (58,59,60,24). Following the tradition, and the recommendations of references (59,54), the Sérendipity family of shape functions were used in this work. In the following section, the derivation of shape functions of this family, for a rectangular element with different number of nodes along the parallel sides is demonstrated.

2.3.2. Shape Functions for Cubic-Quadratic Element

For some practical purposes, it is desirable to have elements with varying number of nodes along different sides. The shape functions for such an element, which is shown in figure 2.2 and will be used in chapters 3 and 5, derived following the procedure given in (59,54).

Shape functions for the midside nodes of this element are the same as a cubic element in ξ and as a quadratic element in η directions.

To derive the shape functions for the corner nodes, one can start from the linear function shown in figure 2.3(a). To obtain the cubic variation of figure 2.3(e), first the variation in figure 2.3(b) is to be subtracted from figure 2.3(a) to give figure 2.3(c), then figure 2.3(d) is to be subtracted from figure 2.3 (c) to give the final form in figure 2.3(e).

A similar process, of course, will be applied for the quadratic variation in η direction.

The curves of figures 2.3 (b) and 2.3(d) are the cubic shape functions for the midside nodes, multiplied by a constant.

The shape function for node 1 of figure 2.2 for instance will be

$$N_1 = N_L - \frac{2}{3} N_5 - \frac{1}{3} N_6 - \frac{1}{2} N_{10} \qquad (2.3.1)$$

where N_L is the linear shape function for node 1. Substitution of the corresponding functions of N_i gives the shape functions as:

$$N_1 = \frac{1}{32} (1-\xi)(1-\eta)\left[-8\eta-9(1-\xi^2)\right] \qquad (2.3.2)$$

or the general form for all the corner nodes:

$$N_i = \frac{1}{32} (1+\xi_o)(1+\eta_o)\left[8\eta_o-9(1-\xi^2)\right] \qquad (2.3.3)$$

with $\xi_o = \xi\,\xi_i$ and $\eta_o = \eta\,\eta_i$

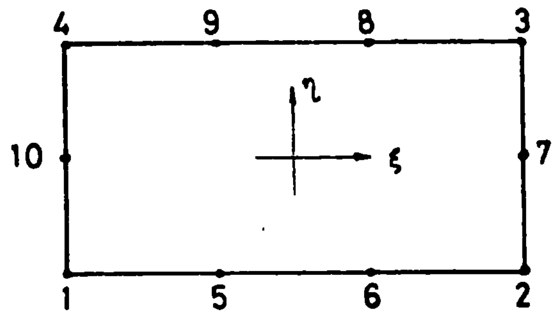

Figure 2.2 : Node numbering system for 10-node element.

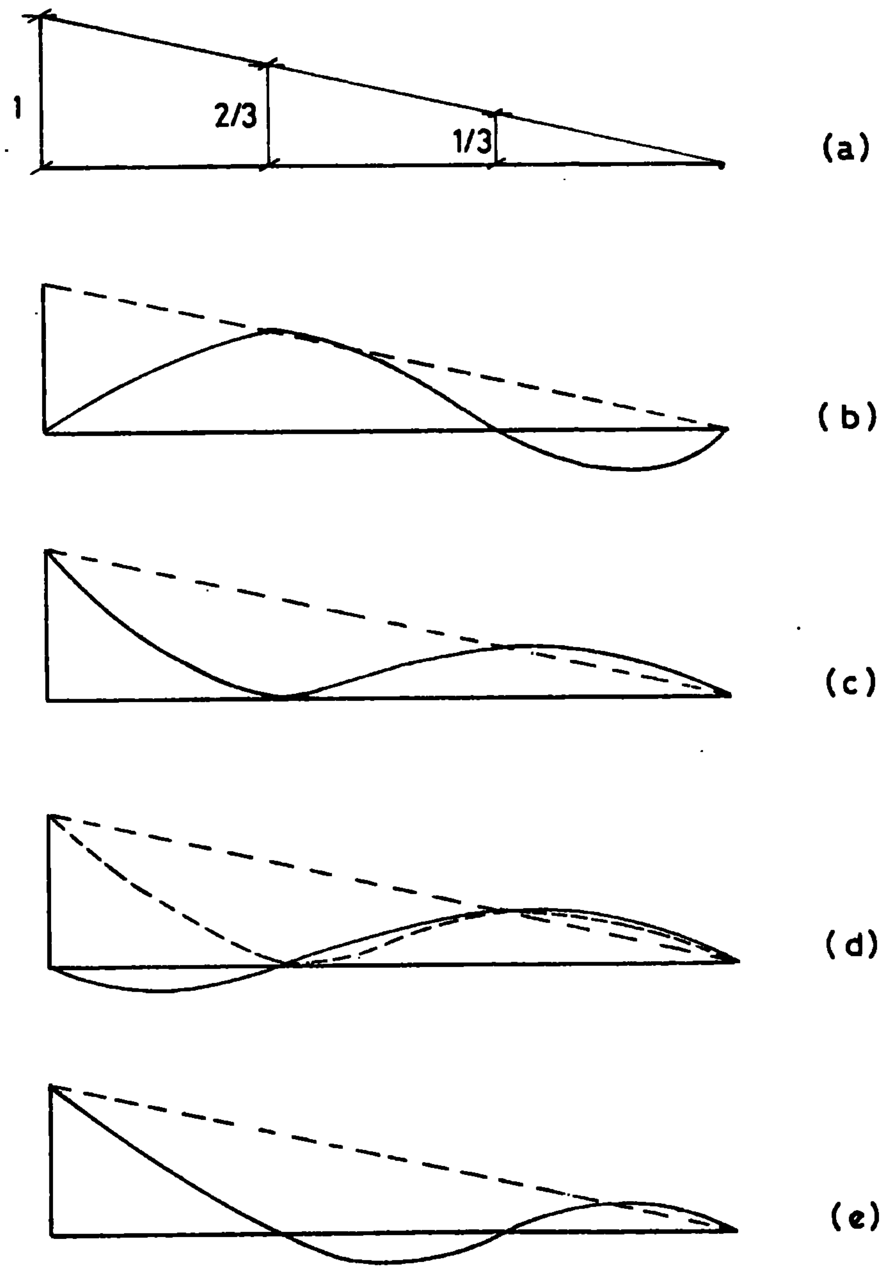

Figure 2.3 : Derivation of Shape Functions for corner nodes.

For the midside nodes the shape functions are:

$$N_i = \frac{1}{2}(1+\xi_o)(1-\eta^2) \qquad \text{for} \qquad \xi_i = \pm 1,\ \eta_i = 0 \qquad (2.3.4)$$

$$N_i = \frac{9}{32}(1+\eta_o)(1-\xi^2)(1+9\xi_o) \qquad \text{for} \qquad \xi_i = \pm\frac{1}{3},\ \eta_i = \pm 1 \qquad (2.3.5)$$

2.4. Reduced Integration

In its original form, the thick shell element was too stiff in representing bending deformations in thin shell and plate applications. Zienkiewicz et al. (61), and Pawsey and Clough (47) had noticed that the overstiffness of the element was due to the displacement function imposing unrealistic restrictions upon the modes of deformation of the element. Following a procedure similar to the one that Doherty et al (20) employed, that is, by reducing the order of integration, is was possible to relax the overstiffness of the element. Accuracy of the reduced numerical integration in finite elements is discussed by Irons (33,34,35,36). The point he emphasises is that the convergence is guaranteed, provided that the determinant of Jacobian does not change sign in the domain, and that the volume of the element is calculated accurately.

To modify the element, Zienkiewicz et al. proposed a uniform low order integration on all stress components, whereas Pawsey and Clough used a selective integration order for different stress components. Pawsey, in a later publication (46) agrees that the eight node quadratic element can be integrated using uniformly reduced integration points. The advantage of the uniform reduction over the selective reduction lies in the fact that it does not require any additional effort in programming, and reduces the computational time due to the lesser number of integration points.

In both of the references (61,47), the improvement achieved by reducing the order of integration is demonstrated by several examples. Vibrational application of the modified element (using uniform reduction) is reported in (30,9). In all examples but one, the element performed very well. Only in the case of a turbine blade, was it found to be overflexible (30). The reason was the high curvature across the width of the blade. Since only one element was used across the width, it was not able to represent rapid local change of curvature.

In the present study , the uniform reduction of integration points is used to modify the element. In general 2 X 2 X 2 integration points are used for the stiffness matrix, and 3 X 3 X 2 for the mass matrix. The effect of using different integration points has been observed on the results of some of the test examples of chapter 3. A survey was carried out to decide the best choice of order of integration for the elements having a high curvature. For these elements it is found out that unless a refined mesh is used, 3 integration points are needed along the curved edge. The comparison of results using different integration orders is given in the next chapter.

2.5. Repetitive use of Element Matrices

Using a regular mesh, makes it easy to produce the input data, and also helps to reduce the computational time. Element matrices, if they were calculated in a local coordinate system having the same orientation with respect to the element geometry, would be the same for similar elements. Once the matrices for one element are evaluated, the same matrices can be used for similar elements, provided that the necessary coordinate transformation is performed. If the similar elements have the same orientation with respect to the global system element matrices need not be transformed but could be used repetitively. If the orientation of similar elements is different with respect to the global coordinate system transformation is only required for the entries of the matrices corresponding to u, v, w degrees of freedoms, since α and β are the rotations of the thickness vector, and by definition, they are independent of the global coordinate system.

2.6. Eigenvalue Economization

The time required to solve the eigenvalue problems increases rapidly with the size of the matrices involved. Frequently, finite element idealization of a structure yields a representation with several hundreds of degrees of freedoms. The eigenvalue solution of a matrix of this size would require a great deal of computer time and storage which may be impossible to supply. Fortunately, these requirements may be reduced by a careful selection of a reduced number of degrees of freedoms which is sufficient to give acceptable results in the solution of the dynamic problems. This can be explained by Rayleigh's principle that a first order error in modal shape causes only a second order error in frequency.

Elimination of unwanted variables have been studied by several researchers (31,32,28,5,50,6,29). The method due to Irons (32,5) has been used in this study, because of its advantage of performing the elimination process during assembly.

The unwanted variables which are called slaves are chosen amongst the degrees of freedoms which have the least contribution to the strain energy. When sth degree of freedom is eliminated from the stiffness matrix $[K]$, the new entries of the reduced stiffness matrix $[K]^*$ are given by the formula

$$K^*_{ij} = K_{ij} - K_{is} (K_{js}/K_{ss}) \qquad (2.6.1)$$

with row and column s being deleted. The corresponding operation on the mass matrix is:

$$M^*_{ij} = M_{ij} - M_{is} (K_{js}/K_{ss}) - M_{js} (K_{is}/K_{ss}) + M_{ss}(K_{is}/K_{ss})(K_{js}/K_{ss}) \qquad (2.6.2)$$

The advantage of the method lies in the fact that the operations (2.6.1) and (2.6.2) can be applied to the M_{ij} and K_{ij} that are incompletely summed, as long as all of the M_{is} and K_{is} are completely summed, and as long as all contributions from later elements will eventually be added in.

CHAPTER 3.

3. TEST EXAMPLES

In order to see the performance of the computer program, it was tested against several plate and shell vibration problems. Either eight-node or ten-node elements were employed for the mathematical modelling of the structures. The effect of the number of Gauss points used in the numerical integration was investigated.

The results are given either in Hertz, or in dimensionless frequency parameter ϕ , which is defined as:

$$\phi = \frac{\omega}{(D/\rho t l^4)^{1/2}} \qquad \text{where} \qquad D = \frac{E t^3}{12(1-\nu^2)} \qquad (3.1.)$$

in which ω is the natural angular frequency, ρ, E and ν are the density, modulus of elasticity and the Poisson's ratio respectively. t and l stand for the thickness and the length of the shell.

3.1 Uniform Cantilever Plates

The first example was a square cantilever plate. The natural frequencies of this plate were determined by using both modified and unmodified elements. The problem was solved for different length/thickness (l/t) ratios. The increase in the stiffness of the unmodified element with the increasing l/t ratio was observed. The dimensionless frequency parameter (ϕ), obtained by using 1 x 1 and 2 x 2 uniform meshes are listed on table 3.1 together with the results reported in references (5) and (8). The results of the unmodified element shows a rapid convergence with the increasing number of elements. The modified element gives acceptable results even with one element for the first two frequencies. In addition to the modes shown on table 3.1., some in-plane modes were also observed. The frequencies corresponding to these modes were independent of the order of integration used.

A similar analysis was performed on a rectangular plate having a length/width ratio of 2. Since the results obtained were very similar to the square plate case, only the results of modified elements with 2 x 2 uniform mesh for three different l/t ratios are given on table 3.2, together with the results of references (5) and (49).

Because of the coarse mesh used, the frequencies corresponding to high mode shapes were overestimated on both tables.

3.2. Tapered Rectangular Plate

In this example, a varying thickness cantilever plate was analysed. The plate had a rectangular plan form with dimensions 127 x 63.5mm (5 x 2.5 inches). The cross section of it was an isosceles triangle with an apex angle of 2.4^{o}. The frequencies were calculated for different l/w ratios. The width of the plate was varied by succesively shaving it down on the thin side. This plate was first studied experimentally by Plunkett (49). He also calculated the fundamental frequencies using the beam theory.

In the present study, four eight-node modified elements were used to represent the structure. Dimensionless frequency parameters reported in reference (49), and the results of the

Number of elements	1/t	Order of Integration for stiffness Matrix	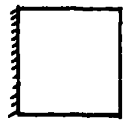	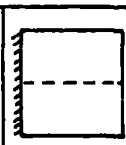	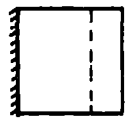	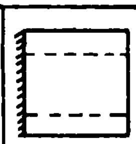	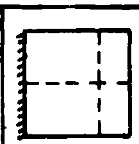
Ref. 8		Ritz Meth.	3.49	8.55	21.44	27.46	31.17
Ref. 5		Finite Element	3.47	8.54	21.45	27.06	-
4	100/2	2x2x2	3.48	8.56	22.40	28.79	32.88
4	100/5	2x2x2	3.47	8.45	22.06	28.02	32.10
4	100/10	2x2x2	3.45	8.17	21.10	26.70	30.06
4	100/2	3x3x2	3.68	9.25	(34.20)	(41.24)	48.00
4	100/5	3x3x2	3.63	9.03	(29.51)	(35.77)	42.90
4	100/10	3x3x2	3.55	8.56	(25.30)	30.17	35.00
1	100/2	2x2x2	3.58	9.04	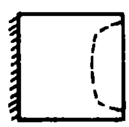	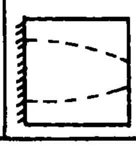	
1	100/3	2x2x2	3.58	9.02			
1	100/5	2x2x2	3.57	8.97			
1	100/7	2x2x2	3.57	8.89			
1	100/10	2x2x2	3.55	8.72			
1	100/2	3x3x2	4.45	11.43			
1	100/3	3x3x2	4.42	11.35			
1	100/5	3x3x2	4.35	11.12			
1	100/7	3x3x2	4.29	10.83			
1	100/10	3x3x2	4.18	10.30			

Table 3.1. Dimensionless frequency parameters of a square cantilever plate determined by using one and four 8-node elements.

(The mode shapes corresponding to the frequencies in parantheaia are shown at the bottom of the column).

Mode Shape	Measured Ref.49	Calculated Ref.5	4 Elements l/t = 100/2	4 Elements l/t = 100/5	4 Elements l/t=100/10
	3.50	3.44	3.47	3.46	3.45
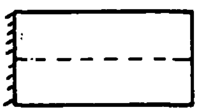	14.50	14.77	14.83	14.72	14.38
	21.70	21.50	22.74	22.66	22.38
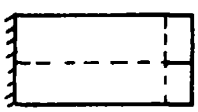	48.10	48.19	50.91	50.45	49.00
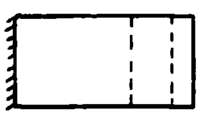	60.50	60.54	75.93	75.08	72.36
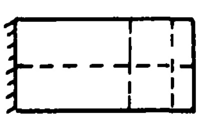	92.30	91.76	111.41	108.87	102.23
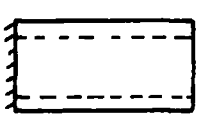	92.80	92.78	99.16	98.12	95.04
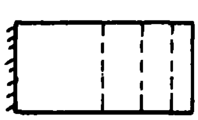	118.70	119.37	There are not enough nodes to identify this mode		
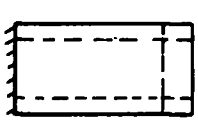	125.1	124.23	137.11	133.12	126.06

Table 3.2 Dimensionless frequency parameter for a rectangular plate of w/l = 1/2

finite element analysis are given on table 3.3. Very good agreement was obtained for the simple mode shapes like 0/0 1/0, 0/1 (m/n, where m indicates the number of nodal lines perpendicular to the support, and n is the number parallel to it). Accurate determination of higher modes would require a finer mesh.

In general, the frequencies were underestimated for small l/w ratios, and overestimated for large ones. This is probably because of the changing element aspect ratio due to the decreasing width.

3.3. Pretwisted Cantilever Blading

The next example was a rectangular cross section pretwisted blading. The experimental values of the frequencies for this blading have been reported by Carnegie (13). He also gave the theoretical values for the fundamental frequencies, and for all torsional frequencies. The blade was 152.4 mm (6 inches) long, 25.4mm (1 inch) wide and 1.6129mm (0.0635 inches) thick.

The calculations in this study were performed for 0°, 30°, 60° and 90° of pretwist angle, using both eight-node and ten-node elements with 1 x 6 and 2 x 6 meshes. The results are listed on table 3.4.

In bending type of modes, the modified eight-node element performed very well with 1 x 6 mesh. But for torsional modes it was overflexible especially for large pretwist angles. In this case, it was possible to increase the accuracy by refining the mesh. Alternatively, by increasing the order of

Mode	1/w	2.00	2.22	2.86	4.00	6.67
0/0	Meas.	2.57	2.57	2.71	2.91	3.15
	Calc.	2.49	2.50	2.58	2.78	3.04
	F.E.	2.43	2.54	2.73	2.97	3.26
1/0	Meas.	11	11.6	15	22	37
	F.E.	10.63	11.50	15.50	23.48	40.79
0/1	Meas.	15.5	16	17	18	19.5
	F.E.	15.85	16.50	18.08	19.96	21.47
1/1	Meas.	30.7	33	49	68	112
	F.E.	30.55	36.34	49.67	75.25	127.42
0/2	Meas.	38	40	42.5	49	54
	F.E.	48.18	53.07	60.35	64.9	72.1

Table 3.3 **Comparisons of the frequency parameters for the tapered rectangular plate.**

integration points in the direction of the curvature, better results were obtained for torsional modes. Another alternative was to increase the number of nodal points in the direction of the curvature. This was achieved by using ten-node elements. The results obtained by using different number of integration points indicate that this element too, exaggerates the flexibility of the structure when a low order of integration is used. The best choice of integration order for this element seems to be 4 x 2 x 2. Using 3 integration points along the length of the blade gives overstiff representation for both eight-node and ten-node elements.

Two different frequencies corresponding to some of the modes are the result of coupled bending-bending due to the pretwist. For instance, the second bending mode at 60° pretwist angle have two frequencies. One of them is around 260 Hz and second bending mode out of the plane of the root, couples with the second bending mode in the plane of the root. The other frequency which lies around 1320 Hz is the coupling between second bending out-of-plane and first bending in-plane modes. The value of this frequency, though, is more likely to correspond to the second value of the third bending frequency (1200 Hz) found experimentally. A similar discrepancy, in the identification of the modes, is seen at 90° pretwist angle. The second values corresponding to the fourth bending frequency almost coincide with the experimental fifth bending frequency.

	MODE	Angle of Twist 0°								Angle of Twist 30°						
		CARNEGIE		FINITE ELEMENT						CARNEGIE		FINITE ELEMENT				
				8 Node Elements			10 Node Elements					8 Node Elements			10 Node Elements	
		Exper.	Theor.	1x6* 2x2x2+	1x6 3x2x2	2x6 2x2x2	1x6 3x2x2	1x6 4x2x2	1x6 4x3x2	Exper.	Theor.	1x6 2x2x2	1x6 3x2x2	2x6 2x2x2	1x6 3x2x2	1x6 4x2x2
BENDING	1	57.5	61.5	58	58.7	58.2	58.7	58.7	59	58	62	58	58.9	58.4	58.8	58.9
	2	362	386 x	364	367	365	367	367	380	320	—	323	326	324	325	325
	3	1031	1081 x	1026	1038	1031	1037	1038	1128	1000	—	924 1084	930 1093	923 1087	928 1092	929 1093
	4	1987	2119 x	2061	2102	2075	2097	2101	2423	1950	—	2041	2077	2051	2072	2076
	5	3283	3502 x	3613	3706	3645	3692	3704	4620	3275 3212	—	3257	3644	3587	3629	3640
TORSION	1	712	700	689	689	685	632	686	700	730	725	689	718	709	662	712
	2	2156	2100	2104	2106	2093	1937	2095	2145	2200	2150	2106	2192	2167	2024	2175
	3	3690	3600	3659	3670	3645	3383	3652	3755	3800	3750	3665	3810	3767	3525	3782
	4	5373	5380	5532	5564	5523	5160	5537	5774	5500	5500	5538	5745	5893	5342	5708

Table 3.4. Carnegie Pretwisted blading comparison

The frequencies given in c/sec.

* Mesh used.

\+ Order of integration for the stiffness matrix

x Calculated using beam theory.

	MODE	ANGLE OF TWIST 60°							ANGLE OF TWIST 90°								
		CARNEGIE		FINITE ELEMENT					CARNEGIE		FINITE ELEMENT						
				8 Node Elements			10 Node Elem.				8 Node Elements				10 Node Elements		
		Exper.	Theor.	1 x 6 2x2x2	1 x 6 3x2x2	2 x 6 2x2x2	1 x 6 3x2x2	1 x 6 4x2x2	Exper.	Theor.	1 x 6 2x2x2	1 x 6 3x2x2	1 x 6 3x3x2	2 x 6 2x2x2	1 x 6 3x2x2	1 x 6 4x2x2	1 x 6 4x3x2
BENDING	1	59	63	59	59.5	59	59.3	59.4	61	65	60	60.4	63.5	60	60.2	60.2	63.4
	2	263	–	258 1321	295 1324	257 1316	258 1321	259 1322	210	–	207	208	227	206	207	207	226
	3	890 1200	–	873	881	873	879	879	812 1500	–	790 1525	796 1532	907 1621	788 1518	793 1527	794 1529	905 1618
	4	1980	–	2002	2028	2005	2023	2026	2000	–	2047 3319	2063 3339	2367 4366	2046 3299	2058 3323	2060 3333	2364 4359
	5	3318	–	3465	3503	3454	3488	3498	3218	–	–	–	–	–	5411	5431	6415
TORSION	1	800 794	790	691	797	778	742	784	900	910	692	913	940	879	857	890	915
	2	2500	2450	2113	2430	2373	2263	2392	2800	2650	2126	2775	2878	2673	2604	2708	2810
	3	4200	4100	3683	4197	4105	3912	4142	4700	4600	5597*	4761	5025	4595	4463	4663	4927
	4	5900	5950	5559	6247	6125	5840	5998	6000	6600	3710*	6989	7701	6761	6555	6871	7582

Table 3.4 (Continued)

* Based on mode recognition

3.4. Curved Fan Blade

First shell problem which was solved to test the program was the fan blade, originally studied by Olson and Lindberg. They performed the experiments on a model which was constructed by rolling a piece of sheet steel 3.048mm (0.12 inches) thick, to a radius of curvature of 609.6mm (24.0 inches). This curved sheet was then cut to size 304.8 x 304.8 mm (12x12 inches) and welded to a steel block to simulate the clamped boundary condition.

Initially Olson and Lindberg (43,44) used a cylindrical shell element, with four nodes and 28 degrees of freedoms, to predict the natural frequencies of this fan blade. Later Lindberg et al (39,45) solved the same problem by using a curved triangular shallow shell element which was more accurate than the previous one. They predicted the first 25 frequencies within a few per cent of error.

The problem was also solved by Bridle (11) using power series method, by Neale (42) using a hybrid shell element, and by Martins and Owen (40) using the semi-loof element. The original form of the thick shell element was used by Ahmad et al. (2) to solve the problem. They noticed that the element was too stiff. After the modifications Hofmeister and Evensen (30), and Bossak and Zienkiewicz (9) applied the element to the same problem obtaining very good results.

Table 3.5 lists the first five natural frequencies reported in the references mentioned above, together with the results of a 4 x 4 mesh of this study which is in excellent agreement with the experimental values. Table 3.6 contains the first seventeen frequencies reported in (43) and (39), and the results of the

Ref.	39	43	39	42	11	40	2	30	9	Present
Grid	Exper.	4 x 4	4 x 4	6 x 6	Power Series		4 x 4	2 x 3	3 x 3	4 x 4
1	85.6 86.6 (43)	93.5	86.6	89	85.8	85.3	113.0	87.0	88.3	86.2
2	134.5	147.6	139.2	143.2	138.3	138.1	147.0	143.0	142.8	139.5
3	259	255.1	251.3	252.6	246.7	245.1	296.0	252.0	257.6	249.8
4	351	393.1	348.6	380.5	342.5	340.4	440.0	367.0	369.2	347.9
5	395	423.5	393.4	428.2	386.8	383.8	475.0	412.0	441.8	405.0
D.O.F.	-	175	300	390	108	275	325	145	288	280

Table 3.5. Predictions of the first five natural frequencies by different references for the curved fan blade.

Freq. No.	Exp. * (39)	Ref. (39)	Present 4 x 4	Ref. (43)
1	85.6 86.6(43)	86.6	86.2	93.5
2	135	139	139.5	148
3	259	251	249.8	255
4	351	348.6	347.9	393
5	395	393	405	424
6	531	533	549	534
7	743	752	771	782
8	751	746	756	792
9	790	790	817	863
10	809	813	911	862
11	997	1008	1100	1002
12	1216	1231	1383	1175
13	1252	1246	1266	
14	1241	1266	1371	
15	1281	1286	1583	
16	1310	1303	-	
17	1706	1652	1762	

Table 3.6. Comparison of the first 17 Natural Frequencies for curved fan blade.

Mode	Exp. (39)	2 x 2	3 x 2	2 x 3	3 x 3	4 x 4
1	85.6 86.6(43)	94.1	91.66	86.6	87.11	86.2
2	135	145	145	143.2	141.8	139.5
3	259	250.6	258	252.5	255.6	249.8
4	351	402.4	385	366	359	347.9
5	395	418	448	411	430	405
6	531	828	595	717	584	549
7	751	807	801	736	755	771
D.O.F.*		80	110	120	165	280

Table 3.7 Frequencies of the fan blade using different meshes.
* Total number of degrees of freedom after the boundary conditions.

Mode	2 x 3 (30)+	2 x 3* 3x2x2**	2 x 3 4x2x2	3 x 3 3x2x2	3 x 3 4x2x2	3 x 3 4x3x2
1	91	90	91	88	88	91
2	149	144	148	143	144	146
3	310	270	298	261	264	282
4	383	374	380	362	364	407
5	556	455	535	461	479	582

Table 3.8. Frequencies of the fan blade using 10-node elements

+ Results for 12-node element ref (30)

* Mesh used

** Order of integration

modified eight-node element with 4 x 4 mesh. The values on table 3.7 demonstrate the importance of the location of the nodal points and the choice of the mesh used. Finally, on table 3.8 the frequencies obtained by using ten-node elements are compared with the results of the twelve-node element of reference (30).

3.5. Circular Cylindrical Shell

This example was chosen to test the program on a cantilevered cylindrical shell. The configuration is shown on figure 3.1. The experimental values of the frequencies for this cylinder were reported by Gill (27). He calculated the frequencies using the method given in (51). Wilson (57) also solved the problem using five axisymmetric shell elements. The experimental and the calculated values of the frequencies of the references (27,57), and the results of the present study are listed on table 3.9.

In the present study, the frequencies were calculated by using modified eight-node elements with different meshes. Due to the symmetry only half of the cylinder was considered. Even with 2 x 2 mesh reasonable results were obtained for the simple modes like 1/1, 2/1, 2/2. A finer mesh was required for the accurate determination of higher frequencies.

3.6. Curved Cantilever Beam-Pipe Segments

The examples solved in sections 3.4 and 3.5, showed that the program is capable of dealing with shallow and closed shell structures. The hollow blading of chapter 5 consists of two

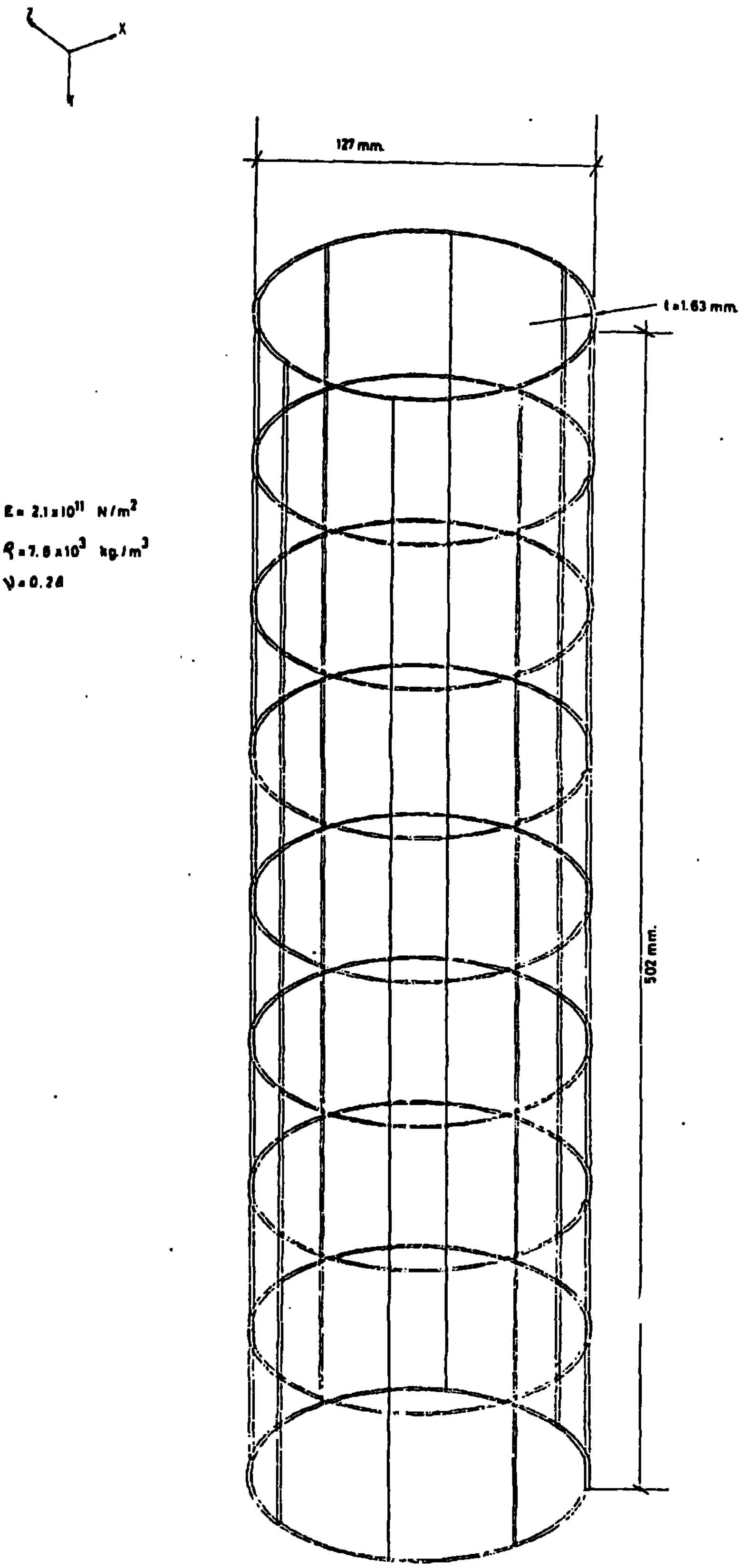

Figure 3.1 Circular Cylindrical Shell

Mode n/m*	Exp.	Ref. (27)	Ref. (57)	** 2 x 2	3 x 5	4 x 8	4 x 10	6 x 8
1/1	364	-	470	466	470	468	468	468
2/1	293	319	315	289	334	320	320	316
3/1	740	767	767	1274	916	821	816	779
4/1	1451	1462	1461	-	-	-	1782	1527
5/1	2236	2361	2359	-	-	-	-	-
1/2	-	-	2061	-	-	-	2025	2055
2/2	827	1017	943	990	960	996	951	941
3/2	886	928	914	-	-	1061	986	932
4/2	1503	1521	1517	-	-	-	1832	1597
2/3	1894	2393	2212	-	-	-	2230	2213
3/3	1371	1511	1459	1632	-	-	1593	1505
4/3	1673	1726	1712	-	-	-	1992	1874
4/4	2045	2158	2122	-	-	-	2338	2494

Table 3.9 Natural frequencies of circular cylindrical shell.

* n/m where n is the number of nodal diameters

and m = number of nodal circles + 1

** Mesh used

shallow shells, similar to the fan blade of section 3.4., connected by two circular pipe segments. The analysis in this section was performed in order to decide on a reasonably accurate representation of these pipe segments.

The cantilever beam with the cross-section shown on figure 3.2 was analysed. Being a slender beam, all of its lower modes of vibration were of bending type. First six natural frequencies - first three bending in X-X plane and first three bending in Y-Y plane - were calculated by using the closed form formula for the natural frequencies of a beam. These modes of vibration coincided with the first six modes of the finite element analysis which was performed by using different meshes and integration points. The natural frequencies were calculated by using both the eight-node and the ten-node elements. The meshes used were either 1 x 8 or 2 x 8. Eight elements along the length were used in order to have compatible results for the analysis of chapter 5 where two beams similar to the present one were used as parts of the oval cross-section blading. The results are given on table 3.10.

The eight-node element with 1 x 8 mesh and 2 x 2 x 2 integration points was too flexible and did not give any reasonable results. Increasing the number of integration points from two to three in the direction of curvature improved the results and brought them within acceptable limits. An additional integration point along the length caused small increases in the higher frequencies. A refined mesh with 2 x 8 elements gave good results with 2 x 2 x 2 and 3 x 2 x 2 integration points,

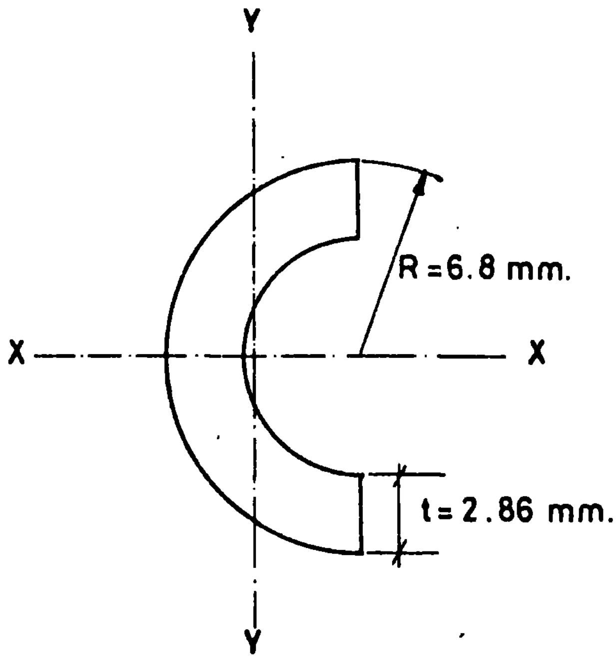

I_{xx} = 745.012 mm^4

I_{yy} = 154.144 mm^4

Area = 48.249 mm^2

Length = 380.0 mm

E = 2.11 $\times 10^{11}$ N/m^2

Density = 7.85 x 10^3 kg/m^3

Figure 3.2 Assumed cross section of the beam segment.

Mode No.		Beam Theory	8 - node Elements					10 - node Elements.				
			1 x 8 2x2x2	1 x 8 3x2x2	1 x 8 3x3x2	2 x 8 2x2x2	2 x 8 3x2x2	1 x 8 3x2x2	1 x 8 4x2x2	1 x 8 4x3x2	2 x 8 3x2x2	2 x 8 4x2x2
x - x	1	79	64	71	71	78	79	80	82	82	79	79
	2	495	394	440	445	480	483	491	502	508	485	485
	3	1385	1079	1215	1246	1321	1333	1348	1382	1416	1336	1337
y - y	1	36	11	34	34	34	36	34	35	35	36	36
	2	225	70	214	214	214	226	218	223	224	227	227
	3	630	201	615	618	603	639	627	644	646	641	642
x-section Area mm^2		48.3	41.1	41.1	41.1	47.6	47.6	48.8	48.8	48.8	48.3	48.3

Table 3.10. Results for the cylindrical pipe segment.

later being more accurate. The results of ten-node element was much better for both 1 x 8 and 2 x 8 meshes. Order of integration did not change the results much, but the use of three integration points along the length caused slight over-stiffness of the element. For this particular problem, the order of integration did not effect the calculated volume of the elements, but in general the volume was calculated more accurately by refined meshes or when ten-node elements were used. More accurate results were obtained when the volume was determined accurately.

The results indicate that the ten-node element is more suitable for the finite element modelling of this beam. A 1 x 8 mesh with 4 x 2 x 2 integration points seems to be the best choice when the economy is taken into consideration.

3.7 Conclusion

A modified eight-node element with the stiffness matrix integrated at 2 x 2 x 2 Gauss points gave excellent results for all plate and shallow shell analysis. Only in two cases, those of pretwisted blading and of pipe segments, was this element found to be too flexible. Increasing the number of integration points from two to three in the direction of curvature, increased the accuracy. In these two cases, the performance of the ten-node element was very good.

For the numerical integration of the mass matrix 3 x 3 x 2 Gauss points were used for both eight-node and ten-node elements. Also 3 x 3 x 3 integration points were tried for integrating the mass matrix of the eight-node element and

4 x 3 x 2 integration points for the ten-node element. Their effects on the results were unnoticeable.

For all the examples the mode shapes determined were in a very good agreement with the mode shapes given in the original references.

CHAPTER 4

4. EXPERIMENTAL METHOD

The majority of the experiments were undertaken to confirm the numerical predictions of the natural frequencies and the mode shapes of an oval cross-section hollow blade. In addition to these, some subsidiary experiments were performed to see the effects of various assumptions on the experimental and numerical results.

Geometry and construction of the shells, and the results of the experiments are given in the related sections of chapters 5 and 6. In this chapter, measurement of the geometry of the shell, apparatus and the procedure will be given.

4.1 Determination of the Actual Geometry of the Shell

After the blade was manufactured (see 5.2), some measurements were taken in order to determine its actual geometry. A grid, which was later used in the finite element analysis, was drawn on the surface of the shell. Relative distances of each node of the grid from a base line was measured by means of a micrometer. The measurements were taken both along y = const. and x=const. lines. Then, taking one of the nodes as the reference point z coordinates of all the nodes were calculated by using the two sets of data, thus cross-checking the results. At the end, the average values were taken, and these were checked against the direct measurement of the distance between the faces of the blade.

In spite of the careful measurements there were some differences between coordinates that were determined by different methods. So, some adjustment had to be made by close visual inspection of the shell. Also, there was no way of measuring the coordinates of the points at the bottom faces of the elements, since they were trapped inside the shell. Coordinates of these points were calculated analytically.

4.2 Apparatus and Procedure

All the experiments were conducted on a vibration table which consisted of a cast-iron bedplate, mounted on a concrete block. The flanged channels on the surface of the bedplate was used to bolt the base of the shells on to the table. To prevent the shell from rocking, it was found to be useful to use as many bolts as possible. In some instances, it was observed that the extra bolts were effecting the bending type of frequencies, increasing them by up to 4 per cent.

The shells were excited over a large range of frequencies, using an oscillator which was driving a coil through an amplifier. In spite of the amplifier, the magnetic field created was not sufficient above 500 Hz .,and it was necessary to have the coil very close to the shell surface. The position of the coil was often changed for a better excitation of different modes. The improvement gained was small, although it marginally helped in the torsional type of modes.

The response of the shell was indicated by piezoelectric strain gauges cemented on the surface of the shell. Up to six gauges were bonded to the shell, different ones being useful for different modes.

Output from the gauges was displayed on the lower trace of an oscilloscope where it was compared with the forcing frequency displayed on the upper trace. Usually the shell responded at some whole number multiple of the forcing frequency. When the core of the coil was not a permanent magnet, the response of the shell was at twice the driving frequency. The output signal of the guages reached their maximum when a natural frequency was excited. This frequency was accurately determined by using a Muirhead-Wigan Decade oscillator.

Once a frequency was detected, the identification of the mode shape was done using a hand-held piezoelectric guaged probe. The guage on the probe converted the displacements of any vibrating surface into an electrical signal which was displayed on the upper trace of the oscilloscope instead of the forcing frequency. By touching a particular point on the shell with the probe, the signals were compared as either in or out of phase with the signals from the strain gauge. A thorough examination of the shell surface yielded the mode shape for the particular frequency.

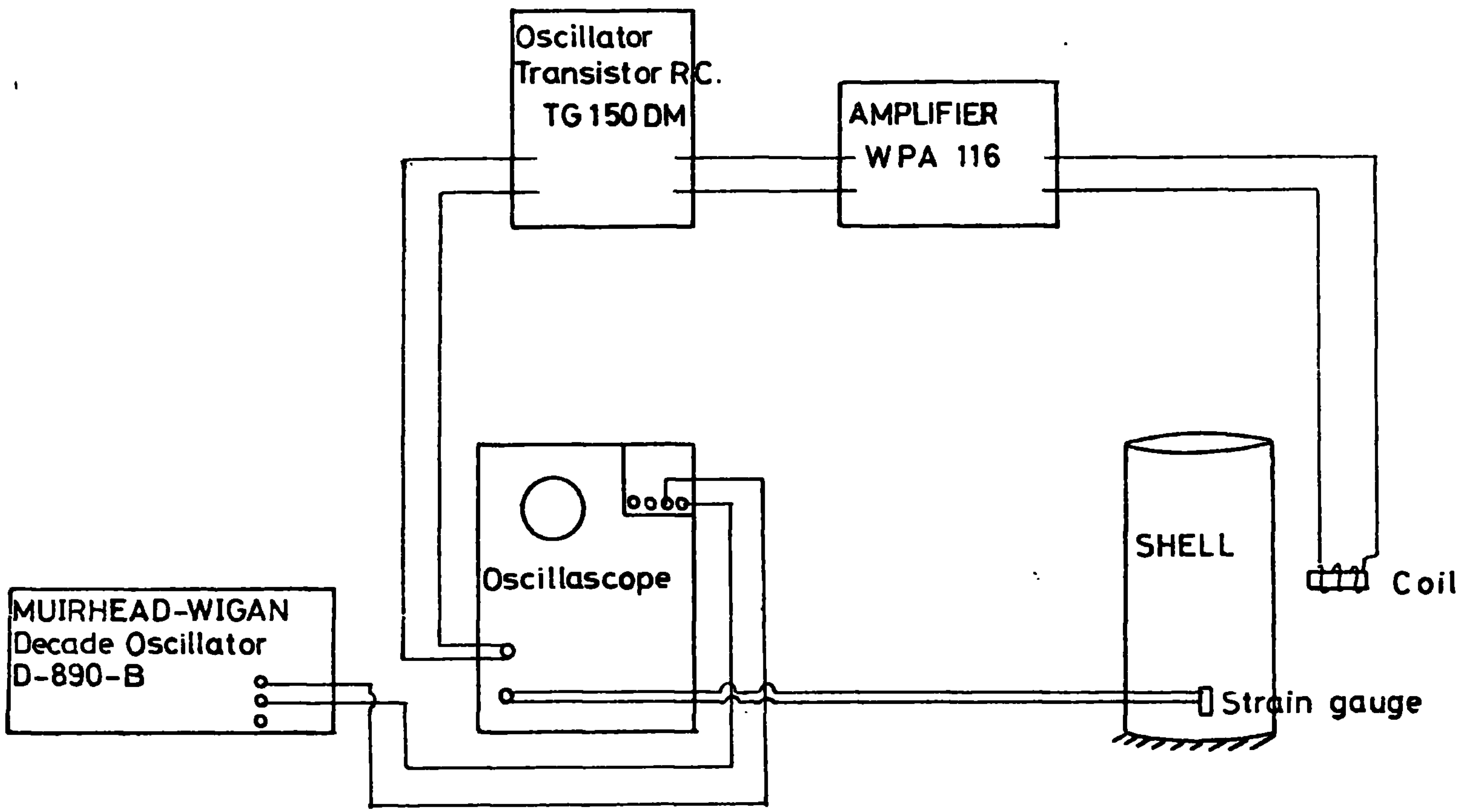

Figure 4.1. Circuit for the determination of the natural frequencies.

CHAPTER 5

5. OVAL CROSS-SECTION HOLLOW BLADE

In this chapter, the computer program which was explained in chapter 2, and checked against several test examples in chapter 3, was used to analyse hollow blading. The natural frequencies predicted by the program were compared with the results of the experiments performed on a model blade, and the causes of some of the differences were studied.

The geometrical descriptions of the experimental and the mathematical models of the blade are given in the following section.

5.1 Geometry of the Blade

The blade was designed to have a constant cross-section of oval shape, consisting of four circular segments with two different radii of curvature along the whole length. (Fig.5.1). To have a continuous surface, the circular segments were so located that they would be tangent at the intersecting points. This condition required the following relationship to be satisfied:

$$R = \frac{a^2 + b^2 - 2\,ar}{2(b - r)} \qquad (5.1)$$

The parameters of this relationship are as shown in Fig. 5.1. and they were chosen as:

a = 105 mm	r = 6.76 mm
b = 20 mm	R = 377.6 mm

The length of the blade was taken to be 420 mm.

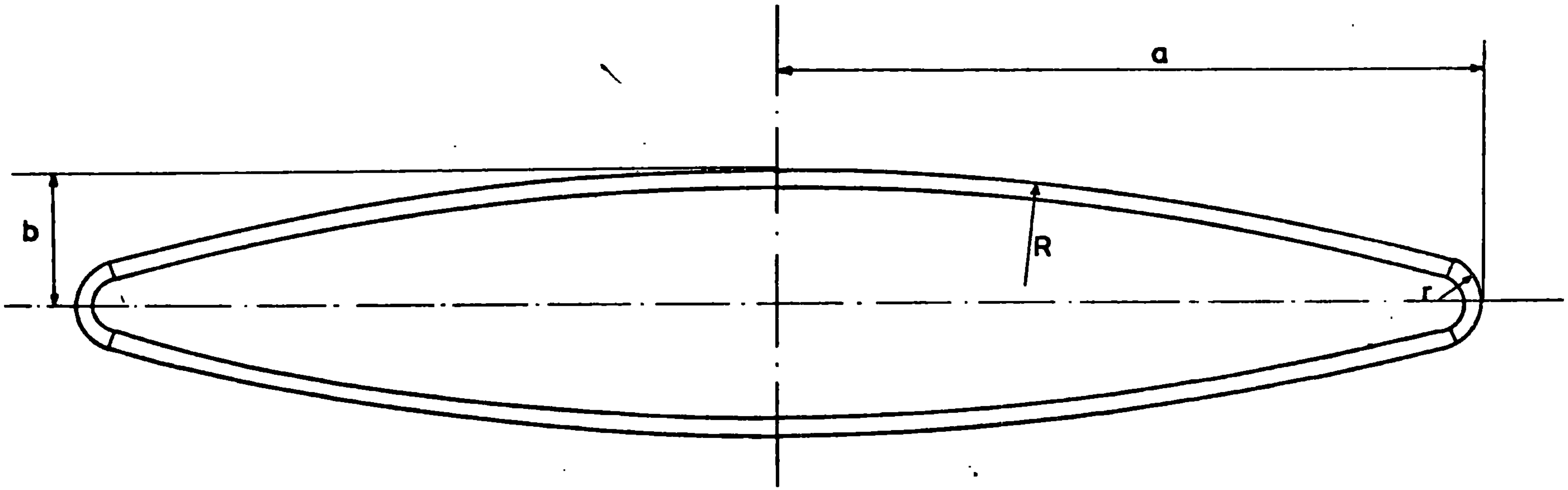

Figure 5.1. The cross-section of the design geometry of oval blade.

Due to the difficulties encountered during the manufacturing process (see Sec. 5.2.), the experimental model of the blade had some geometrical imperfections. To achieve a smooth surface then, was only possible by filing it along the intersecting lines, and the true mathematical description of the experimental model became impossible.

5.2 Manufacturing the Experimental Model

A model of the blade described in the previous section was manufactured for laboratory testing. Two larger cylindrical segments were obtained by rolling two 200 x 420 mm steel sheets of 2.54 mm thickness, to a radius of curvature of 380 mm. The two small segments were cut out of a steel pipe of 13.5 mm outer diameter. The wall thickness of the pipe was 2.75 mm.

Two successive different methods were employed to connect the four pieces together and to fix the root of the assembly. The experiments were performed for both cases.

5.2.1 Solder Assembly

In the first case brazing was used to connect the pieces. The idea was to avoid welding, thus to prevent the pieces from warping under high temperatures. But the pipe segments were inevitably bent during the cutting process due to stress relaxation, so the final assembly was a doubly curved shell with an unwanted curvature along the length, (see fig. 5.2). Since this curvature was non-uniform the symmetry of the blade was lost. Measurements taken on the blade showed that the geometric parameter b was varying from 16.5 mm at the tip to 23 mm at the middle cross-section.

The root fixing was achieved by embedding 40 mm of the blade into a solder base. The clear length of the blade for this case was 380 mm.

The analysis in Section 5.3 has shown that the brazing was not stiff enough to assume the blade as a single piece of metal. Also the solder which was used to fix the root was too flexible to simulate the clamped boundary condition. These difficulties were overcome in the second method at the expense of using welding.

5.2.2 Weld Assembly

In the second case the aim was to have the inter-connections of the pieces stiff enough to treat the whole blade as a single piece of metal, also to have the root fixing as stiff as possible to be able to assume that it was clamped. For this purpose the brazing along the inter-connecting lines was replaced by welding. Also the solder base was removed and the blade was welded onto a steel plate. As expected, the high temperature caused some irrecoverable local distortions in the geometry. The measurements that were taken to determine the final shape of the blade indicated that, in addition to the unwanted curvature now, there was also a slight pretwist on the blade.

To use for numerical analysis the coordinates of each node were calculated. The finite element model of the blade shown in figure 5.2 was drawn using these coordinates. This geometry of the blade will be referred as the real geometry of the blade in the following sections.

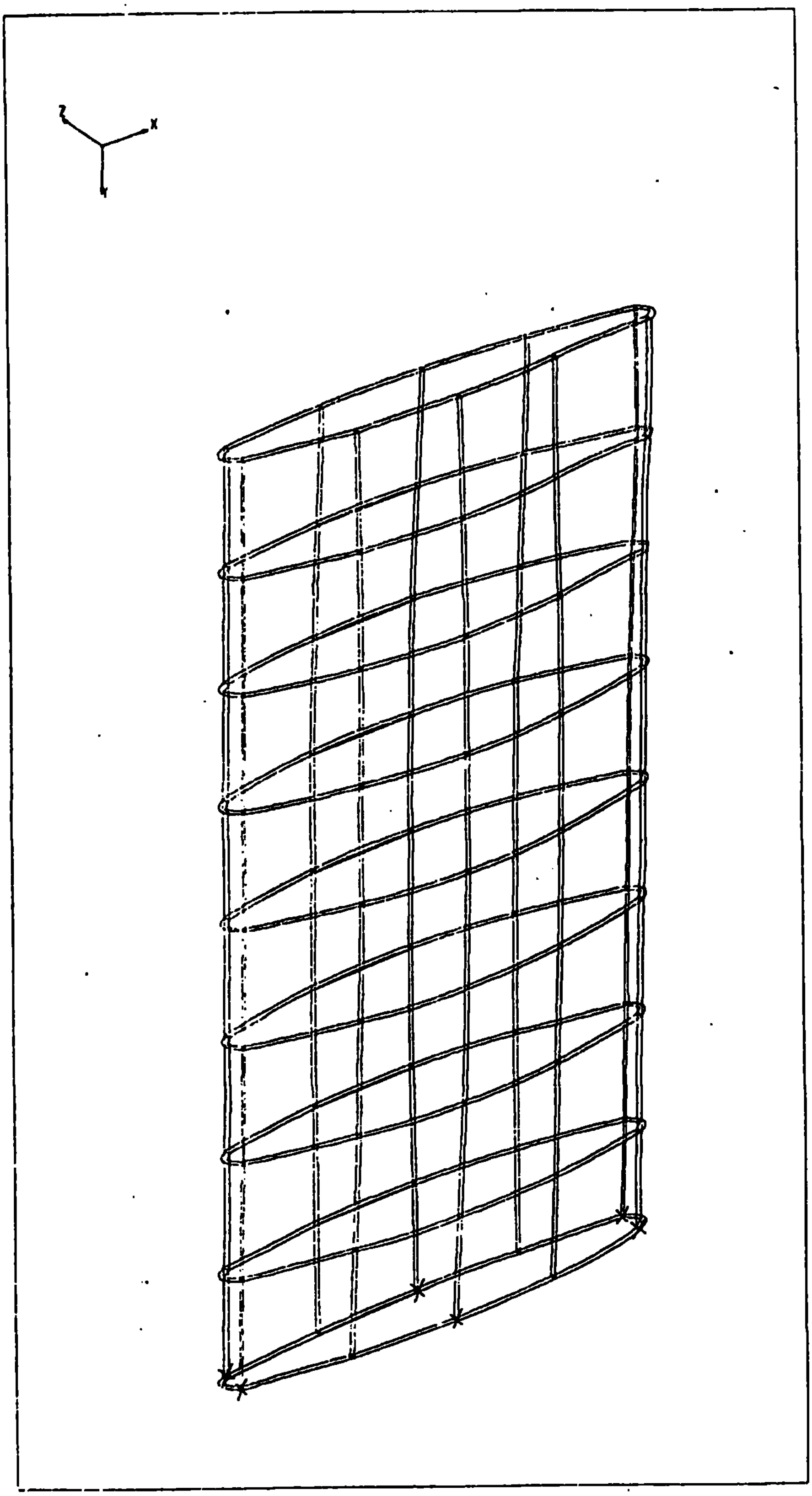

Figure 5.2 Real Geometry finite element model of the blade.

X See footnote on page 56.

The average values of these coordinates yield to the following approximate parameters for the geometry:

a	=	105 mm	r	=	5.5 mm
b	=	19 mm	R	=	410 mm

The geometry of the blade described by these parameters was used to determine the ideal mode shapes in Section 5.5.1. and will be referred as ideal geometry.

5.3 Analysis of the Blade Assembled using Solder

In this section, the experimental model of the blade described in section 5.2.1. is analysed. First three natural frequencies obtained from the analyses are listed on table 5.1. Column 1 contains the experimental frequencies, columns 2 and 3 give the results of the finite element analyses. As the results indicate the experimental model was too flexible to give any comparable results. The frequencies listed in column 3 were obtained by representing the brazing between the pieces as hinges* in the finite element model. The effect of this assumption on the ovalling and torsional modes was to reduce them considerably, although it did not change the bending mode at all.

The results showed that a rigid connection between the pieces was not achieved in the experimental model, and over-flexibility of these connections were resulting low torsional and ovalling frequencies. Bending mode of vibration which was independent of the type of connections between the pieces, depends greatly on the type of root fixing which is discussed in the next section.

* See addendum on page 52.

Mode	Exp.	8 x 10 F.E.*	8 x 8 F.E.**
Bending	151	232	233
Ovalling	197	345	198
Torsion	256	317	135

Table 5.1: First three frequencies obtained experimentally and by finite element analysis.

* rigid connections

** hinged connections

Frequencies given are in Hertz.

ADDENDUM

The representation of the hinged connections was achieved in a simple way during the elimination process. The rotational degrees of freedom, at the nodes along the line connecting the pipe segment to the shallow shell, were eliminated as soon as the contribution of the elements along the pipe segment were completed but before any contribution from the elements of the shallow shell was included. The process was reversed when crossing the connecting line from shell to pipe segment. The elimination of u, v and w degrees of freedom was done following the usual procedure.

5.4 Effect of the Root Fixing on the Natural Frequencies

To achieve the idealized clamped boundary conditions in the experiments is very difficult. In this part of the study, the behaviour of different experimental simulations of the clamped boundary conditions was examined.

A set of experiments were performed on two identical cylindrical steel pipes. The pipes had an outer diameter of 50.8 mm and a wall thickness of 1.59 mm.

The first piece of pipe was 260 mm long and it was welded on a steel block of dimensions 305 x 82.5 x 25.4 mm. The pipe responded to the first bending mode (which also was the fundamental mode of vibration) at two different resonant frequencies. When it was excited to vibrate parallel to the length of the base plate the resonant bending frequency was found to be 602 Hz , whereas the same pipe responded to the same mode of vibration at 564 Hz when it was excited to vibrate normal to the previous direction. The second mode of vibration was the first ovalling mode and it was found to be 1783 Hz , independent of the direction of excitation. The The third natural frequency was the second ovalling mode at 2300 Hz.

The root fixing of the second piece of pipe was achieved be embedding it into a block of solder having dimensions 84 x 75 x 26 mm. The average length of the pipe was 251 mm. The resonant frequencies corresponding to the first bending mode were determined to be 395 Hz and 417 Hz in two normal directions. The ovalling mode responded to a resonant frequency of 1796 Hz.

Table 5.2 lists these experimental results, together with the results obtained from the computer program. For the numerical analysis a 6 x 8 grid was used, and due to the symmetry, only half of the cylinders were considered. Clamped boundary conditions were assumed for both cases.

Case	Exp.	Num.	Exp.	Num.
length (mm) / Mode	260	260	251	251
1	564/602	706	395/417	755
2	1783	1773	1796	1776
3	2300	2297	-	2358

Table 5.2. Comparison of the experimental and numerical frequencies of two similar cylinders. Different methods for root fixing were used for the experiments.

As expected the results of the finite element analysis gave a higher bending frequency for the shorter cylinder. But in the experimental case, due to the effect of the different methods of root fixing, the situation was reversed. The solder base is definitely not suitable to represent the clamped boundary conditions for the experiments.

5.5 Weld Assembled Blade

5.5.1 Finite Element Analysis using Ideal Geometry

The numerical analysis was first performed on a regular geometric shape, approximated by the average geometric parameters given in section 5.2.2., to determine the ideal mode shapes for the blade.

A 10 x 8 grid (same as on figure 5.2) was used in the analysis, and the length of the blade was taken to be 420 mm. To represent the pipe segments at the sides, the cubic-quadratic element of section 2.2. was used. The number of integration points for these elements were 3 along the curvature, 2 along the length and through the thickness.

The sketches of first 20 mode shapes, and deflection curves for some of these modes are given in appendix 3. Since these mode shapes were obtained by using a regular geometry, and they show a regularity themselves, they are referred as ideal mode shapes. In general, it is possible to classify them in different groups except for the last, mode number 20. Inconsistent shape of this mode could be due to the coupling of bending mode with two nodal diameters, and the mode type 8 with three nodal diameters.

Table 5.3 lists the frequencies obtained by using different number of master degrees of freedoms with 10 x 8 grid. In addition the frequencies for some of the symmetric modes which were calculated by using only half of the blade (making use of the symmetry around z -axis) are included.

The frequencies listed in column 1, were calculated by keeping both u and w displacements as master degrees of freedoms at 92 nodes. Two different frequencies corresonding to mode 6 are the result of the coupling with the bending mode in x - direction. Detailed tip deflections for these two frequencies are given in figure A.3.1. in appendix 3.

Frequencies given in column 2 were obtained by keeping only w displacements at 102 nodes. Since the master degrees of freedoms were distributed more evenly over the blade than they were in the previous case, they gave better results especially for the mode shapes with three nodal diameters. A similar comparison can be made between the second and third columns where only 88 w displacements were kept as masters.

Columns 5 and 6 contain the frequencies which were calculated by using only half of the blade. The retained master degrees of freedoms which gave the frequencies in column 5 were equivalent to the ones of column 3.

The frequencies given in columns 4 and 7 were calculated by restraining only six* and four* nodes respectively at the root of the blade, to simulate more flexible root fixing condition. The greatest effect of this assumption was reflected on the bending frequencies which were reduced by about 30 per cent.

5.5.2. Finite Element Analysis - Real Geometry

The analysis in this section was performed on the geometry that was described by the coordinates of nodes as measured directly on the blade (Section 5.2.2). Thus, a closer approximation to the geometry of the experimental model was achieved.

The finite element idealization used was very similar to the ideal geometry case of section 5.5.1, with the grid shown in figure 5.2. The y-coordinates of the tip nodes were changing between 413 mm and 417 mm, giving an average total length of 415 mm to the blade. In all the analyses in this section the

* See figure 5.2 on page 50 for the location of these nodes.

Column	1	2	3	4*	5	6	7*
Grid	10 x 8	10 x 8	10 x 8	10 x 8	5 x 8	5 x 8	5 x 8
DOF / Mode	184	102	88	104	48	88	48
1	196.5	195.6	197	142	197	197	139
2	302.5	302.5	304	299	304	303	299
3	335.5	335.7	337	327	-	-	-
4	562	562	590.4	564	-	-	-
5	553	553	589.8	551	589.8	581	567
6	809/879	821.5	837	830	-	-	-
7	804.7	804.5	873	809	873	866	809
8	953.6	955	962	961	961.5	961	961
9	950	951	1040	1029	-	-	-
10	1062	1064	1148	1144	1148	1143	1144
11	1047	1047	1372	1338	-	-	-
12	1042.7	1042	1378	-	1378	1356	1363
13	1191	1191	1485	-	-	-	-
14	1359	1359	1754	-	-	1696	1696
15	1418.7	1436	1434	-	-	-	-
16	1510	1502	-	-	-	-	-
17	1589	1583	-	-	-	-	-
18	1604	1598	-	-	-	-	-
19	-	1733	1755	-	-	-	-
20	1514	1513	-	-	-	-	-

Table 5.3. Predicted natural frequencies for the ideal geometry oval blade.

* Partial restraining of the root.

master degrees of freedoms were chosen among the w displacements only.

First seven natural frequencies are listed on table 5.4 with the sketches of the tip deflections of the modes, and the results of experimental and ideal geometry analyses. Higher frequencies, corresponding mode shapes, and some of the deflection curves are included in appendix 3.

5.5.3. Experimental Analysis

Some of the natural frequencies and the corresponding mode shapes of the experimental model of the blade were determined following the procedure given in chapter 4.

The location of the nodal lines were very much effected by the imperfections of the geometry of the blade, especially for high natural frequencies. Also, for these natural frequencies the magnetic field created by the coil was relatively weak. These, together with the suppressive effect of the hand-probe when in contact with the shell, made it extremely difficult to identify the mode shapes of high frequencies.

First seven frequencies are listed on table 5.4. Sketches of the mode shapes of these and some higher frequencies are given in appendix 3.

5.5.4. Comparison of the Results

Table 5.4 lists the first seven natural frequencies obtained from experimental and finite element analyses. These frequencies and the corresponding mode shapes are in a good agreement in all three analyses.

The biggest difference between the frequencies is seen in the bending mode. This is an expected situation since the effect of the simulation of the clamped boundary condition is greatest for this mode (this was pointed out both experimentally and numerically in sections 5.4 and 5.5.1.). Comparison of the frequencies listed for real geometry and ideal geometry analyses also indicate that this mode is very sensitive to the geometry used in idealization. Although the nodal coordinates of the real geometry case were taken directly from the experimental model of the blade, the accuracy of these measurements is subject to discussion. Considerations of these facts make the difference in the frequencies of the bending mode tolerable.

Fifth mode, which is the second ovalling mode, of real geometry and experimental analyses seems to couple with the second tortion mode (figure A.3.20, and A.3.32). Also slight coupling of sixth mode with the second bending can be seen on figure A.3.20.(a). These are the first signs of the affect of imperfections of the geometry on the mode shapes. Similar couplings were observed in section 6.3.1, where the pretwist of the blading was considered. Although the pretwist of the geometry considered in this section was very small, the frequencies corresponding to these two sets of modes were fairly close (within about 10%) and the overall irregularity of the geometry may account for these couplings.

During the experiments a frequency at 708.5 Hz was detected, but the identification of the mode shape was not possible due to the difficulties explained in section 5.5.3. This frequency is inserted into the table as the experimental second bending mode which is in a good agreement with the finite element analyses.

Effects of the imperfections of the geometry on the mode shapes become visible at fifth mode, and increases as the mode shapes get more and more complicated. Coupling occurs between two or even three close modes, and the identification of the resulting mode shape becomes very difficult, sometimes impossible. In appendix 3, the shapes of some of the modes above 7 are examined, and possible matchings between the results of different analyses are pointed. Some of the mode shapes that were obtained either by the finite element analysis of the real geometry, or by the experimental analysis are not included at all, because of the extreme difficulties of identifying them.

5.6 Effects of the Material Properties and the Choice of Degrees of Freedoms on the Natural Frequencies and the Mode Shapes.

In all the numerical calculations performed in this chapter the following nominal material data was used.

Young's Modulus	=	0.211×10^{12} N/m^2
Density	=	0.785×10^{4} kg/m^3
Poissons Ratio	=	0.285

In order to observe the variation of the natural frequencies with the changes in material properties, the numerical calculations were repeated for the real geometry of the blade using 10 x 4 grid for different material data.

Mod. No.	Cross-section	Experiment.	R.G.	I.G.
1	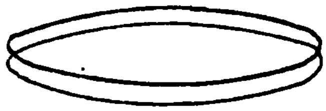	142	158	196.5
2	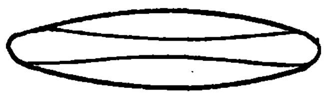	296	306.8	302.5
3	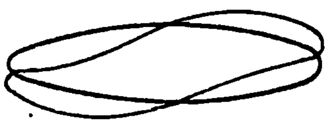	355	371.5	335.5
4	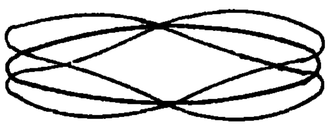	561	588.4	562
5	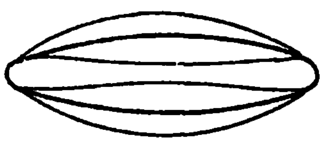	595	648	553
6	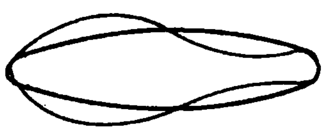	812	836	821.5
7	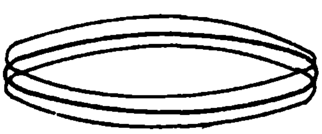	(708)*	739	804.5

Table 5.4. Comparison of the results of the experimental and finite element analyses. The frequencies given are in

* Mode shape was not identified experimentally.

The results obtained are listed on table 5.5. An increase of 2.03% in Young's Modulus caused 1.014% increase; and 0.637% decrease of the density caused 0.32% increase in all frequencies. These changes are exactly as expected, since the frequencies are directly proportional to $(E/\rho)^{1/2}$. Changing the poissons ratio, in the possible range of 0.25 to 0.33 effected different frequencies in different ways, but in all cases the change in the frequencies was less than 2%.

A similar observation was made by changing the master degrees of freedoms retained. The results are given on table 5.6. Again 4 x 10 grid was used, and there were total 640 degrees of freedom after the insertion of boundary conditions. In general keeping more w displacements distributed over the blade gives better results than any other combination of master degrees of freedoms. An exception to this reasoning was seen only for mode 6, and it was the effect of the bending mode in x-direction.

5.7. Discussions of Results

Natural frequency analysis of an oval cross-section hollow blade has been presented. The geometry chosen is interesting from the point of view that it contains both thin-shallow and thick-deep shell properties in it. The interesting part of the numerical analysis on the other hand, is that the same type of finite element was used to represent both types of shell properties.

Difficulties that arose in manufacturing the experimental model, imposed some limitations on accurate representation of the mathematical model. Two different mathematical representations

E	0.211×10^{12}	0.2153×10^{12}	0.211×10^{12}	0.211×10^{12}	0.211×10^{12}	0.211×10^{12}
ρ	0.785×10^{4}	0.785×10^{4}	0.780×10^{4}	0.785×10^{4}	0.785×10^{4}	0.785×10^{4}
ν	0.285	0.285	0.285	0.250	0.300	0.330
1	162.23	163.874	162.749	162.745	162.029	161.664
2	320.111	323.356	321.136	318.677	320.837	322.497
3	375.274	379.078	376.474	374.120	375.883	377.317
4	621.429	627.730	623.418	621.060	621.733	622.614
5	660.429	666.754	662.174	659.237	660.541	661.738
7	782.532	790.466	785.036	782.689	782.534	782.674
6	870.081	878.902	872.866	864.331	872.888	879.153
8	1011.85	1022.11	1015.09	1006.29	1014.62	1020.85

Table 5.5. Variation of natural frequencies with the material properties.

D.O.F. / MODE	118 w	60w	60w+60u	60w+60v	60w+60α	60w+60β
1	162.23	162.24	162.24	162.24	162.238	162.243
2	320.111	320.261	320.227	320.257	320.160	320.253
3	375.274	375.953	375.580	375.945	375.355	375.939
4	621.428	624.996	624.275	624.830	623.348	624.601
5	660.062	667.445	665.841	666.719	666.546	666.330
6	870.081	876.025	827.181 937.434	856.149	871.007	875.804
7	782.532	790.022	786.725	789.004	780.832	789.476
8	1011.85	1031.49	1028.26	1021.58	1018.83	1030.10

Table 5.6. Variation of the Natural Frequencies with different choice of master degrees of freedoms.

were used for the finite element analysis. First, using a regular but approximate geometric shape, general trend of the idealized mode shapes were determined. Seven of these predicted modes and the natural frequencies were confirmed by the experiments. Later, the accuracy of the predictions were further increased by describing the geometry of the mathematical model closer to the experimental one.

Some of the causes of the differences between the results of various analyses were studied experimentally and numerically. The studies indicated that the clamped boundary conditions were not simulated properly on the experimental model. In spite of that, the results obtained were quite satisfactory.

CHAPTER 6

6. FUTURE APPLICATIONS

The range of application of the computer programs which are developed to serve a particular purpose is usually limited. The limitations that isoparametric shell element has, are the difficulties of modelling the sharp corners and multiple junctions in the structures. For a structure where these type of connections are dominant, it might be better to employ some other element, for instance semiloof, for which they do not represent any difficulty. On the other hand this new element may not offer the same facilities as the original one, for instance it may not be able to represent the properties of a thick shell.

In this chapter, some simple modifications are introduced to extend the range of applicability of the isoparametric shell element. Some assumptions are made for very sharp corner connections and mulitple junctions. Also the stiffeners are considered for hollow shells. However, if the nature of the problem in hand changes considerably, it may be more practical to employ a general purpose program for the solution.

6.1. Sharp Corner Connections

Instead of an oval cross-section, when an aerofoil cross section is assumed for the hollow blading, as shown in figure 6.1, immediately a difficulty arises in representing the sharp corner. To satisfy the continuity of the displacement between the elements joining at this corner, the nodes which are common to these elements must be defined uniquely. A unique definition of the nodes at the sharp corner is achieved by assuming the nodal connections between the elements as shown in figure 6.2. Application of this assumption to the section shown in figure 6.1 introduces another difficulty. When one defines the top and bottom points of the thickness vector at the corner, and goes around the aerofoil cross-section by defining the thickness vectors at every node, it is apparent, when reaching the corner node again, that the top and bottom points of the node have to be reversed. This does not affect the continuity of the u, v and w displacements since they are defined at the midpoint of the node, but may affect the rotational degrees of freedoms, α and β since their definition depends upon the thickness vector. Defining two different thickness vectors for the same node is discussed and illustrated on a cantilever plate in the next section.

6.1.1. Cantilever Plate

The rectangular cantilever plate shown in figure 6.3 is represented using three elements. The direction of the curvilinear axes of each element are so chosen that the thickness vectors corresponding to nodes 6,7 and 8 are pointed in opposite directions for the elements 1 and 2. Since the displacements u, v and w are the displacements of the mid-point of the thickness vector in the global system, they do not represent any difficulty in joining the element matrices. On the other hand, α and β are defined as the rotation of the thickness vector $\underset{\sim}{V}_{3i}$ around two orthogonal axis, $\underset{\sim}{V}_{1i}$ and $\underset{\sim}{V}_{2i}$ normal to it.

For a unique definition of $\underset{\sim}{V}_{1i}$ and $\underset{\sim}{V}_{2i}$ the following convention was used.

$$\underset{\sim}{V}_{1i} = \underset{\sim}{j} \times \underset{\sim}{V}_{3i} \qquad (6.1)$$

where $\underset{\sim}{j}$ is the unit vector in the global y direction.

$$\underset{\sim}{V}_{2i} = \underset{\sim}{V}_{3i} \times \underset{\sim}{V}_{1i} \qquad (6.2)$$

For the simple geometry of the figure 6.3, the local orthogonal axis $\underset{\sim}{V}_{1i}$, $\underset{\sim}{V}_{2i}$ and $\underset{\sim}{V}_{3i}$ are shown on figure 6.4. In every case, with the scheme given above, it is only the $\underset{\sim}{V}_{1i}$ vector which will change direction when the sense of the thickness vector $\underset{\sim}{V}_{3i}$ is changed. Thus, only the β displacement will be affected when top and bottom points of a thickness vector are interchanged for different elements. So, the displacements u, v, w, α and β of $\underset{\sim}{V}_{3i}$ vector of figure 6.4(a) correspond to the u,v,w, α and $-\beta$ of $\underset{\sim}{V}_{3i}$ vector of figure 6.4.(b). When the necessary transformation is done for β degree of freedom, the assembly process can continue in the usual form.

The transformation requires the multiplication of the entries of the matrix corresponding to β degrees of freedom of the nodes 6,7 and 8 by (-1). Physically, m_{ij} entry of an element matrix represent the force acting on degree of freedom i due to the unit acceleration (or displacement) of degree of freedom j. Transformation, therefore, is achieved by keeping the i (and then j) entry fixed for the β degree of freedom of the reversed node, and multiplying the j (and then i) entries of the whole matrix by (-1).

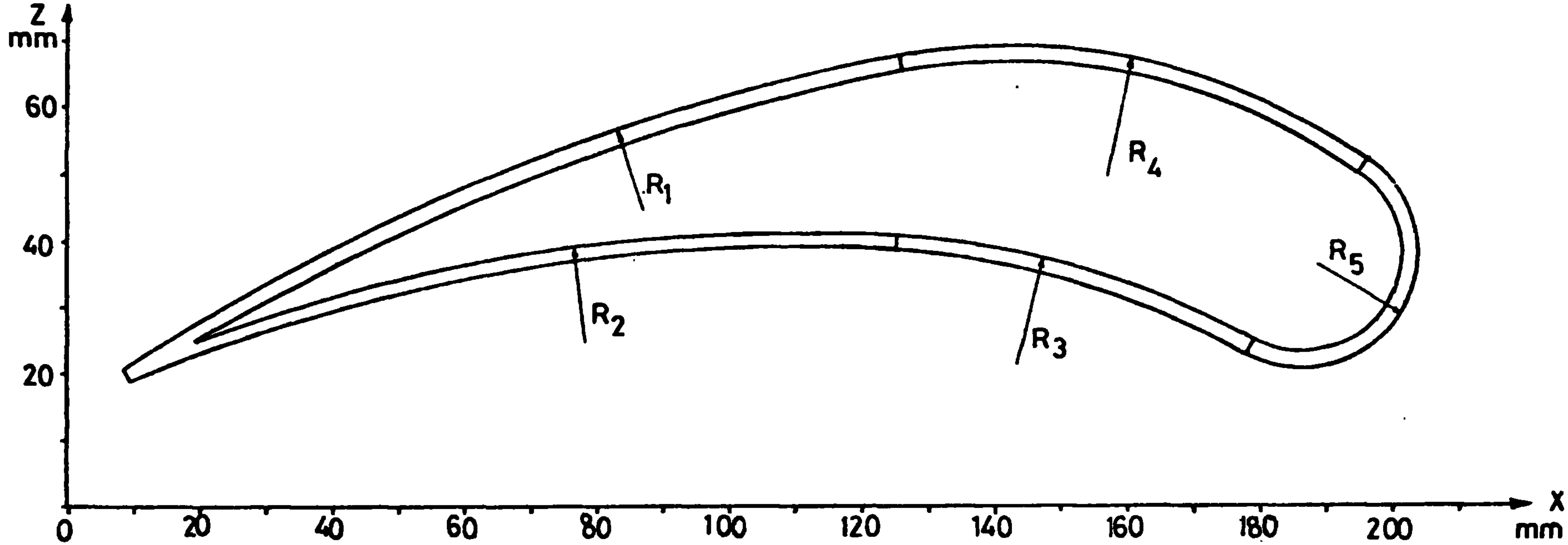

Subscript	Radius R (mm)	Coor. of Centre X (mm)	Z (mm)	Suspends the Arc from α_i^o	to α_f^o
1	331.8	188.5	-257.4	100.9	123.1
2	253.7	109.0	-212.5	86.4	113.5
3	127.0	117.0	-85.6	61.0	86.4
4	91.9	143.0	-22.4	54.6	100.9
5	17.4	186.1	38.2	54.6	-119.0

Figure 6.1. Geometry of the cross-section of the aerofoil blading.

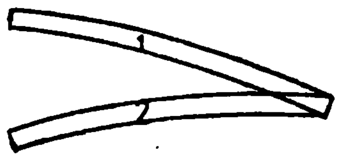

Figure 6.2. Assumed connection of two isoparametric elements at a sharp corner.

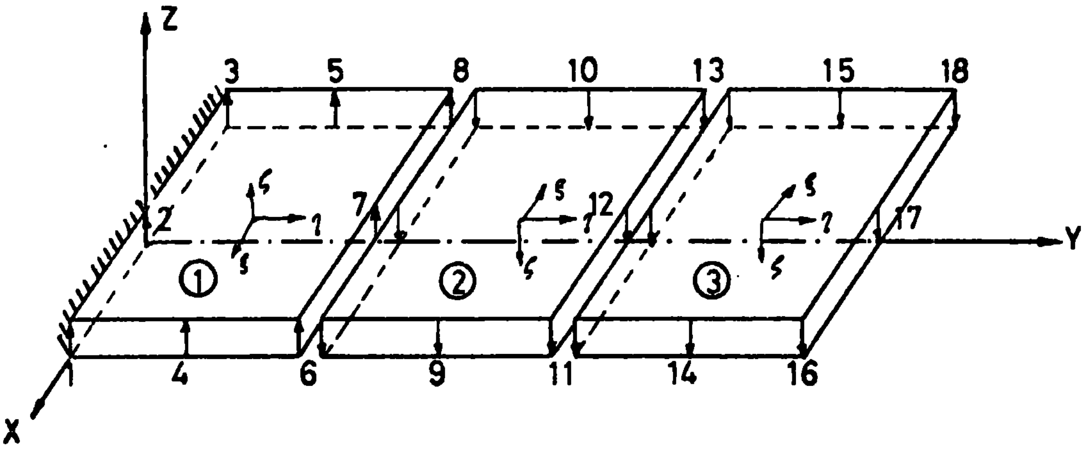

Figure 6.3. Finite element idealization of a rectangular cantilever plate with the thickness vectors mis-matching between elements 1 and 2.

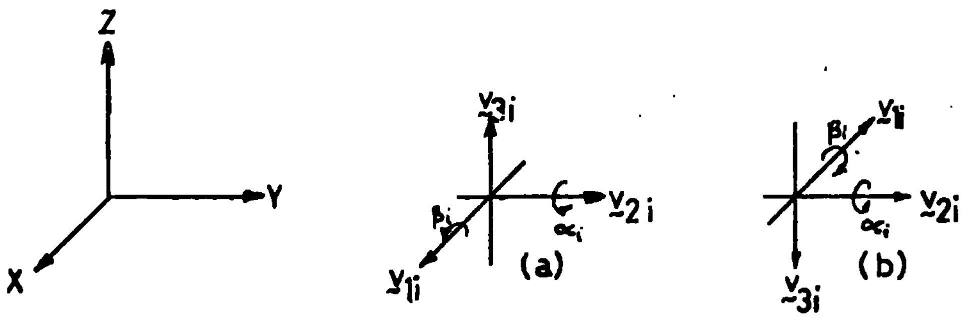

Figure 6.4. Local orthogonal axis and the rotational degrees of freedoms for the elements 1,(a), 2 and 3,(b) of figure 6.3.

6.1.2. V- Shape Cross-Section Cantilever

To assess the validity of the assumption made for the sharp corner connections, the cantilever having the V-shape cross-section, shown on figure 6.5, was studied both experimentally and numerically.

The experimental model was constructed by welding two 200 x 100 x 2.54 mm steel plates together, with an angle of 27° between them. To simulate the clamped boundary condition, it was then welded on a steel block. The determination of the frequencies and the identification of the mode shapes followed the procedure explained in chapter 4.

For the finite element idealization two different meshes, one with two, the other with twelve* elements, were used. The connections of the sharp corner were idealized using both top-to-top and top-to-bottom matching of the thickness vectors. In either assumption the same results were obtained.

The experimental and the numerical results are given on table 6.1. The sketches of some of the typical mode shapes are shown on figure 6.6. The agreement between the results is quite good, and suggests that the assumption made for the sharp corner connections is acceptable.

* This was a uniform mesh with three elements along the length and two across each plate.

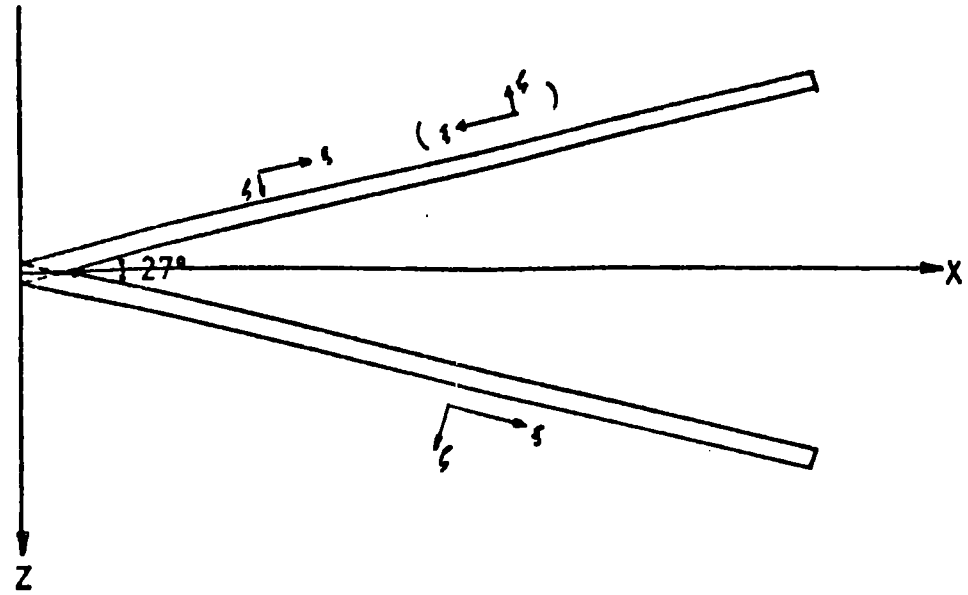

Figure 6.5. Cross section of the cantilever with sharp corner connection.

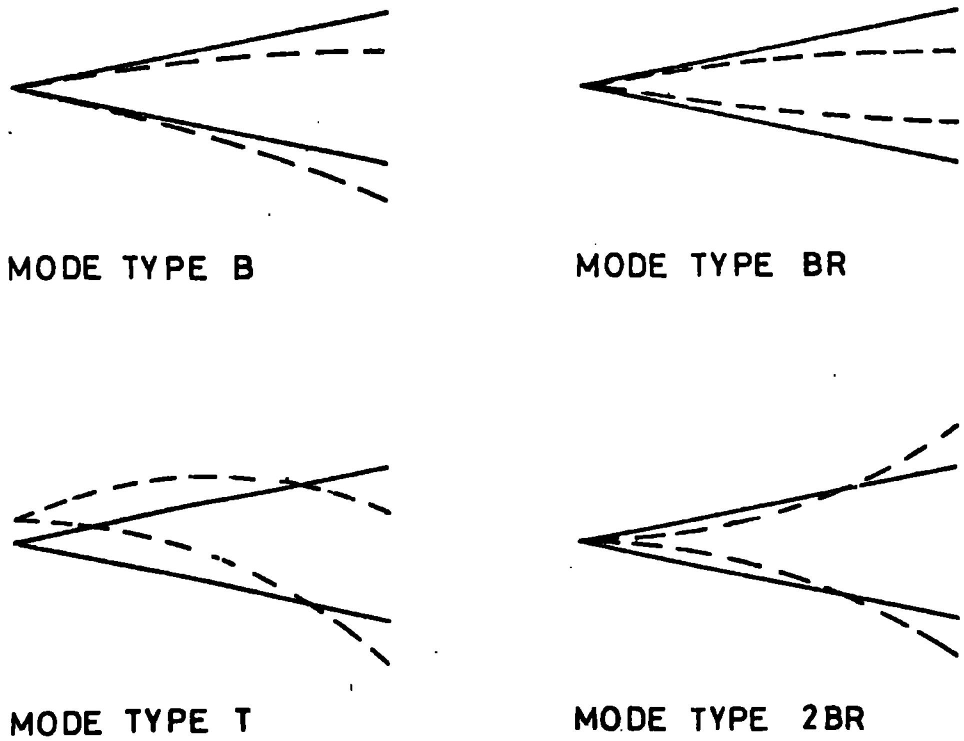

Figure 6.6. Some of the typical mode shapes of the V- cross-section cantilever.

Mode No	Mode Shape	Frequencies (Hz) Experimental	12 Elem.	2 Elem.
1	B/O	130.9	127.1	134.8
2	BR/O	235.0	254.3	304.9
3	B/1	459.3	471.3	545.7
4	BR/1	545.9	616.8	
5	T/O	772.5	822.9	891.1
6	B/2	1065.9	1156.2	
7	BR/2	1128.2	1252.7	
8	2BR/O	1194.4	1357.0	
9	T/1	1284.5	1385.4	

Table 6.1. Comparison of the experimental and numerical frequencies for the V-Shape cross section cantilever. The number given after / in the mode shapes indicates the number of nodal lines parallel to to the root.

6.1.3. Aerofoil Cross-Section Hollow Blading

Sharp corner connection idealization which was studied in the previous section has been applied to two hollow bladings having the aerofoil cross-section shown on figure 6.1. One of the bladings was 400 mm long, shown on figure 6.7, and the other was 200 mm long. Each used a 9x10 mesh.

The first five of the predicted frequencies and the corresponding mode shapes of these blades are given in figures 6.8 and 6.9. The broken lines show the relative displacements of the tip cross-sections. The displacements of a lower cross-section is included if the mode had a nodal line parallel to the base and they are shown by dotted lines. The frequencies given are in Hertz.

The results given in this section are not supported by any experimental analysis, since the foreseen difficulties of manufacturing an experimental model have discouraged any such attempt. Yet, the analyses performed on the individual parts of the structure, like sharp corners, shallow shells or cylindrical segments, have given good results previously. Also, the studies reported in Section 6.4 where the analysis of a hollow turbine blade with a similar geometry gave very good results, imply that the results presented here should be reliable.

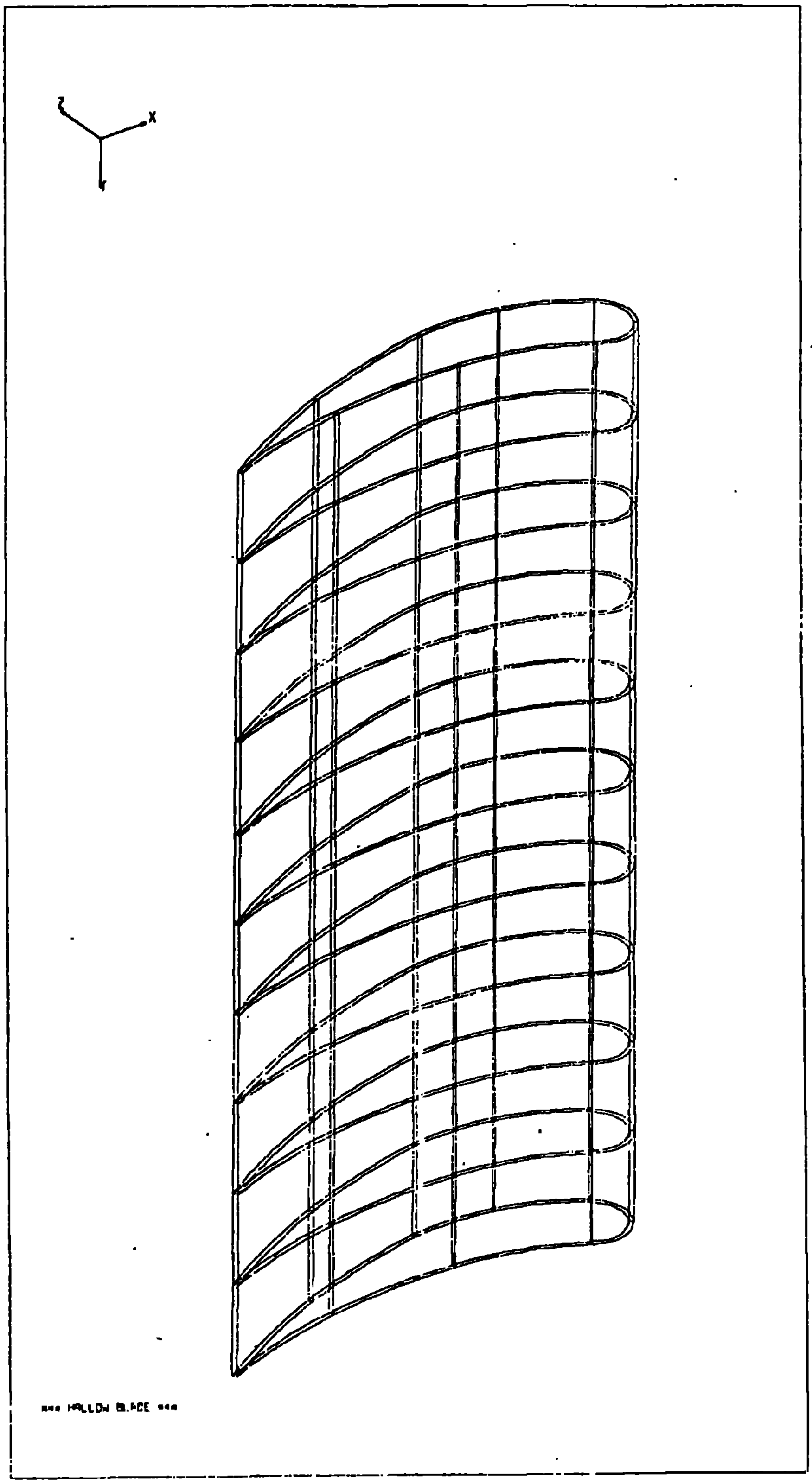

Figure 6.7. Finite element idealization of the 0.4 m long aerofoil cross-section hollow blading.

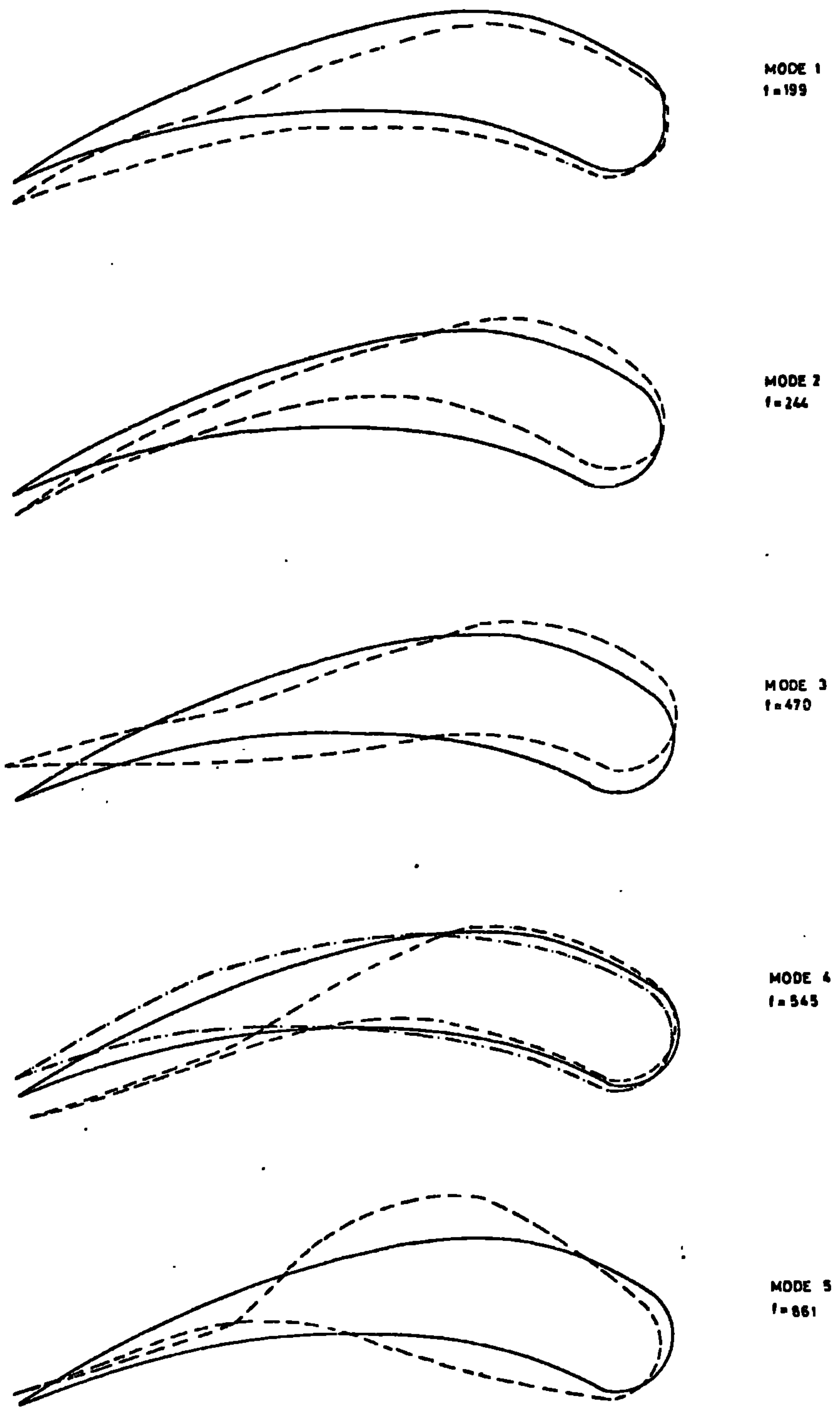

Figure 6.8. First five mode shapes and the corresponding frequencies of the 0.4 m long hollow blading.

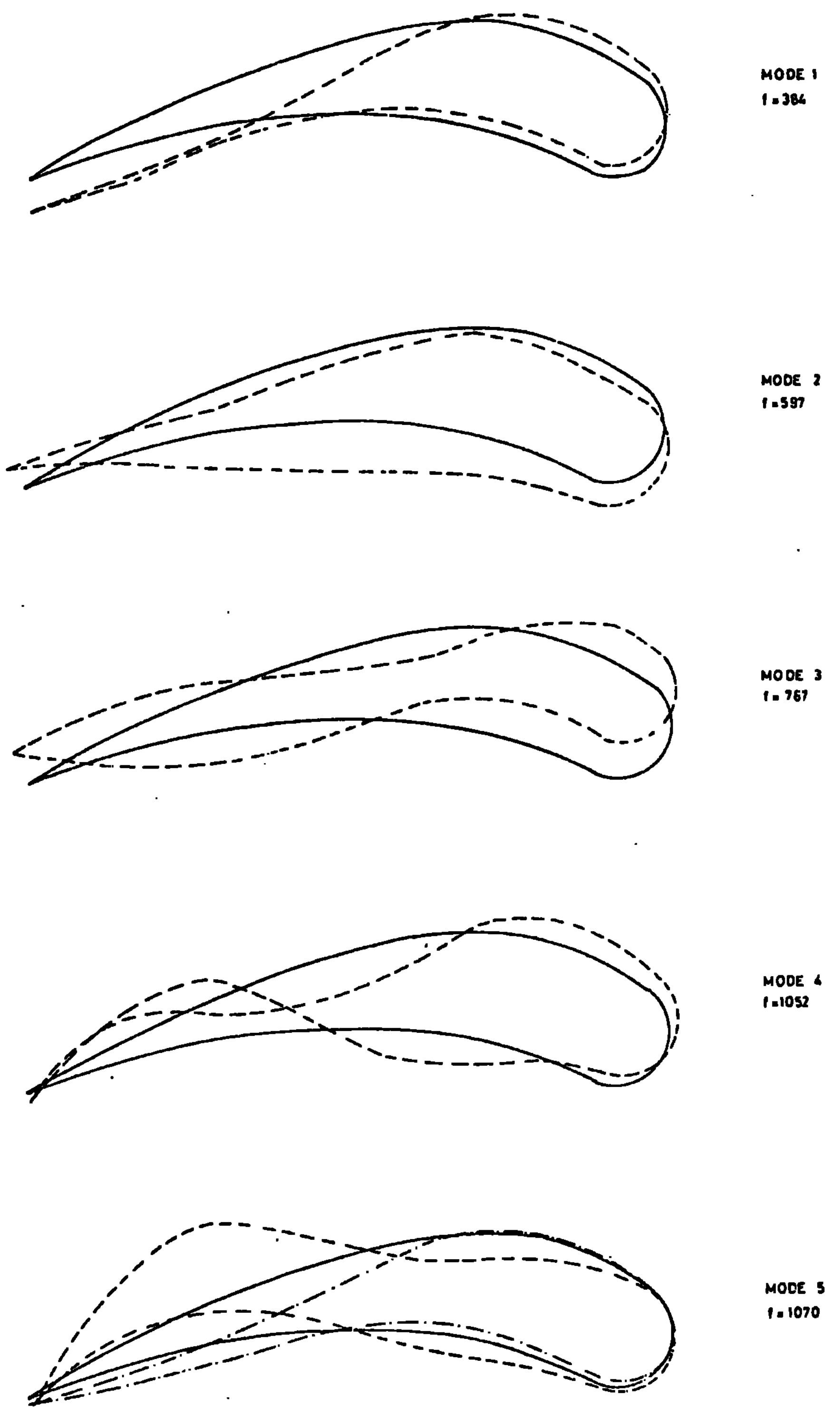

Figure 6.9. First five mode shapes and the corresponding frequencies of the 0.2 m long hollow blading

6.2. Stiffeners

The stiffeners that may be used in a hollow blading are approximated by massless rods connecting the nodes as shown on figure 6.10. The rods are assumed to carry only the axial forces. Thus they have only three degrees of freedom at each end and they do not create any problem in the assembly process.

The configuration shown on figure 6.10 was solved with and without stiffeners. The effect of the stiffeners was to suppress the modes which require the relative displacements of the opposite faces. The frequencies corresponding to other modes were identical for both cases.

The only apparent difference was seen at mode 6 (see figures A.32 and A.33), where two modes were coupling. The frequencies corresponding to this mode for the non-stiffened case were 809 Hz and 879 Hz. With the stiffeners the mode became pure in-plane bending with a frequency equal to 866 Hz

6.3. Effect of Pretwist

In section 3.3, the program was used to calculate the natural frequencies of a pretwisted plate, and good results were obtained. In this section, the effect of the pretwist on the natural frequencies and the mode shapes of oval and aerofoil cross-section blades have been considered. The analysis was performed only numerically, and the results still require experimental verification.

Figure 6.10. Hollow Blading with Stiffeners.

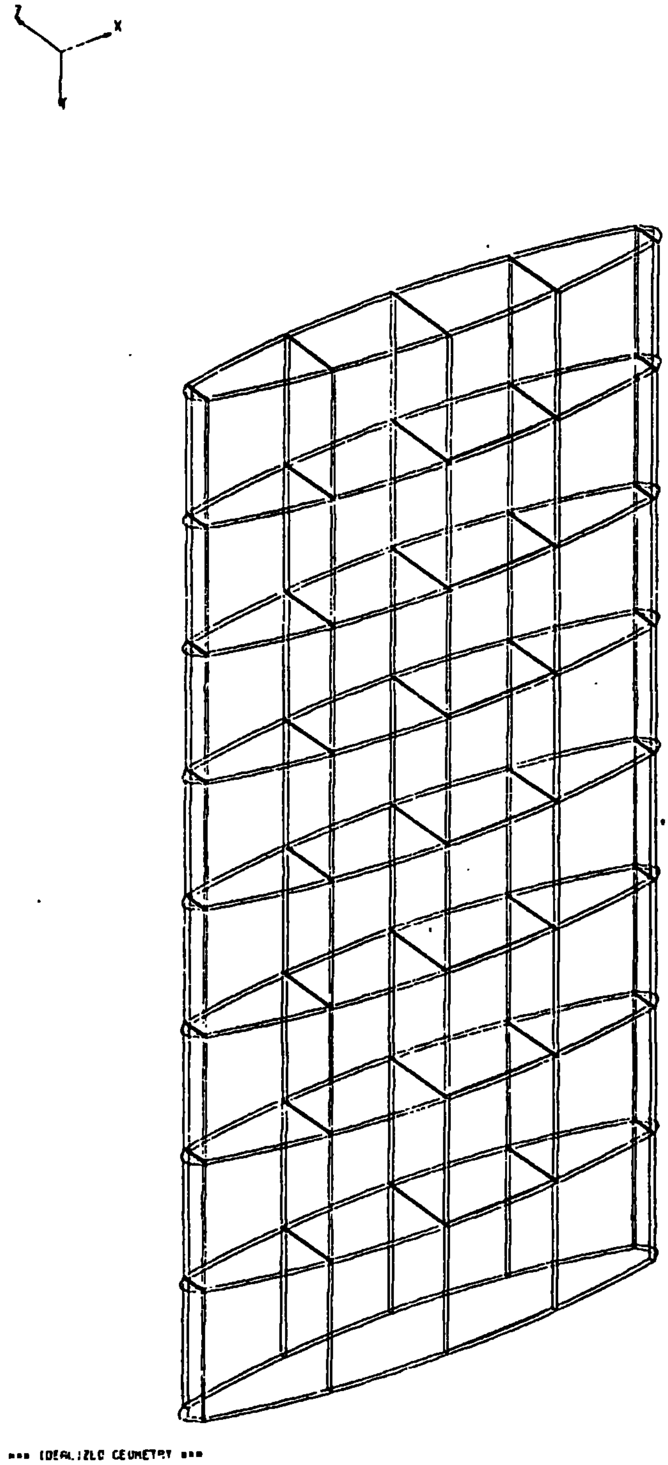

6.3.1. Pretwisted Oval Blading

The oval cross-section blading having the idealized geometry described in Section 5.2.2. was assumed to be twisted linearly about the centroid of its cross-section up to an angle of 60 degrees. The results are presented on figure 6.11 as graphs of natural frequencies in Hz , plotted against the pretwist angle.

The numbers next to each line correspond to the mode number, for the non-twisted blade, as shown on figure A.3.3.

The mode shapes were much influenced by the pretwist. Coupling took place between several modes, and this made it difficult, especially for higher frequencies, to decide the origin of the contributing modes. All frequencies but one, increased with increasing pretwist angle. In some modes the increase was preceded by a slight decline of frequencies at the beginning. In order to reduce the effect of coupling, the same problem was also solved with the stiffeners fitted between the faces. The results are shown with dotted lines on figure 6.11.

The rapid increase of the frequencies was suspected to be due to the stiffening of the deformed elements and this possibility is discussed in section 6.3.3.

6.3.2. Pretwisted Aerofoil Blading

An analysis, similar to the previous one was performed for the aerofoil blading of section 6.1.3. The mode shapes were effected by pretwist even more than the oval blading.

Only two of the modes were identified relatively easily through different pretwist angles, and they are plotted on figure 6.12. This time a rapid decrease of the frequencies was observed. Since a relatively fine mesh was used, the possibility of not being able to inegrate the stiffness terms properly due to the reduced integration order (30) seems to be unlikely.

6.3.3. Pretwisted Cylinder

In order to see the effect of the distortions of the elements on the natural frequencies, the cylinder of section 3.5 was reanalysed by assuming different pretwist angles. It was observed that the frequencies corresponding to the simple modes, like bending and torsion, were totally unaffected by the amount of pretwist assumed. For more complex mode shapes some stiffening was observed in the elements, increasing with the complexity of the mode in consideration.

The mode shapes, with a large number of nodal lines and circles, of a circular cylinder are unsuitable to be reproduced by isoparametric shell elements. The difficulty comes from the assumed displacement functions being relatively simple compared with the mode shapes. In order to reproduce a figure similar to the mode shape with the mathematical model, the elements have to be over strained. As a result, the elements become overstiff for certain modes, and to be able to obtain accurate results, one has to use a very fine mesh. When the elements are distorted due to the pretwist, the shape that the elements have to take, in order to describe a mode shape, becomes even

Figure 6.11. Frequencies of oval cross-section blade as function of the pretwist angle.

Broken lines show the coupling modes. Dotted lines are the results with the stiffeners. B/X stands for bending in X direction.

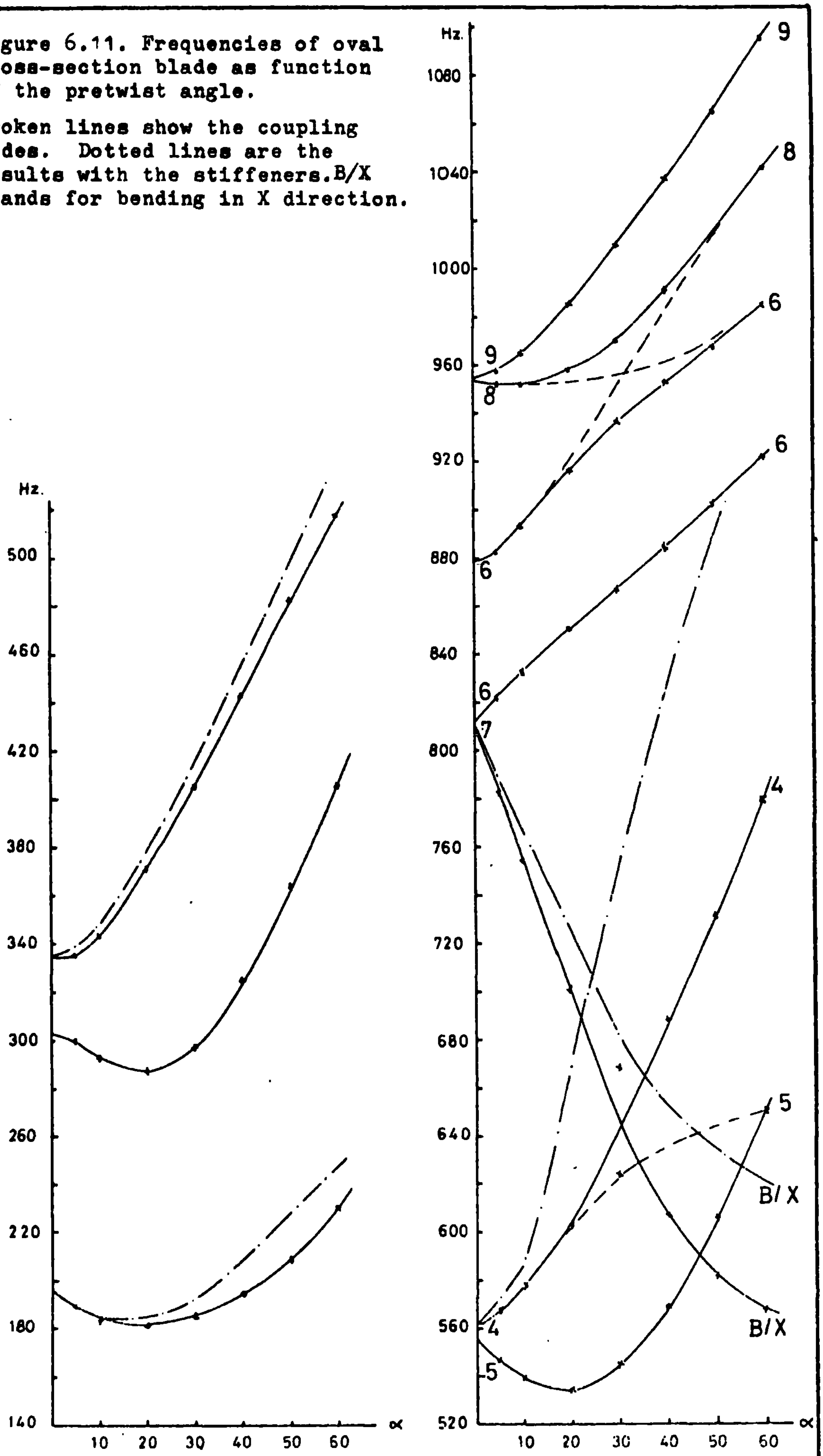

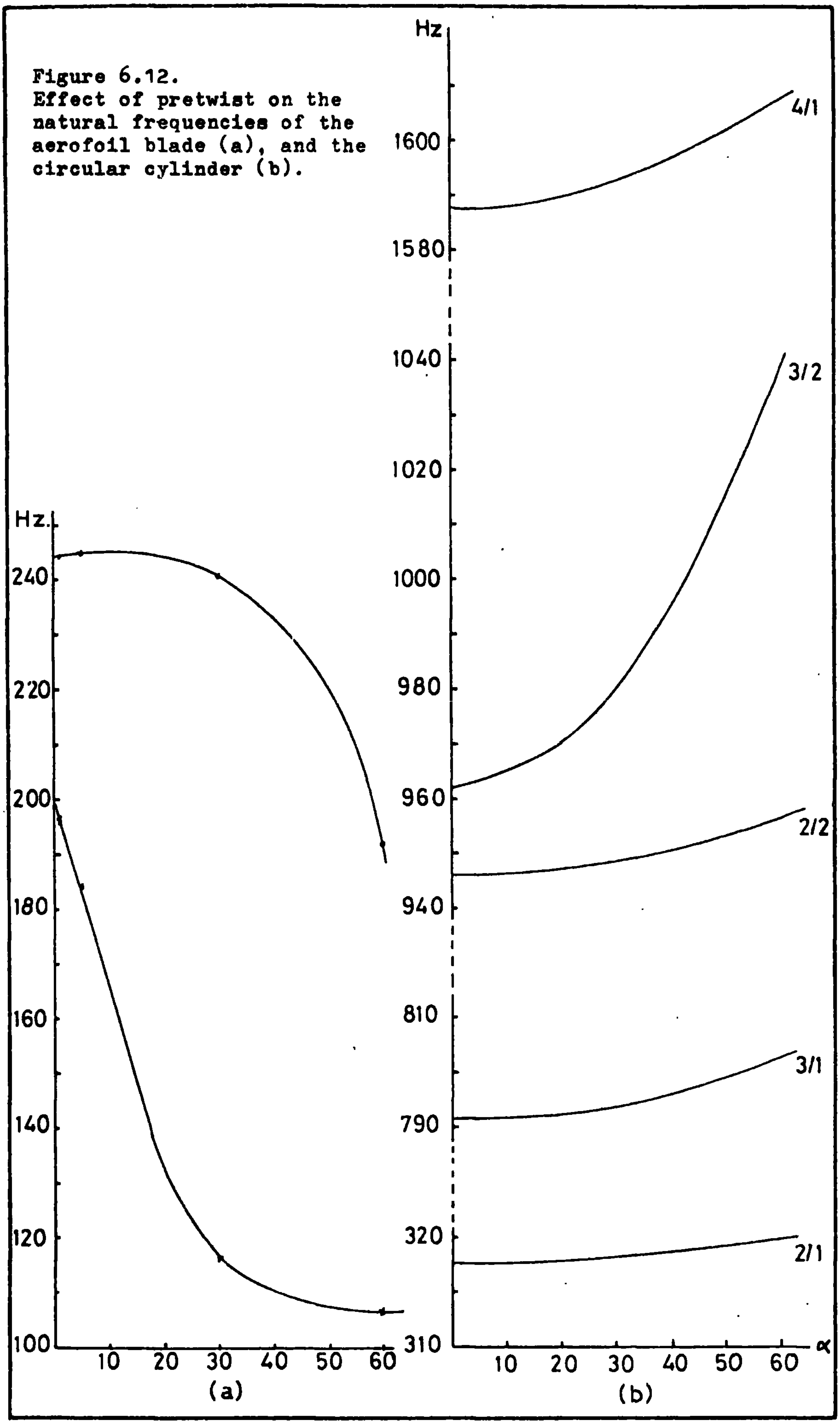

Figure 6.12.
Effect of pretwist on the natural frequencies of the aerofoil blade (a), and the circular cylinder (b).

more complicated. So in fact one should expect the stiffening of the elements with the increasing angle of pretwist. The fact that the bending and torsion modes are unaffected by the pretwist should again be expected because of the regularity of the displacements of indicidual nodes.

It is clear, from figure 6.12 (b), that the effect of the distortions of the elements on the natural frequencies of simpler modes is very small. The largest difference is only 8% and it corresponds to the mode 3/2. The changes in all the other frequencies are well under 1.5%.

Figure 6.13 shows the computer plotting of the cylinder which was twisted 60 degrees. Figure 6.14 shows the oval blading again with 60 degrees of pretwist angle. The meshes shown are the meshes used in calculations. A close examination of the two figures give the impression that the elements of the oval blading are not distorted as much as the elements of the cylinder. Also, a review of the mode shapes, shown on figure A.3.3, shows that they are much simpler in the sense of the relative displacements of the nodes, than the mode shapes of a cylinder.

As a result of this discussion it may be said that the stiffening of the elements should effect the results of the pretwisted oval blading less than it does the results of the pretwisted cylinder. Still, the lack of a convincing explanation for the common trend of some of the lines in figure 6.11 - i.e. a negative slope followed by a sharp increase - and the lack of any experimental confirmation make it necessary that care should be taken in accepting the results, especially for large pretwist angles, and complicated mode shapes.

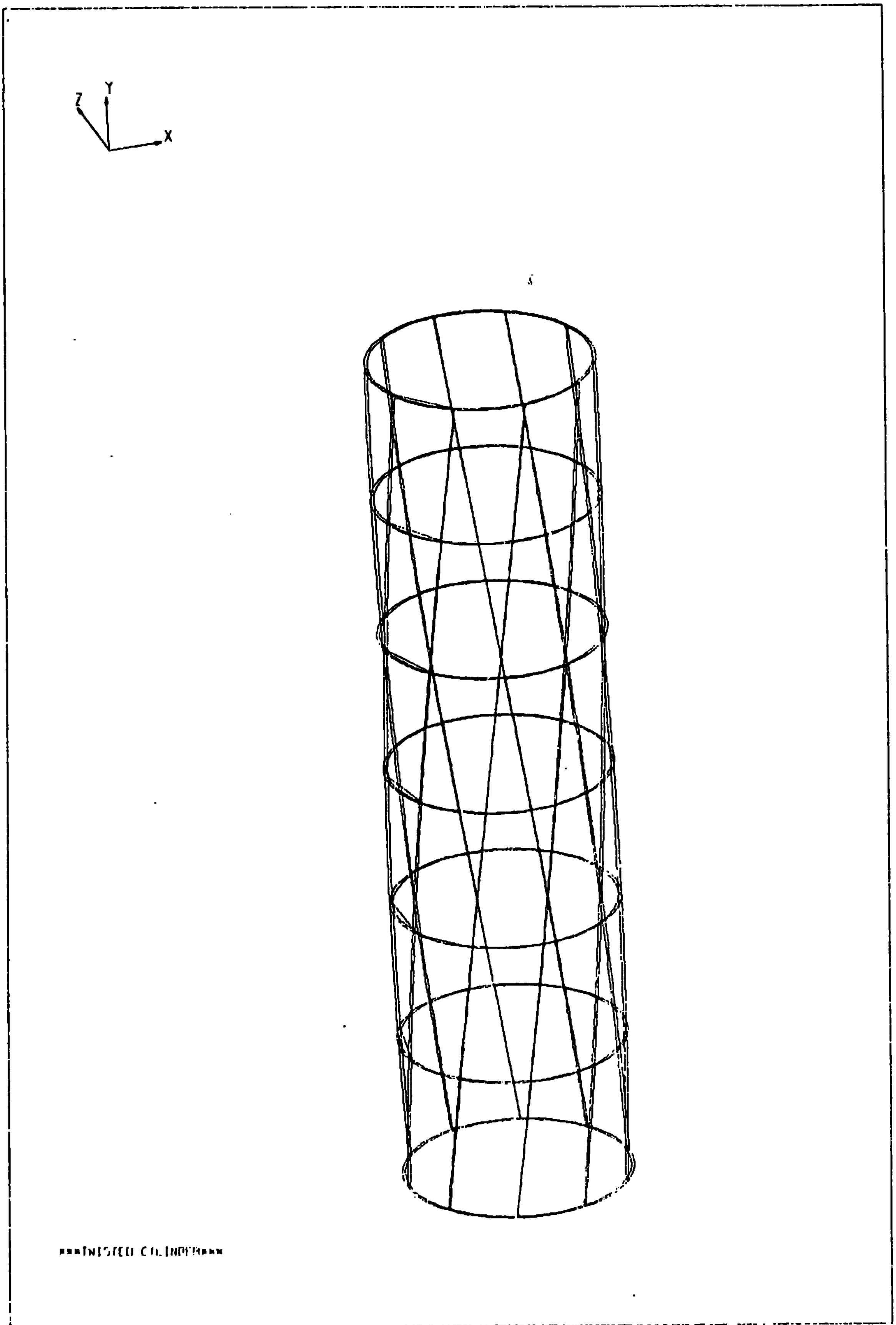

Figure 6.13. Finite element idealization of the cylinder with 60° of pretwist angle.

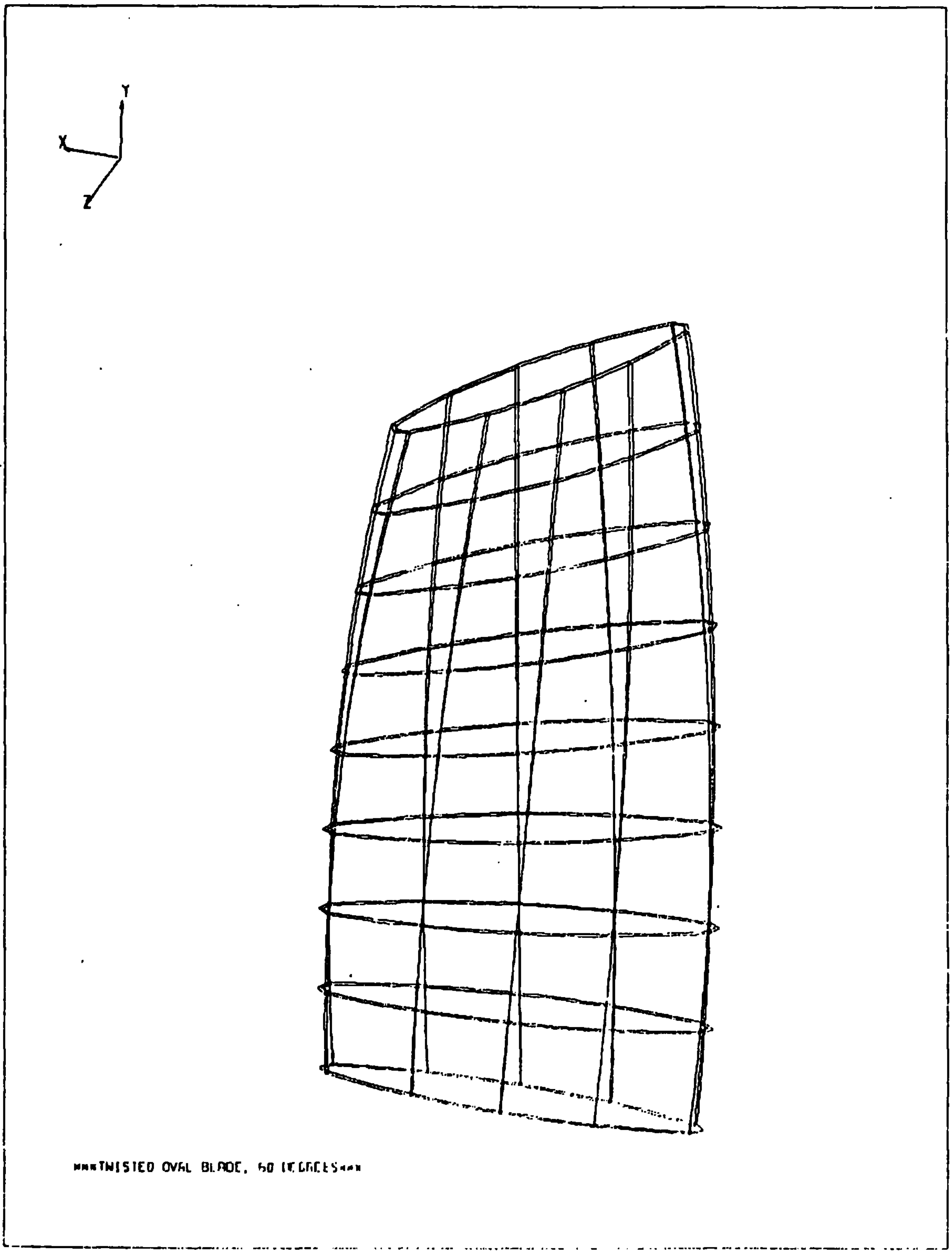

Figure 6.14. Finite element idealization of oval blading with 60° of pretwist angle.

6.4. A Real Turbine Blade

The final excercise was performed on a real hollow turbine blade (supplied by G.E.C.).

The experimental analysis of this blade was done by G.E.C. They encased the root of the blade in lead alloy surrounded by a large mass of cast iron. The method of excitation was electro-mechanical. The natural modes of vibration, between the frequency limits of 0-6 kHz were reported.

For the finite element analysis of the blade the idealization shown on figure 6.15 was used. Nodal coordinates for this idealization were determined by taking direct measurements on the blade. With these measurements it was possible to determine the geometry of the blade only approximately. In the idealization two sharp connections were used, and they were approximated as discussed in section 6.1. The root of the blade was assumed to be clamped at the platform level. The mesh contained 40 elements with 600 degrees of freedoms, 160 of them were retained as masters.

The frequencies and the mode shapes obtained from the finite element analysis are given on figures 6.16 - 6.19, together with the matching experimental results. The positive and negative signs on the figures indicate the transverse displacements of the faces, and "s" shows the stationary regions. The sketches on the left show the pressure side, and those on the right show the suction side. Plottings of the tip and the middle cross section displacements are included in appendix 4.

In spite of the difference between the root fixing of the experimental and the finite element models excellent agreement was obtained for most of the modes. First tortional mode was found to be exactly the same in both analysis. Results for the second mode were very close. Third mode did not exactly meet the experimental mode shape where the areas indicated with negative sign were much lower along the blade length. The big difference seen between the frequencies of the fourth mode was possibly due to the different assumptions of root fixing. Fifth and eighth modes are again in very good agreement both mode shape and frequencywise. Modes seven and twelve show slight differences from the experimental mode shapes. Modes 6,9,10 and 11 have not been detected during the experiments, and one experimental mode found at 3005 Hz was not encountered in finite element analysis.

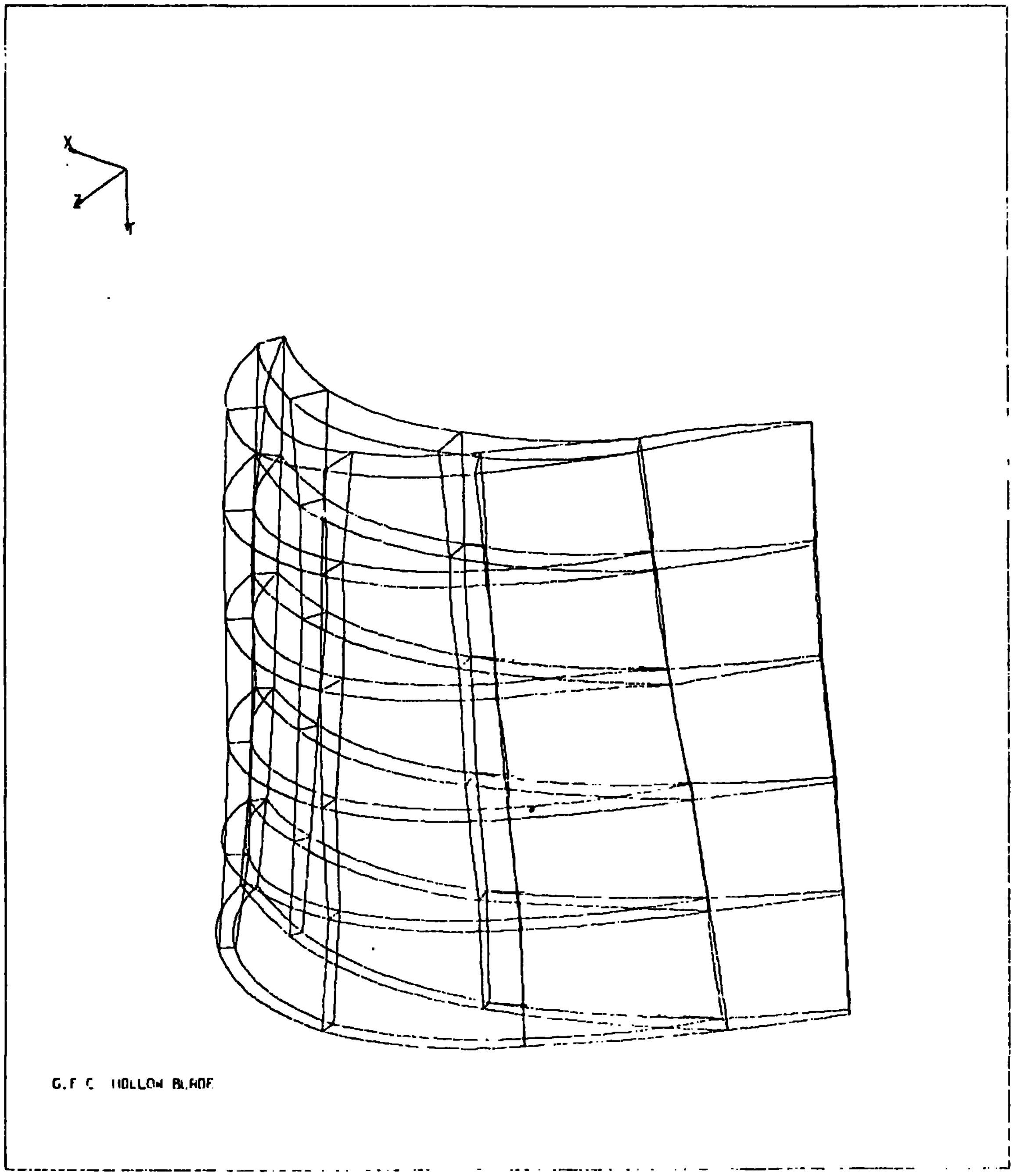

Figure 6.15. Finite element representation of the hollow Turbine Blade.

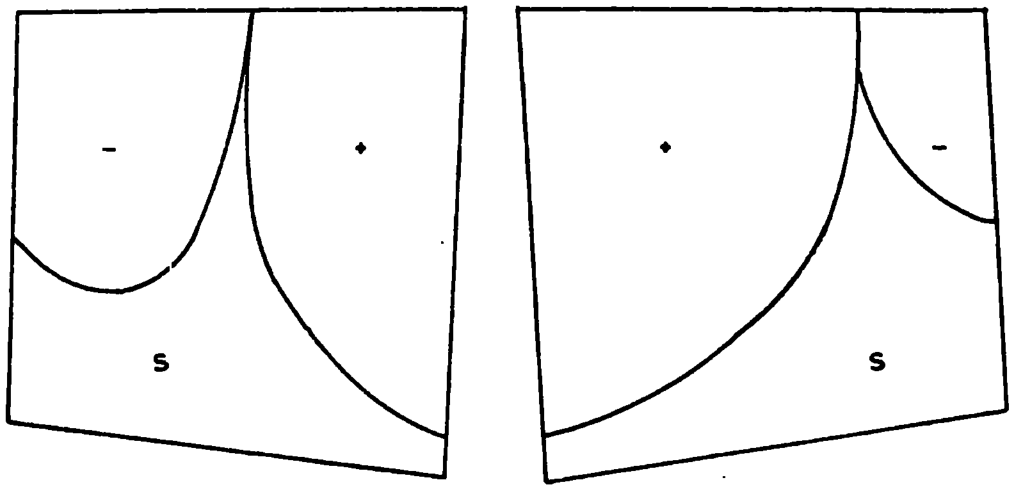

Mode 1 FE: 1064 EX: 1064

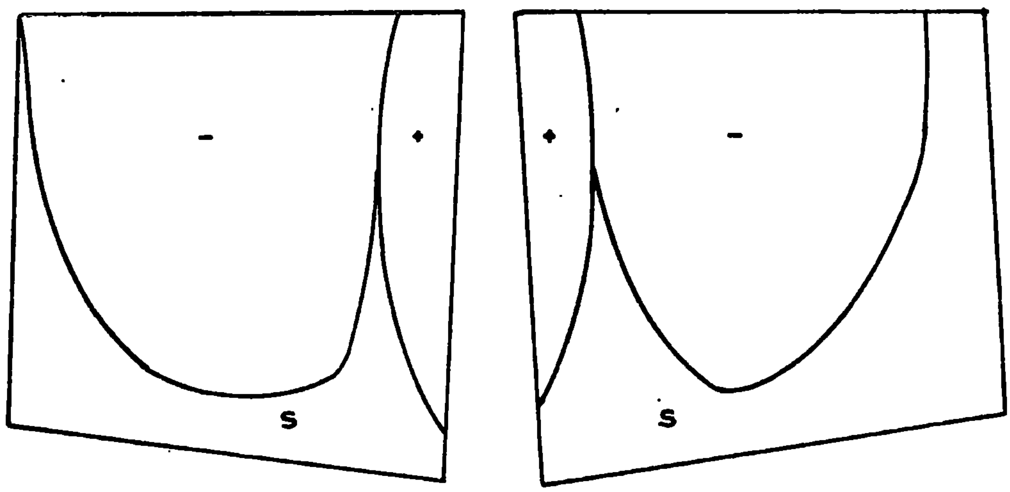

Mode 2 FE: 1713 EX: 1717

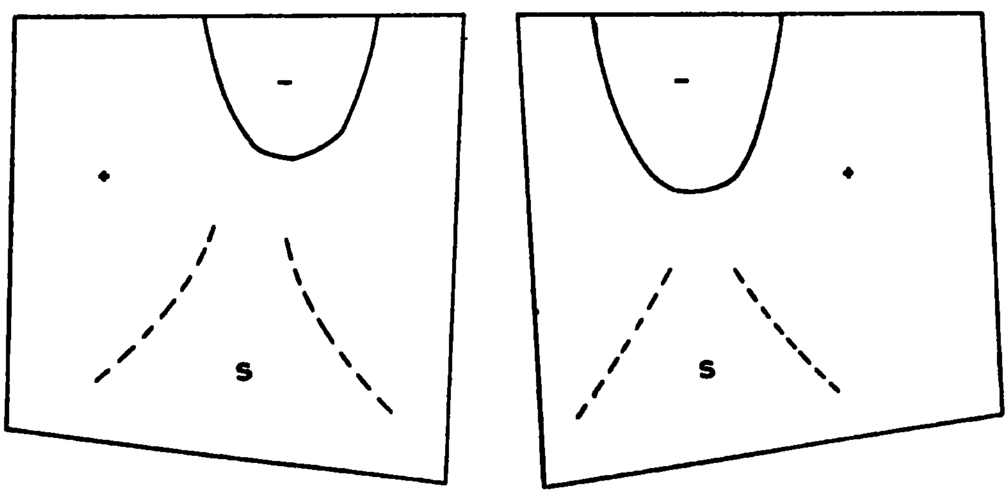

Mode 3 FE: 1915 EX: 1875

Figure 6.16. Mode shapes and the natural frequencies of the hollow turbine blade.

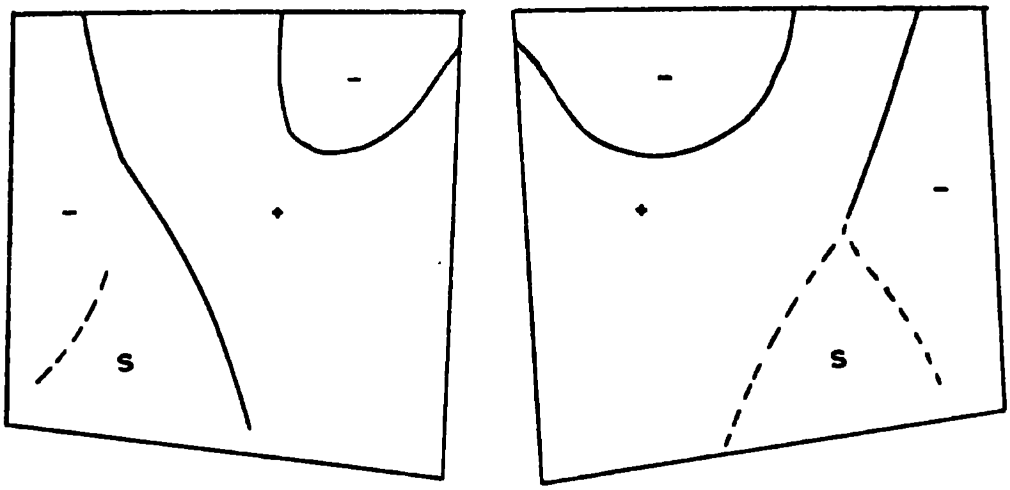

Mode 4 FE: 2787 EX: 1533

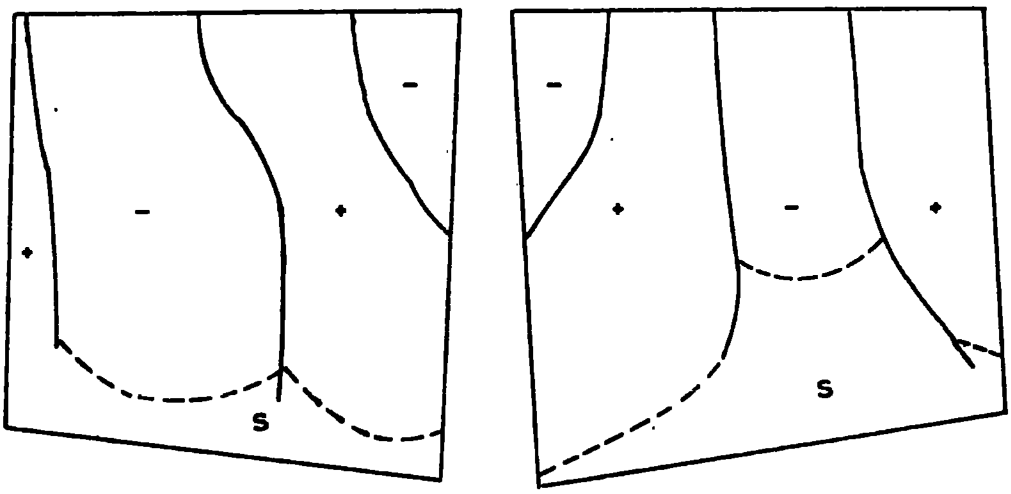

Mode 5 FE: 3310 EX: 3274

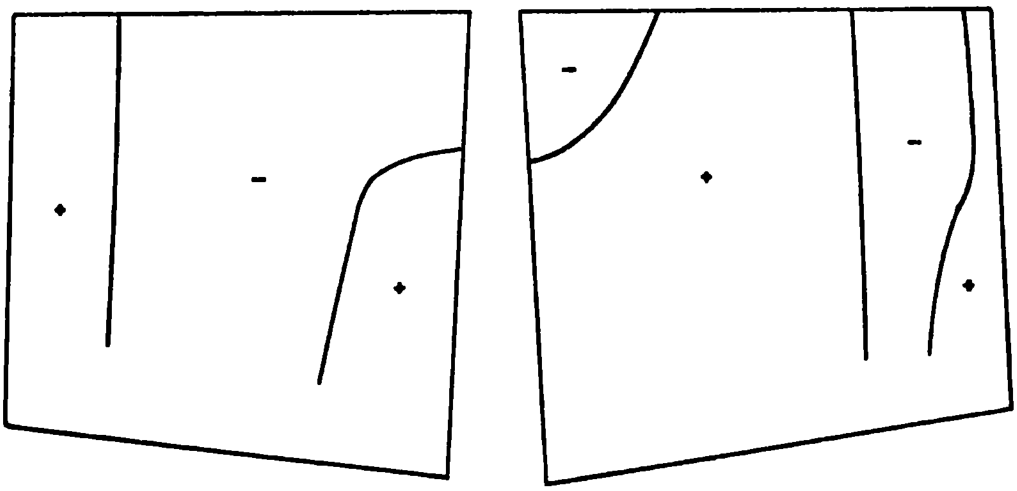

Mode 6 FE: 3864

Figure 6.17. Mode shapes and natural frequencies of the hollow turbine blade .

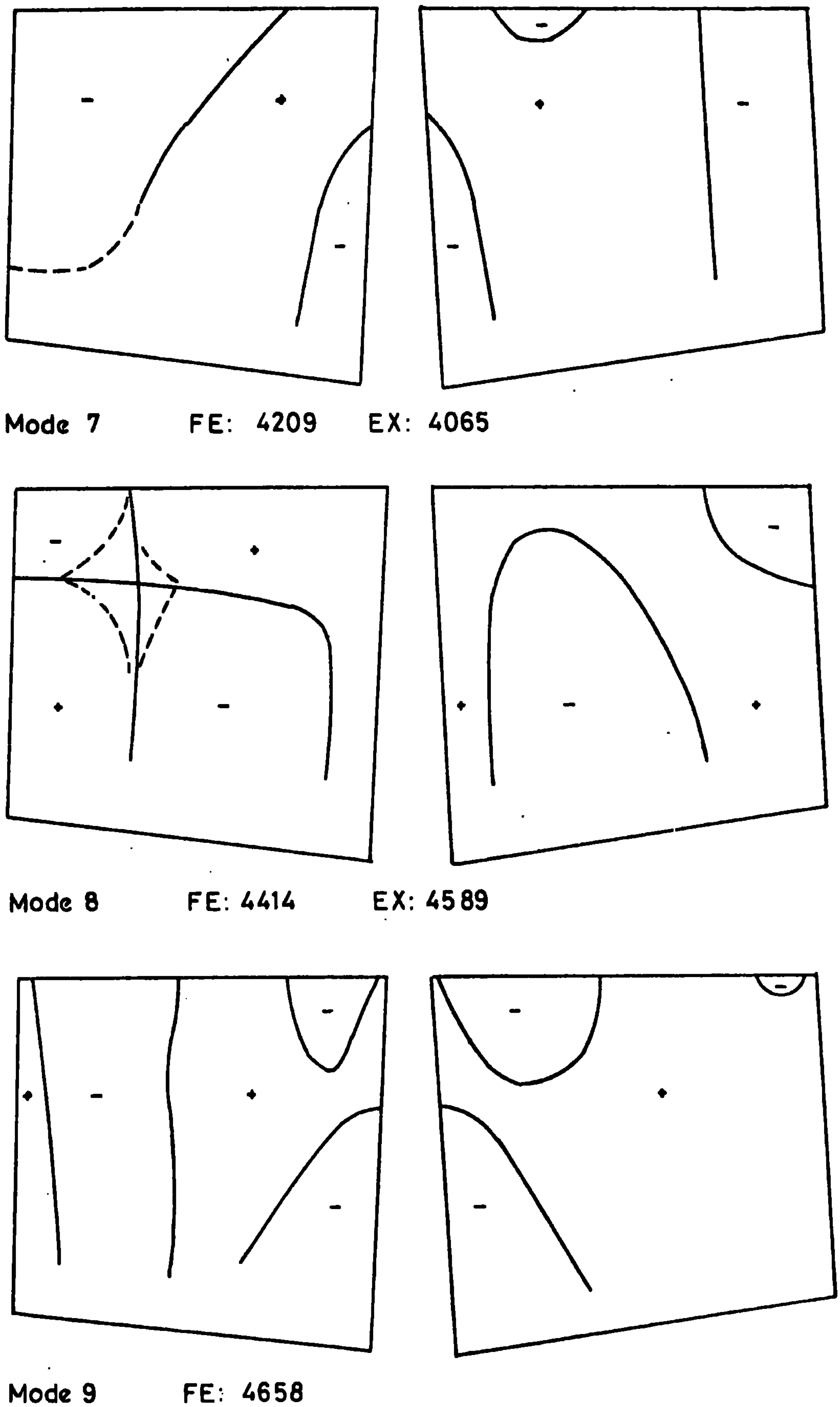

Figure 6.18. Mode shapes and the natural frequencies of the hollow turbine blade.

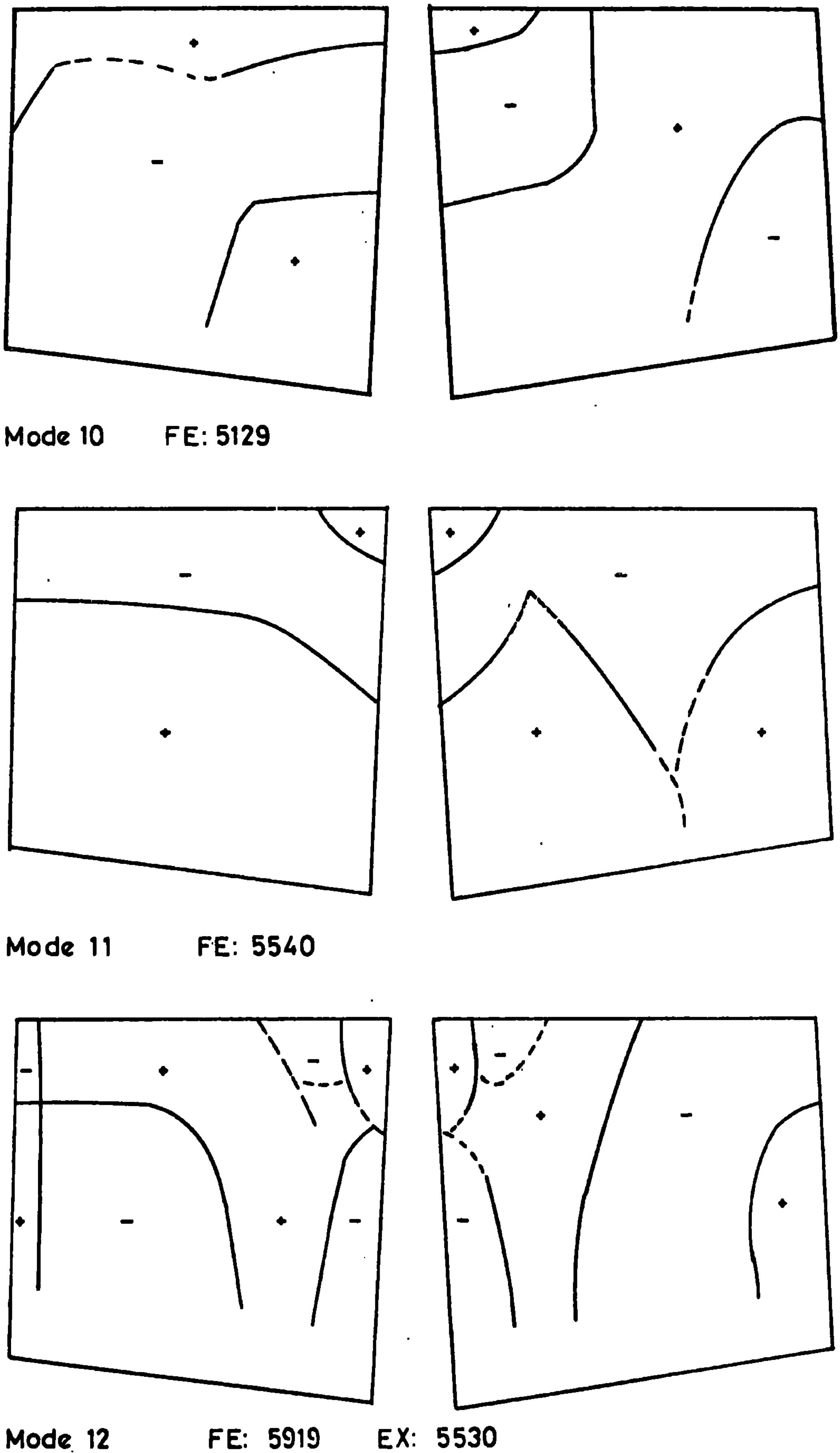

Figure 6.19. Mode shapes and the natural frequencies of the hollow turbine blade.

CHAPTER 7

7. CONCLUSIONS

A numerical and experimental study of the vibrations of arbitrary shell structures is presented. In particular, closed, non-circular cylindrical cantilever shells have been studied, as a preliminary step towards the understanding of the dynamical behaviour of hollow bladings.

Finite element method was employed for the numerical analysis, and a computer program based on the isoparametric thick-shell element has been developed. At the beginning, the element was inefficient in representing sharp curvatures. Later, improved efficiency was achieved by increased the order of integration and with the help of the additional nodes inserted along the curvature. Some assumptions were suggested to represent the sharp corners and multiple junctions in the structure. As a result, the program has become applicable to a large range of vibration problems. It has been used to solve the problems of uniform and variable thickness plates, pretwisted plates and shells, axi-symmetric and non-axisymmetric cylinders, shallow shells and hollow bladings. The results obtained agreed very well with the available experimental and theoretical results of other researchers.

The imperfect geometry of the experimental model of the oval blade was an inevitable result of the difficulties encountered during manufacturing. In spite of that the experimental results agreed reasonably well with the finite element predictions. The difference between the results was within 5 per cent for most of the lower modes. Sensitivity of some of the modes to the geometry and the boundary conditions was observed and the difference in the results for these modes was within 11 per cent.

Experiments have shown that by embedding the blade into a solder base, it is not possible to achieve a root fixing which is stiff enough to simulate the clamped boundary condition. A similar observation was made for brazing which was found to be too flexible to join the components of the oval blading together. Welding, on the other hand, provided stiffer joints both for connecting the components and for fixing the root.

Further experiments with a better experimental model would be interesting to perform for pretwisted and stiffened oval blading.

The method and element used proved to be satisfactory for the dynamic analysis of arbitrary shell structures. The program is well tested and reliable.

REFERENCES

(1) Ahmad, S., "Curved Finite Elements in the Analysis of Solid, Shell and Plate Structures". Ph. D. Thesis, University College of Swansea, 1969.

(2) Ahmad, S., Anderson, R.G., Zienkiewicz, O.C., "Vibration of Thick Curved Shells, with Particular Reference to Turbine Blades". J. Strain Analysis, Vol. 5, No. 3, 1970

(3) Ahmad, S., Irons, B.M., Zienkiewicz, O.C., "Curved Thick Shell and Membrane Elements with Particular Reference to Axisymmetric Problems". Proc. 2nd Conf. on Matrix Meth. in Structural Mech. AFFDL-TR-68-150, part 1 of 2, pp.539-572 1968

(4) Ahmad, S., Irons, B.M., Zienkiewicz, O.C., "Analysis of Thick and Thin Shell Structures by Curved Finite Elements". Int. J. Num. Meth. Eng., Vol. 2, pp. 419-451, 1970.

(5) Anderson, R.G., Irons, B.M., Zienkiewicz, O.C., "Vibration and Stability of Plates Using Finite Elements". Int. J. Solids Structures, Vol.4. pp. 1031 - 1055, 1968.

(6) Appa, K., Smith, G.C.C., Hughes, J.T., "Rational Reduction of Large-Scale Eigenvalue Problems". AIAA. J., Vol.10, No.7, pp. 964-965, 1972.

(7) Barth, W., Martin, R.S., Wilkinson, J.H., "Calculation of the Eigenvalues of a Symmetric Tridiagonal Matrix by the Method of Bisection". Numerische Mathematik, Vol.9, pp. 386-393, 1967

(8) Barton, M.V., "Vibration of Rectangular and Skew Cantilever Plates". J. Applied Mechanics, Vol.18, pp.129 - 134, 1951.

(9) Bossak, M.A.J., Zienkiewicz, O.C., "Free Vibration of Initially Stressed Solids, with particular reference to centrifugal-force Effects in Rotating Machinery". J.Strain Analysis, Vol. 8, No. 4, pp. 245 - 252, 1973.

(10) Brebbia, C.A., Connor, J.J., "Fundamentals of Finite Element Techniques". Butterworth & Co. Ltd., 1973.

(11) Bridle, M.D.J., "Vibration of Thick Plates and Shells". Ph. D. Thesis, University of Nottingham, 1973.

(12) Cantin, G., Clough, R.W., "A Curved, Cylindrical-Shell, Finite Element". AIAA.J., Vol. 6, pp. 1057-1062, 1968.

(13) Carnegie, W., "Vibrations of Pre-twisted Cantilever Blading". Proc. Inst. of Mech. Eng., Vol.173, No.12, pp 343-374, 1959.

(14) Cheung, Y.K., Cheung, M.S., "Vibration Analysis of Cylindrical Panels". J. Sound Vib., Vol.22 (1), pp 59-73, 1972.

(15) Clough, R.W., Johnson, C.P., "A Finite Element Approximation for the Analysis of Thin Shells". Int. J. Solids Structures, Vol.4, pp.43-60, 1968.

(16) Clough, R.W., Johnson, C.P., "Finite Element Analysis of Arbitrary Thin Shells". ACI publication SP-28, Concrete Thin Shells, pp.333-363, 1971.

(17) Connor, J.J., Brebbia, C.A., "Stiffness Matrix for Shallow Rectangular Shell Element", Proc. ASCE, Vol. 93, EM5, pp. 43-65, 1967.

(18) Cowper, G.R., Lindberg, G.M., Olson, M.D., "A Shallow Shell Finite Element of Triangular Shape". Int. J. Solids Structures, Vol.6, pp.1133-1156, 1970.

(19) Desai, C.S., Abel, J.F., "Introduction to the Finite Element Method". Van Nostrand Reinhold Co., 1972.

(20) Doherty, W.P., Wilson, E.L., Taylor, R.L., "Stress Analysis of Axisymmetric Solids Utilizing Higher-order Quadrilateral Finite Elements". Structural Engineering Lab. Report No.69-3, Univ. of California, Berkeley, 1970.

(21) Dungar, R., Severn, R.T., Taylor, P.R., "Vibration of Plate and Shell Structures Using Triangular Finite Elements". J. Strain Analysis, Vol. 2, No.1, pp 73-83, 1967.

(22) Dunne, P.C., "Complete Polynomial Displacement Fields for Finite Element Method". The Aeronautical Journal of the Royal Aeronautical Society, Vol.72, pp.245-246, 1968.

(23) Dunne, P.C., "Comments on Complete Ploynomial Displacement Fields for Finite Element Method". The Aeronautical Journal of the Royal Aeronautical Society, Vol.72.pp.709-710, 1968.

(24) Ergatoudis, I., Irons, B.M., Zienkiewicz, O.C., "Curved, Isoparametric, Quadrilateral Elements for Finite Element Analysis". Int. J.Solids Structures, Vol.4, pp. 31-42, 1968.

(25) Gallagher, R.H., "Shell Elements". World Cong.on Finite Elem. Meth. in Structural Mech., Bournemouth, Dorset, Vol.1., pp E.1 - E.35, 1975.

(26) Gallagher, R.H., "Problems and Progress in Thin Shell Finite Element Analysis". Finite Elements for Thin Shells and Curved Members, Edited by D.G. Ashwell and R.H. Gallagher, John Wiley & Sons, pp. 1-14, 1976.

(27) Gill, P.A.T., "Vibrations of Clamped-free Circular Cylindrical Shells", J. Soumd Vib. Vol. 25 (3), pp.501-503, 1972.

(28) Guyan, R.J., "Reduction of Stiffness and Mass Matrices". AIAA. J., Vol.3, No.2, p.380, 1965

(29) Henshell, R.D., Ong, J.H., "Automatic Masters for Eigenvalue Economization". Earthquake Engineering and Structural Dynamics, Vol.3, pp375-383,1975

(30) Hofmeister, L.D., Evensen, D.A., "Vibration Problems Using Isoparametric Shell Elements". Int.J.Num. Meth. Eng. Vol.5, pp.142-145, 1972.

(31) Irons, B.M., "Eigenvalue Economisers in Vibration Problems". Journal of the Royal Aeronautical Society, Vol. 67, pp. 526-528, 1963.

(32) Irons, B.M., "Structural Eigenvalue Problems: Elimination of Unwanted Variables". AIAA. J. Vol.3, No.5 pp. 961-962, 1965.

(33) Irons, B.M., "Engineering Applications of Numerical Integration in Stiffness Methods". AIAA. J. Vol.4, No.11, pp. 2035-2037, 1966.

(34) Irons, B.M., "Finite Element Techniques in Structural Mechanics, Discussions". H. Tottenham and C. Brebbia (Eds.), Southampton University Press, pp. 328 - 331, 1970.

(35) Irons, B.M., "Quadrature Rules for Brick Based Finite Elements", Int. J. Num. Meth. Eng. Vol.3. pp. 293-294, 1971.

(36) Irons, B.M., Razzaque, A., "A Further Modification to Ahmad's Shell Element". Int. J. Num. Meth. Eng., Vol. 5, pp.588-589, 1972-73.

(37) Jones, R.E., Strome, D.R., "A Survey of Analysis of Shells by the Displacement Method". Matrix Methods in Structural Mechanics, Wright-Patterson Air Force Base, Ohio, AFB, AFFDL-TR-80, 1966.

(38) Kurt, C.E., Boyd, D.E., "Free Vibrations of Noncircular Cylindrical Shell Segments". AIAA. J., Vol. 9., No.2, pp 239-244, 1971.

(39) Lindberg, G.M., Olson, M.D., Sarazin, A.C., "Finite Element Dynamic Analysis of Shallow Shell Structures". National Research Council of Canada, Aeronautical Report, LR-540, 1970.

(40) Martins, R.A.F., Owen, D.R.J., "Structural Instability and Natural Vibration Analysis of Thin Arbitrary Shells by Use of the Semiloof Element". Int. J. Num. Meth. Eng., Vol. 11, pp. 481 - 498, 1977.

(41) McDaniel, T.J., Logan, J.D., "Dynamics of Cylindrical Shell with Variable Curvature". J. Sound Vib. Vol. 19, pp. 39-48, 1971.

(42) Neale, B.K., "Vibration of Shell Structures". Ph.D.Thesis University of Nottingham, 1971.

(43) Olson, M.D., Lindberg, G.M., "A Finite Cylindrical Shell Element and the Vibrations of a Curved Fan Blade". National Research Council of Canada, Aeronautical Report LR-497, 1968.

(44) Olson, M.D., Lindberg, G.M., "Vibration Analysis of Cantilevered Curved Plates Using a New Cylindrical Shell Finite Element". Proc. 2nd Conf. on Matrix Meth. in Structural Mech., Part 1 of 2, AFFDL-TR-68-150, pp.247-269, 1968

(45) Olson, M.D., Lindberg, G.M., "Dynamic Analysis of Shallow Shells with a Doubly-Curved Triangular Finite Element". J.Sound Vib., Vol. 19 (3),pp.299-318,1971.

(46) Pawsey, S.F., "Discussion of Papers by O.C.Zienkiewicz, R.L. Taylor and J.M. Too and S.F.Pawsey and R.W. Clough". Int. J. Num. Meth. Eng., Vol.4, pp.449-450, 1972

(47) Pawsey, S.F., Clough, R.W., "Improved Numerical Integration of Thick Shell Finite Elements". Int. J. Num. Meth.Eng., Vol.3, pp. 575-586, 1971.

(48) Petyt, M., "Vibration of Curved Plates". J. Sound Vib., Vol. 15 (3), pp. 381-395, 1971.

(49) Plunkett, R., "Natural Frequencies of Uniform and Non-Uniform Rectangular Cantilever Plates". J. Mech. Eng. Sci., Vol.5, No.2,pp. 146-156, 1963.

(50) Ramsden, J.N., Stoker, J.R., "Mass Condensation: A Semi-Automatic Method for Reducing the Size of Vibration Problems". Int. J. Num. Meth. Eng., Vol.1, pp 333-349, 1969.

(51) Sharma, C.B., Johns, D.H., "Vibration Characteristics of Clamped-free and Clamped-Ring-Stiffened Circular Cylindrical Shell". J. Sound Vib., Vol.14, pp.459-474, 1971.

(52) Srinivasan, R.S., Bobby, W., "Free Vibration of Non-circular Cylindrical Shell Panels". J. Sound Vib., Vol. 46(1) pp.43-49,1976.

(53) Strickland, G.E., Loden, W.A., "A doubly Curved Triangular Shell Element". Proc. 2nd Conf. Matrix Meth. in Structural Mech., Part 1 of 2 AFFDL-TR-68-150, 1968.

(54) Taylor, R.L., "On Completeness of Shape Functions for Finite Element Analysis". Int. J. Num. Meth. Eng., Vol. 4, pp 17-22, 1972.

(55) Warburton, G.B., "Dynamics of Shells". Proc. of a Symposium on Structural Dyn., Loughborough University, 1970.

(56) Wilkinson, J.H., "Calculation of the eigenvalues of a symmetric tridiagonal matrix by the method of bisection". Numerische Mathematik, Vol.4, pp.362-367, 1962.

(57) Wilson, J.M., Private communication, Durham University, 1978.

(58) Zienkiewicz, O.C., "The Finite Element Method in Engineering Science", McGraw-Hill, 1971.

(59) Zienkiewicz, O.C., "Isoparametric and Allied Numerically Integrated Elements - A Review". Numerical and Computer Methods in Structural Mechanics, Edited by Fenves, Perrone, Robinson, Schnobrich, Academic Press 1973.

(60) Zienkiewicz, O.C., Irons, B.M., Ergatoudis, I., Ahmad, S., Scott, F.C. "Isoparametric and Associated Element Families for Two-and Three-Dimensional Analysis". Finite Element Methods in Stress Analysis, Edited by I. Holond and K. Bell, Tapir, 1970.

(61) Zienkiewicz, O.C., Taylor, R.L., Too, J.M., "Reduced Integration Technique in General Analysis of Plates and Shells". Int. J. Num. Meth. Eng., Vol.3, pp. 275-290, 1971.

APPENDIX 1

A.1. Explanations on the Program

A.1.1. General Outline.

The computer program developed for the numerical analysis in this thesis consists of four main parts.

i) Data preparation.

ii) Construction of element matrices.

iii) Assembly and reduction.

iv) Eigenvalue solution.

The program uses three devices. Device numbers 5 and 6 are reserved for input and output respectively. Device number 7 is used to store the topology and the nodal coordinates, so that they can be referred whenever necessary during the computations.

A complete listing of the program is given in Appendix 5.

A.1.1.1. Data Preparation

Preparation of the input data to the program is given in detail in Appendix 2. This data consists of two parts.

The first part contains the control integers, material properties and the geometric parameters.

The second part corresponds to the finite element idealization of the structure. According to the control integers, the topology of the elements and the nodal coordinates are either read in through device number 5, or calculated by the data generation subroutines. In either case they are stored on device 7.

Data generation is performed by three subroutines called GENOD, GENTOP and DOF (See Section A.1.2). By using them, the amount of the input data can be reduced considerably. They can be employed for any structure having a constant cross-section in one direction, provided that a regular mesh is accepted in that direction. The input data describes the nodal coordinates at one cross-section, and they are repeated (with twisting if desired) along the length at different levels.

A.1.1.2 Construction of Element Matrices

This is simply achieved by programming the formulation given in Sections 2.1.and 2.2. of Chapter 2. Element stiffness and mass matrices are evaluated simultaneously in the main program. After the first evaluation, if the consecutive elements are similar, this step is either left out or replaced by a coordinate transformation procedure (see Section 2.5. of Chapter 2). In either case the computation time is reduced considerably (See Table A.1.1.).

A.1.1.3. Assembly and Reduction

Assembly of the element matrices into the system matrices, and the condensation of the system matrices are performed by subroutine REDUCE. To reduce the required space, only the lower triangles of the system matrices are stored. They are stored row by row in a one dimensional array. Thus, the $(i,j)^{th}$ entry of a matrix is stored in the kth entry of the array, where $k = j + i x (i - 1) /2$. The assembly procedure follows the standard form given in the first Chapter of reference (58). Then according to the information supplied with each node, the system matrices are either condensed as explained in Section 2.4, or left as they were.

A.1.1.4. Eigenvalue Solution.

For the solution of the eigenvalue problem of equation (2.1.18) a subroutine available within the Engineering Science Department was used. The routine is based on the technique given in references (56,7). It solves the eigenvalue problem provided that [K] and [M] are real symmetric matrices, and [M] is positive definite.

The routine, first factorizes matrix [M] using Choleski decomposition method, and then combines the [K] and [M] into one matrix, reducing the problem into a standard form. Evaluation of eigenvalues are done by tribisection, and of the eigenvectors by inverse iteration method.

A.1.2. List of Sub-programs

In addition to the main part, the following function and subroutines take part in the program.

GENTOP: Generates the mesh for the finite element idealisation.

GENOD: Calculates the coordinates of the nodes.

DOF: Determines the master degrees of freedoms as instructed by the input data.

CONEL: Constructs the elasticity matrix [D]

INTEGR: Determines the abscissae and weight coefficients for the Gaussian quadrature according to the number of integration points given in the input data.

VECI: Determines the local orthogonal axes v_{1i}, v_{2i}, v_{3i}.

JAKOB: Calculates the inverse Jacobian matrix and/or the determinant of the Jacobian.

THETA: Determines the direction cosine matrix.

SHODEN: This is the only function used in the program. It gives the contribution of node i to the shape function (or its derivative) of any point (ξ, η).

REDUCE: Performs the assembly and condensation of the system matrices (See Section A.1.1.3).

MAPRIN: Prints the system matrices which are stored in vector form, after converting them into matrix form.

MATUNI: Any matrix given as argument is put into unit form.

MATCOP: Copies the first argument matrix [A] into the second argument matrix [B]

MATNUL: Matrix [A] given as argument is returned as a zero matrix.

TRNPOZ: Takes the transpose of the first argument matrix [A] and stores it into the second argument matrix [B]

FORMT: Constructs the transformation matrix, for coordinate transformation.

TRNSFR: Performs the necessary transformation when top and bottom coordinates of a thickness vector are defined interchangeably.

DEIGS: Solves the eigenvalue problem (See Section A.1.1.4).

F01CKF: A routine from *NAG library of NUMAC. Three matrices A,B,C are given as arguments. Performs the matrix multiplication [A] x [B] = [C]

F01AAF: Another routine from *NAG Library. Calculates the inverse of a matrix.

A.1.3. CPU Time and Storage

The program was written in "FORTRAN IV" computer language using double precision. The machine used for the analysis was IBM 370/168 under MTS. Since the system was using virtual pages for storage, it was unnecessary to use dynamic allocation. The dimensions of the system matrices allow them to expand up to a size of 300 x 300 during the assembly process. The program uses about 250 virtual memory pages which corresponds to just over 1000 K bytes.

The run time of the program is affected by many variables. In general most of the CPU time is used for the evaluation of element matrices and for the reduction of the size of the system matrices. The time required for reduction depends upon their instantaneous size. By employing a careful node numbering system this size might be reduced considerably.

The following table is included to give a rough idea about the allocation of CPU time used within the program.

CPU Time Used sec.	Operation Performed
1.30	Evaluation of an element stiffness matrix for an 8-node element. Integration points 2 x 2 x 2.
1.92	Evaluation of a mass matrix for an 8-node element. 3 x 3 x 2 integration points were used.
1.67	Transformation of mass and stiffness matrices of one element to use for another element.
2.22	Evaluation of a stiffness matrix for a 10-node element integrated at 3 x 2 x 2 points.
2.16	Evaluation of a mass matrix for a 10-node element integrated at 3 x 3 x 2 points.
0.01	Assembly of one element into system matrices.
0.25	Reduction of the size of the system matrices from 85 to 80
0.42	Reduction of the size of the system matrices from 105 to 100
1.66	Reduction of the size of the system matrices from 180 to 175
3.52	Reduction of the sixe of the system matrices from 180 to 165
2.86	Reduction of the size of the system matrices from 220 to 215
4.70	Reduction of the size of the system matrices from 220 to 207
10.19	Reduction of the size of the system matrices from 255 to 233

TABLE A.1.1. CPU Time used during difference operations.

APPENDIX 2

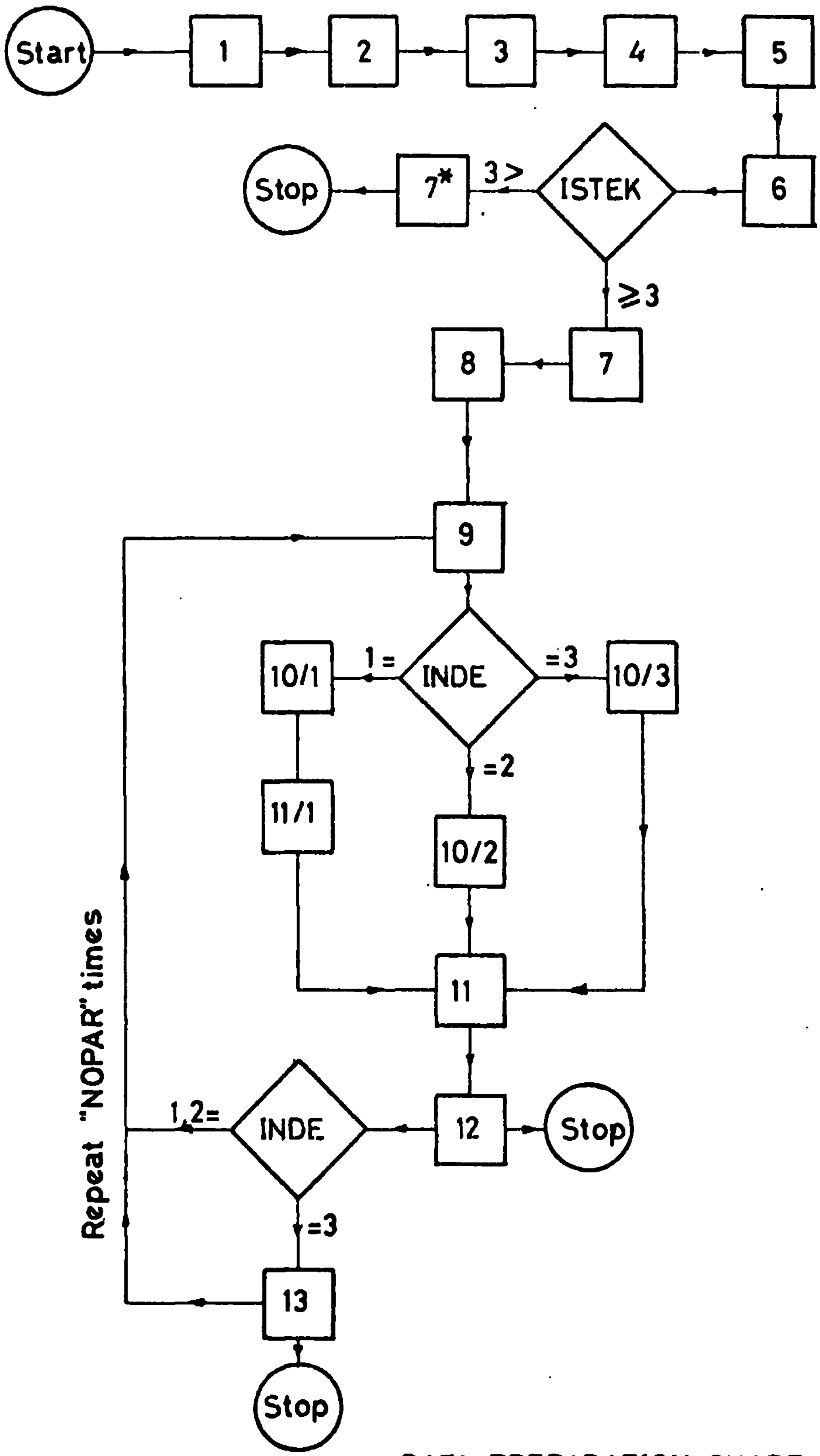

DATA PREPARATION CHART

DATA PREPARATION

1) Job description card; 1 card; FORMAT (20A4); Columns 1-80.

2) Control integers; 1 card; FORMAT (9I5)

Col:	5	10	15	20	25	30	35	40	45
	NO	NONO	NNC	M1	M2	ISTEK	IPRINT	MAPRO	NEY

NO: If ISTEK < 3 NO= total number of elements in the structure

If ISTEK ≥ 3 NO= total number of elements in the first row of the mesh

NONO: Total number of nodes in the structure.

NNC: Total number of nodes that are to be constrained.

M1: Number of the first eigenvalue to be found.

M2: Number of the last eigenvalue to be found.

ISTEK: Control integer for data generation program (GENDAT)

If ISTEK < 3 GENDAT not to be used. All the coordinates of the nodes and master d.o.f. are to be given explicitly.

If ISTEK ≥ 3 GENDAT is to be used and;

when ISTEK = 5, for the elements beyond the first row ITYPE= 2

when ISTEK > 5, for the elements beyond the first row ITYPE= 3

when ISTEK < 5, for the elements beyond the first row ITYPE is the same as the elements in the first row.

IPRINT: Output control integer.

= 1 instantaneous size, frequencies and eigenvectors printed.

= 2 1 + topology and coordinates printed.

= 3 2 + element information printed.

= 4 3 + restrained nodes are printed

= 5 4 + physical and geometrical properties printed

9 > IPRINT $\geq$ 7   5 + Element coordinates, topology, boundary condition, degrees of freedom printed

= 9   7 + Structural stiffness matrix printed

> 10   9 + Stiffness matrix for stiffening rods printed.

Recommended value for IPRINT = 8

MAPRO: Number of different material property sets.

$1 \leq$ MAPRO ≤ 5

NEY: Number of elements along the shell.

3) Material properties; MAPRO cards; FORMAT (3 E 10.5)

Col:	10	20	30
	E	RO	PR

E = Modulus of elasticity

RO = Density

PR = Poisson's ratio

This card is also used to give the sectional properties of stiffening rods. When stiffeners are used, the value of MAPRO is increased by 1 and on the additional card following information is given:

E = Modulus of elasticity of the rods

RO = 0.0 (since the rods are assumed massless)

PR = Cross-sectional area of the rods.

4) Geometric properties; 1 card; FORMAT (2F 10.4)

Col:	10	20
	RLEN	THIC

RLEN: Length of Shell

THIC: Thickness of the shell at a reference point.

5) Restrained nodes; NNC/16 cards; FORMAT (16I5)

(used to display the restrained nodes, also in GENDAT)

6) Topology and element information; NO cards; FORMAT (14I5,4I2)

Col:	50	55	60	65	70	80
	TOPOLOGY	INTEG	LTIP	ITYP	IPRO	INVER

<u>TOPOLOGY</u>: Topology of the element is given. Nodal numbers must be entered in the order shown in figure 2.1.

<u>INTEG</u>: Three digit integer. Each digit shows the number of integration points for the stiffness matrix of the element in ξ, η, ζ directions respectively. In case of a 2-node element INTEG = INC (see 7)

<u>LTIP</u>: Shows the type of element

= 2 2-node stiffening bar

= 8 8-node quadratic element

= 10 10-node cubic-quadratic element.

<u>ITYPE</u>: Makes repetitive use of the element matrices by transformation.

= 1 Matrices are calculated independently.

= 2 Element has the same orientation and geometry and the same material properties as the previous one.

= 3 Element has different orientation but the same geometry and material properties as the previous one.

<u>IPRO</u>: Element material property set number. IPRO$\leqslant$ MAPRO

<u>INVER</u>: An integer array of dimension 4. It is used when one node is defined in two different ways for two adjacent elements, i.e. when top and bottom coordinates are interchanged. Nodal numbers in the element numbering system corresponding to the nodes which are to be inverted are given in this array. When not in use it is left blank.

7*) Coordinates and d.o.f. of the nodes; NONO cards;
FORMAT(6E10.4, 2I5)

Col:	10	20	30	40	50	60	65	70
	XT	XB	YT	YB	ZT	ZB	NDOF	IDIS

XT, YT, ZT: Top coordinates of the node.

XB, YB, ZB: Bottom coordinates of the node.

NDOF: Total number of degrees of freedom at that node
$0 \leq NDOF \leq 5$

IDIS: Five digit integer. Each digit represents the d.o.f. u, v, w, α, β respectively. Each digit can take any value between 0÷3. Their meanings are:

0: Slave d.o.f. It is to be eliminated when contributions of the elements to this node are completed.

1: Master d.o.f., to be kept in the eigenvalue problem.

2: Restrained d.o.f., not to be included in the structural matrix.

3: Slave d.o.f. Indicates that a hinge is assumed at that node.

7) Control integers for GENDAT; 1 card; FORMAT (13I5)

Col:	5	10	15	20	25	30	35	40	45	50-70
	NOPAR	INC	ID	IR	IBC1	IBC2	IS2	MIS1	MIS2	ISAR

NOPAR: Total number of substructures used for the determination of coordinates and topology by GENDAT. (In one substructure there can not be more than 10 nodes along the side).

INC: Increment between first and second level nodes.

ID: Number of levels where there are master d.o.f.

IR: Master degrees of freedoms. IR=IDIS (see 7*) at that level. It can only contain 0's and 1's. 2's and 3's are given separately.

IBC1 : NDOF (see 7*) of constrained end. If all restrained IBC1 = 0.

IBC2: IDIS of constrained nodes. If all d.o.f. are constrained then IBC2 = 22222.

IS2: IDIS of hinged nodes. It can not contain 1 or 2. If no hinges, leave blank.

MIS1: Only needed when making use of the symmetry. Then it equals to NDOF of the nodes along the axis of symmetry.

MIS2: IDIS of nodes along the axis of symmetry. It can only contain 0's and 2's.

ISAR: An integer array of dimension 4. If the number of any node along the reference side of the substructure is put in this array, its XT and XB coordinates are corrected as XT = XB = (XT+XB)/ 2.0.

8) Angle of pretwist and master d.o.f. levels; (1+ID)/8 cards; FORMAT (8 E 10.4)

```
Col.          10          20               80
             TOTAN       WS(1) ........WS(7)
             WS(8).....................WS(ID)
```

TOTAN: Total angle of pretwist in degrees. The structure is twisted linearly along the length around the coordinate centre. If no pretwist TOTAN = 0.0.

WS: An array containing the y-coordinates of the levels (along the length) where there are master d.o.f.

9) **INDE**: An ineger which indicates the type of substructure whose particulars are to be given. 1 card; FORMAT (I5)

= 1 Plate type substructure (reference line is straight)

= 2 Circular cylindrical substructure.

= 3 Any cylindrical geometry.

10/1) Geometry of the plate; 1 card; FORMAT (8 E 10.4)

Col:	10	20	30	40	50	60	70	80
	XTI	YTI	XBI	YBI	XTF	YTF	XBF	YBF

XTI, YTI, XBI, YBI: Coordinates of the node at one end of the reference line of substructure.

XTF, YTF, XBF, YBF: Coordinates of the node at the other end of the reference line.

11/1) Division of the line along the reference side of substructure. 1 card, FORMAT (2I5)

Col:	5	10
	NOPT	NTERS

NOPT: Total number of nodal points between the two end coordinates given in 10/1.

NTERS: When a negative value is given to NTERS top and bottom coordinates of all the nodes for that substructure are interchanged. Otherwise NTERS = 0.

10/2) Geometry of the circular cylindrical substructure; 1 card; FORMAT (6 E 10.4, 2I5)

Col:	10	20	30	40	50	60	65	70
	XC	YC	RAD	THIC	AINI	AFIN	NOPT	NTERS

XC: X-coordinate of the centre of circular segment) if in x - z plane.

YC: Z-coordinate of the centre of circular segment)

RAD: Outer radius of curvature of the segment.

THIC: Thickness of the segment.

AINI: Angle(in degrees) between the positive X-axis and the radius which connects the first node on the segment to the centre. Angle is measured +'ve from X to Z following the shortest path.

AFIN: Angle (in degrees) between X-axis and the radius which connects the final nodal point to the centre.

NOPT: Number of nodal points between AINI and AFIN.

NTERS: See 11/1.

10/3) Control integers for general cylindrical geometry; 1 card; FORMAT (2I5).

Col:	5	10
	NOPT	NTERS

NOPT: Number of nodal points along the reference line of the prismatic section.

NTERS: See 11/1.

11) Node numbers; 1 card; FORMAT (10I5)
Node numbers, given in order, between the initial and final nodes of substructure. There are NOPT $\leq$ 10 such points.

12) Topology indication number; 1 card; FORMAT (10I5)
Gives the midside nodes, next to the nodes given in 11.

O : no midside node next to the node given in 11.

n : number of the midside node next to the node given in 11.

-n : nodes along this node are hinged or along the axis of symmetry.

-1 : coordinates of this node are calculated in another substructure.

13) Geometry of the general cylindrical section; NOPT cards; FORMAT (4 E 10.4).

Col:	10	20	30	40
	XATI	XABI	YATI	YABI

coordinates of each node in the reference plane of substructure are given in the order from initial to final.

<u>Care must be taken on the following points</u>:

1) The coordinate system chosen must be right handed.

2) When data generation subroutines are to be used, choose global y-direction along the length of the structure.

3) Top and bottom points of a node are decided according to ζ and corresponding global coordinates must be in accordance.

4) Symmetry and hinge facilities in GENDAT can only be used if the axis of symmetry or the hinges are on a line parallel to one of the global coordinates.

5) To use hinge facilities, element numbering system must go faster in the direction of hinged line.

6) Symmetry and hinge condition in GENDAT can not be used for the same run of the program.

APPENDIX 3

This appendix contains some additional figures to Chapter 5. Also a comparison of these figures is included.

Some abbreviations are used for the identification of difference mode shapes. In this convention IG stands for idealized geometry, similarly RG and EX for real geometry and experimental. For instance, IG-8 indicates the 8th mode given in idealized geometry finite element analysis.

List of Figures

<u>Comparison of the Modes</u>

I.G. Mode No:	Comparison with R.G. and EX.
1 - 4	Mode shapes match in all cases perfectly.
5	Very little coupling with 2nd tortion is seen in experimental and RG finite element analyses. Frequency increases with respect to the I.G. analysis.
6	Experimental mode determination was difficult, probably requires a better excitation. Effect of imperfect geometry can be seen in R.G. mode shape. Frequencies agree in all three analyses.
7	Difference between the frequencies of I.G. and R.G. analyses is similar to the difference in first bending mode. Experimentally a frequency was detected at 708.5 Hz, identification of the mode shape was not possible, accepted as 2nd bending mode.
8/9	Frequencies are very close. EX-7/8 and R.G.-8/9/10 have similar mode shapes, possibly coupling of I.G.8 and I.G.9. Deflection curves of R.G.9 are very similar to the deflection curve of I.G.9.
10	A remarkable resemblance between EX-10 and R.G.13/14. Equivalent I.G. mode is I.G.10. Effect of choice of degrees of freedom can be seen by comparing R.G.13 and R.G.14.
11	R.G. 11/12 are quite similar to EX - 9, and their equivalent is I.G.11. R.G.11 and R.G.12 represents the same mode, slight difference is due to the different master degrees of freedoms.

I.G. Mode No.	Comparison with R.G. and EX
12/13	EX-11 and EX-12 have more or less the same shape which is similar to R.G.15. Although sketches of I.G.12 resemble to this shape, deflection curve for I.G.13 and R.G.15 show the same pattern. A coupling between the two might have taken place.
15	EX-13 and I.G.15 are quite similar, no corresponding mode in R.G. group.
16	Deflection curves are similar to R.G.18's, no corresponding mode identified experimentally.
18	Examination of the deflection curves show a resemblance with R.G. 17.
19	EX-15 and R.G.19 have similar mode shapes. The only possible mode corresponding to them in I.G. group is I.G.19.

Similar frequencies pointed above are listed on table A.3.1.

Ideal Geometry		Real Geometry		Experimental	
Mode No.	Frequency Hz	Mode No.	Frequency Hz	Mode No.	Frequency Hz.
1	196.5	1	158	1	142
2	302.5	2	306.8	2	297
3	335.5	3	371.5	3	355
4	562	4	588.4	4	561
5	553	5	648	5	598
6	821	6	837	6	812
7	804.5	7	739		708
8/9	954/950	8/9/10	979/1027/1004	7/8	905/935
10	1042	13/14	1155/1249	10	1096
11	1047	11/12	1052/1109	9	980
12/13	1062/1191	15	1299	11/12	1136/1157
15	1419	-	-	13	1313
16	1502	18	1638	-	-
18	1598	17	1541	-	-
19	1733	19	1818	15	1633

Table A.3.1. Frequencies corresponding to similar mode shapes in three different analysis.

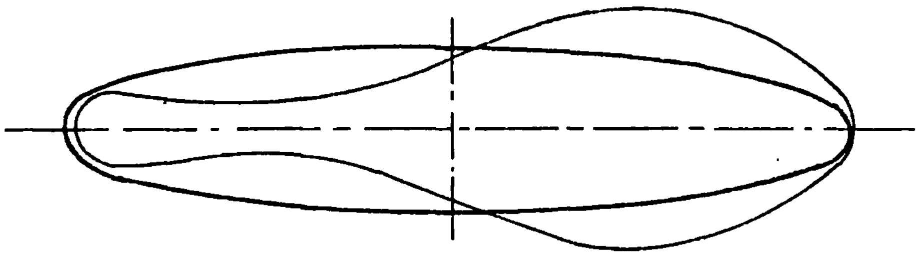

Figure A.3.1.(a): Tip deflection for mode 6 at frequency = 809 Hz.

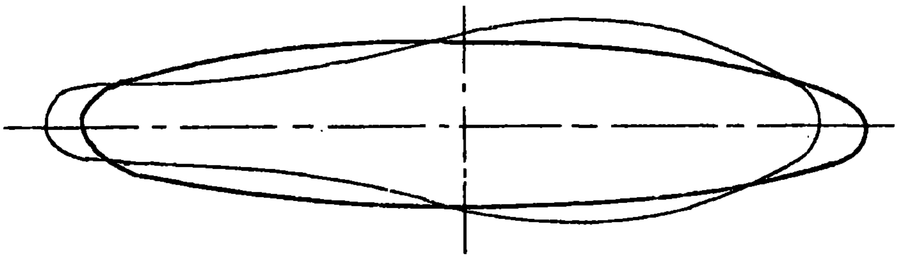

Figure A.3.1.(b): Tip deflection for mode 6 at frequency = 879 Hz.

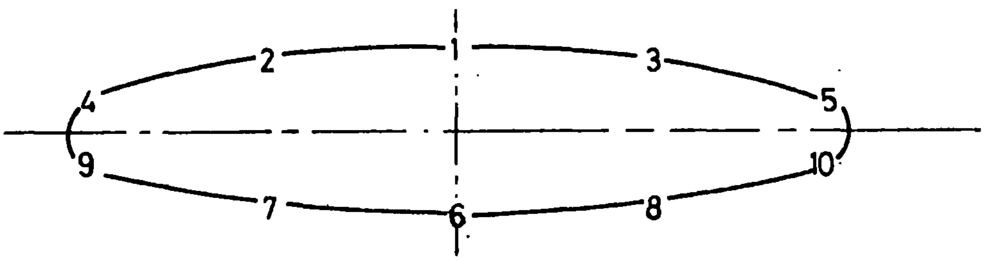

Figure A.3.2: Key to the deflection curves.

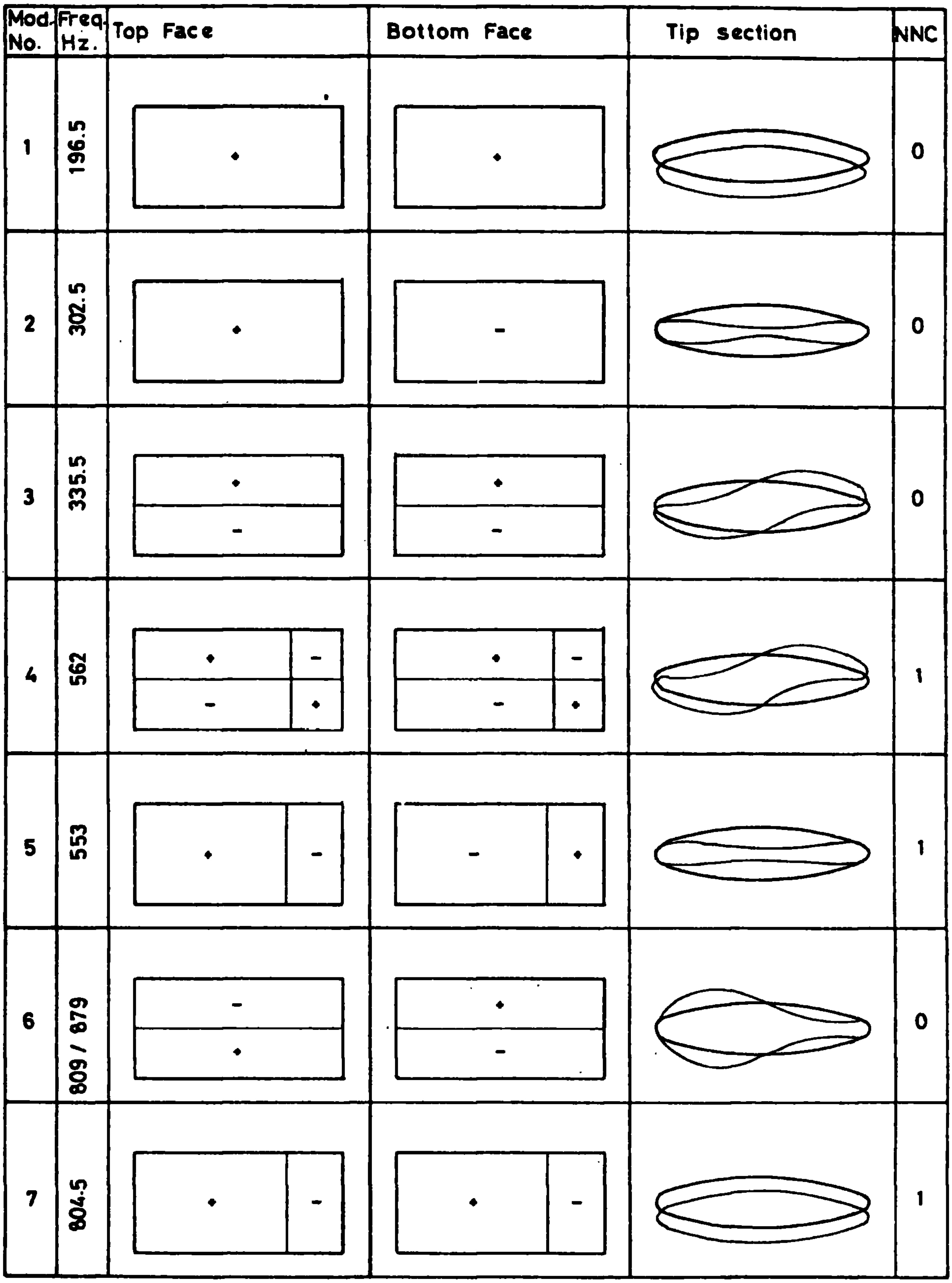

Figure A.3.3.(a): Predicted ideal mode shapes of the Oval X-Section blade using the idealized geometry. NNC stands for number of nodal circles.

Mod. No.	Freq Hz.	Top Face	Bottom Face	Tip section	NNC
8	954	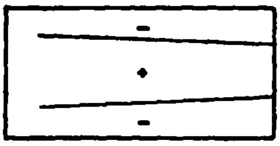	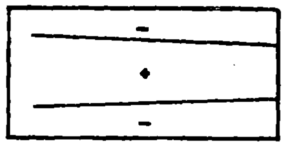	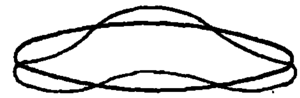	0
9	950	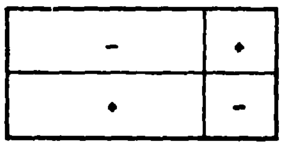	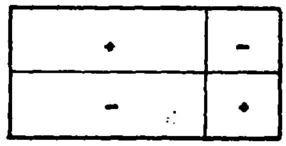		1
10	1042	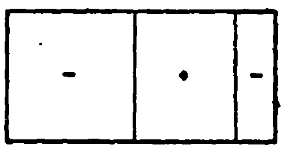	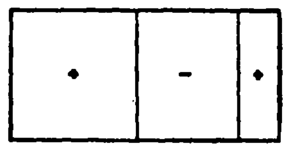	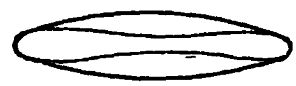	2
11	1047	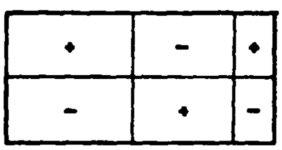	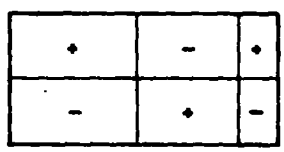		2
12	1062	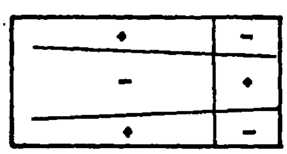	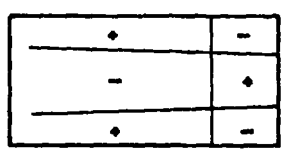		1
13	1191	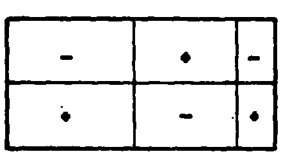	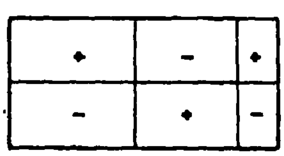		2
14	1359	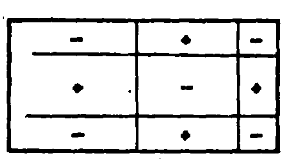	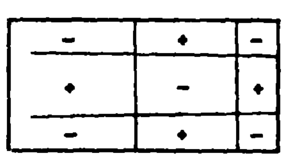		2

Figure A.3.3.(b).

Mod No.	Freq Hz.	Top Face	Bottom Face	Tip section	NNC
15	1419	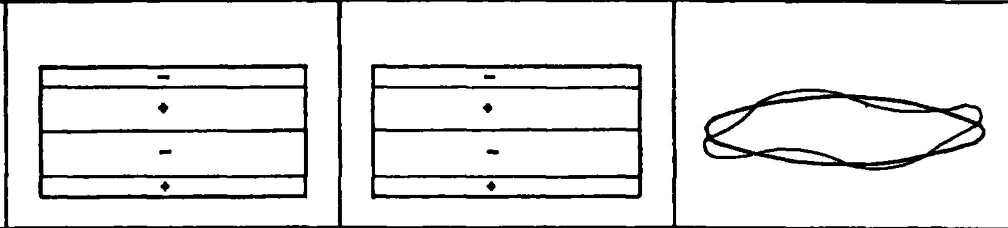			0
16	1502	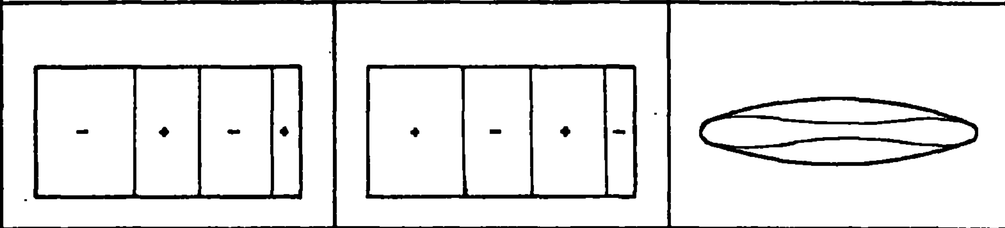			3
17	1583	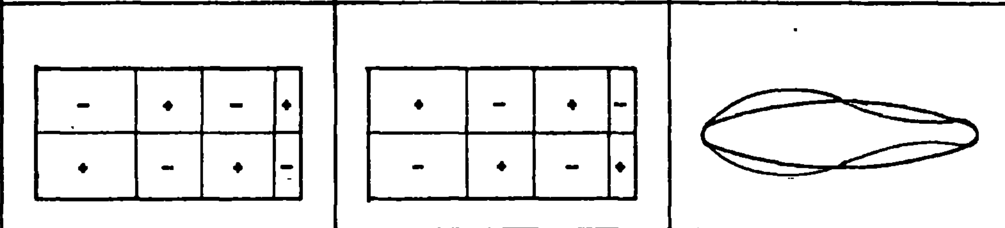			3
18	1598	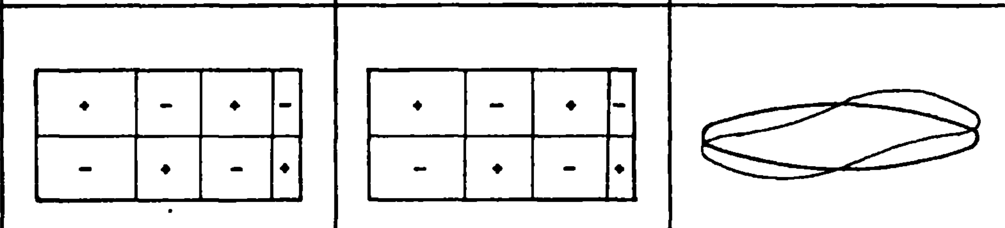			3
19	1733	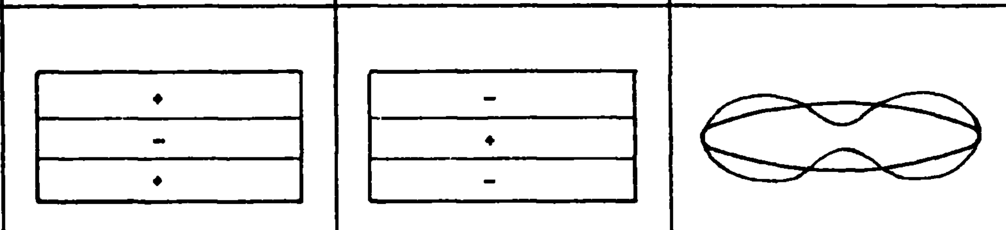			0
20	1513	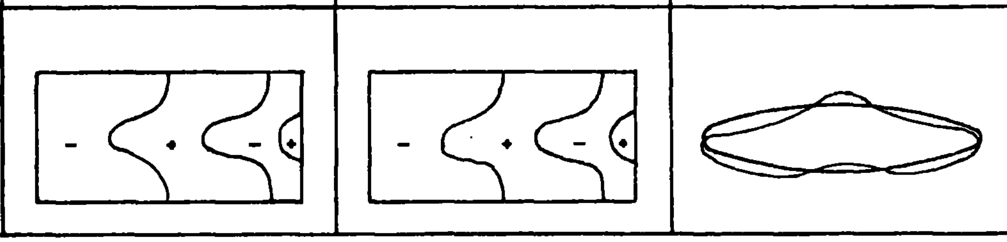			?

Figure A.3.3.(c).

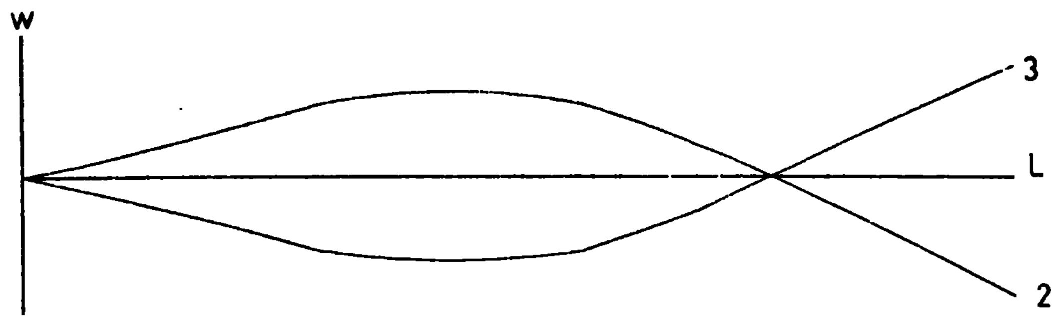

Figure A.3.4: Mode 4, (S), f = 562 Hz.

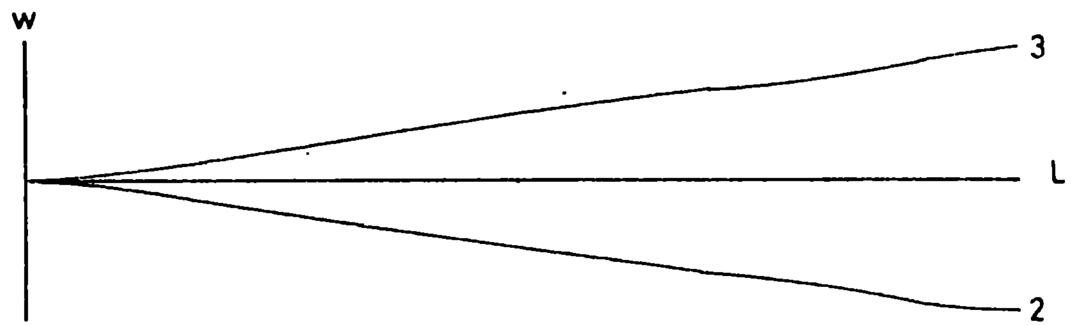

Figure A.3.5: Mode 6, (MI), f = 821.5 Hz.

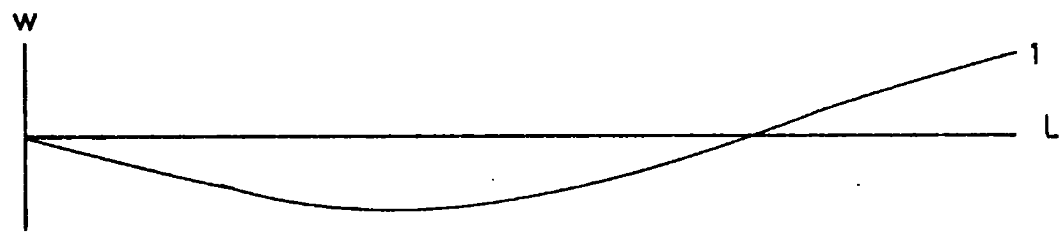

Figure A.3.6: Mode 7, (S), f= 804.5 Hz.

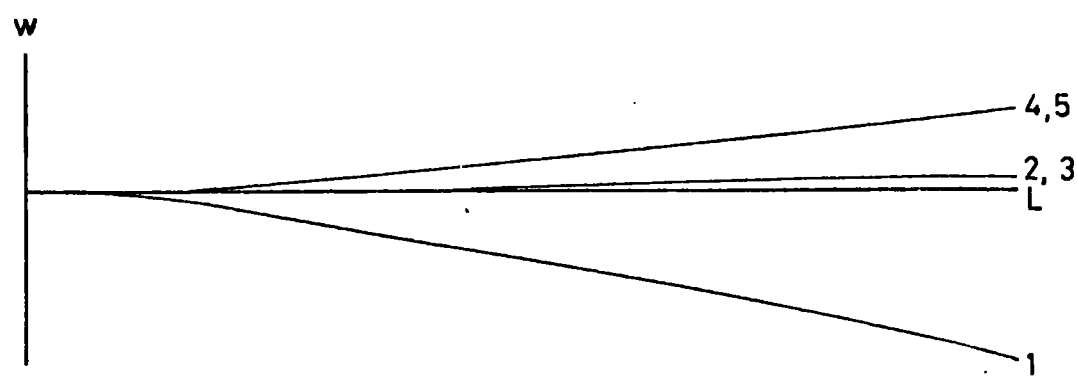

Figure A.3.7: Mode 8, (MI), f= 954 Hz.

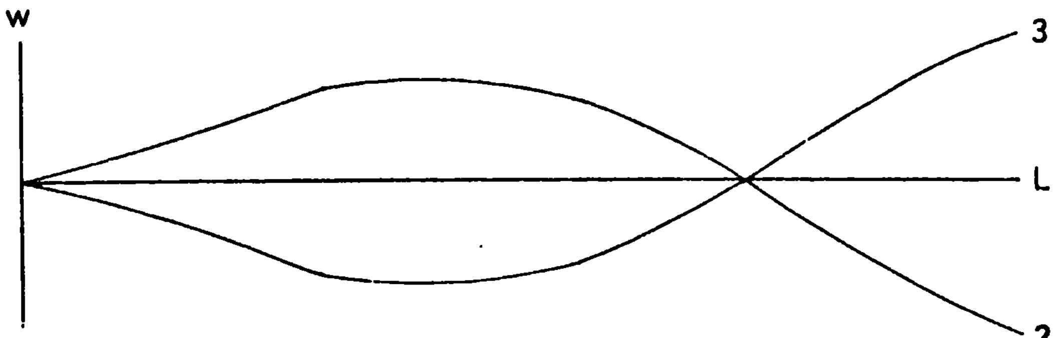

Figure A.3.8: Mode 9, (MI), f = 950 Hz.

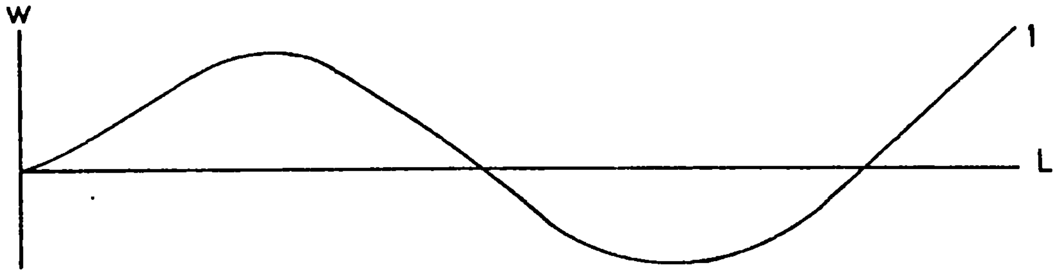

Figure A.3.9: Mode 10, (MI), f= 1042 Hz.

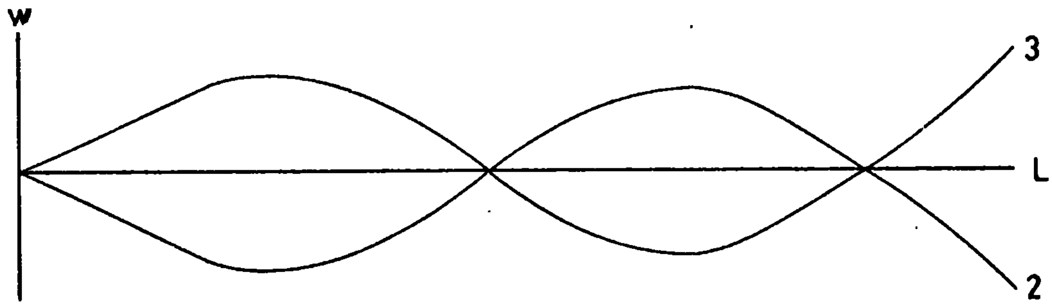

Figure A.3.10: Mode 11, (S), f= 1047 Hz.

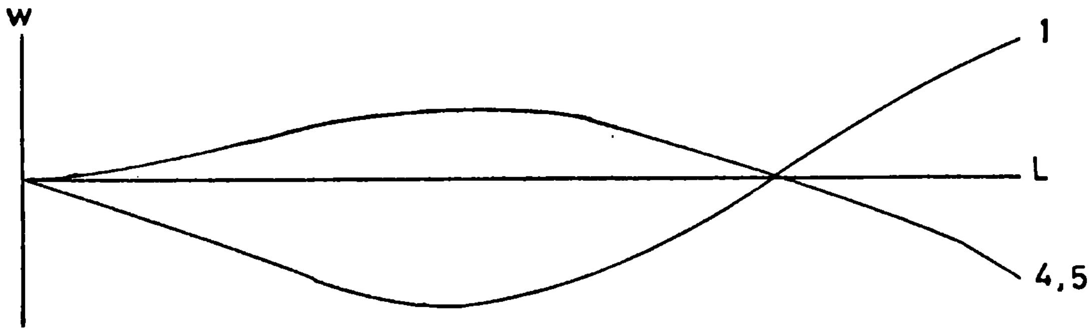

Figure A.3.11: Mode 12, (S), f= 1062 Hz.

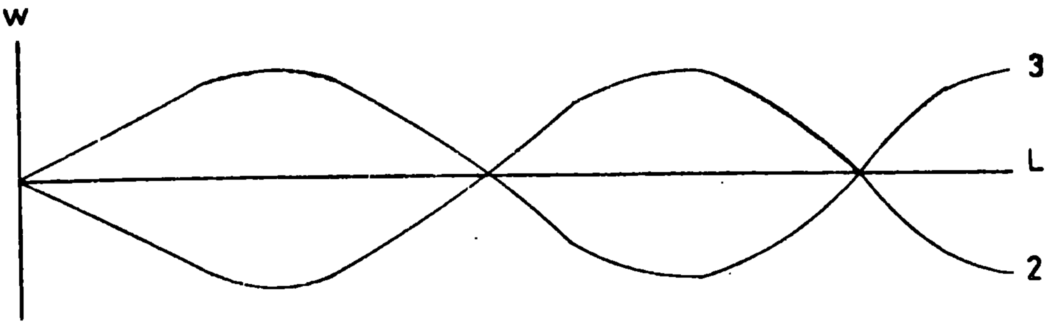

Figure A.3.12: Mode 13, (MI), f = 1191 Hz.

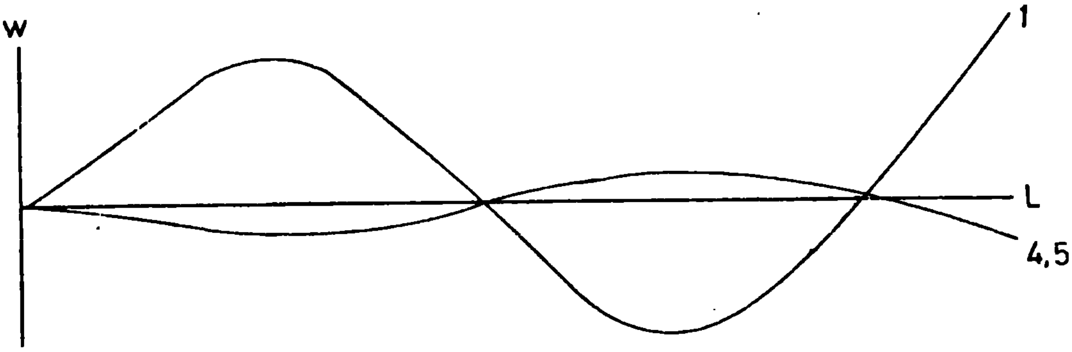

Figure A.3.13: Mode 14, (S), f = 1359 Hz.

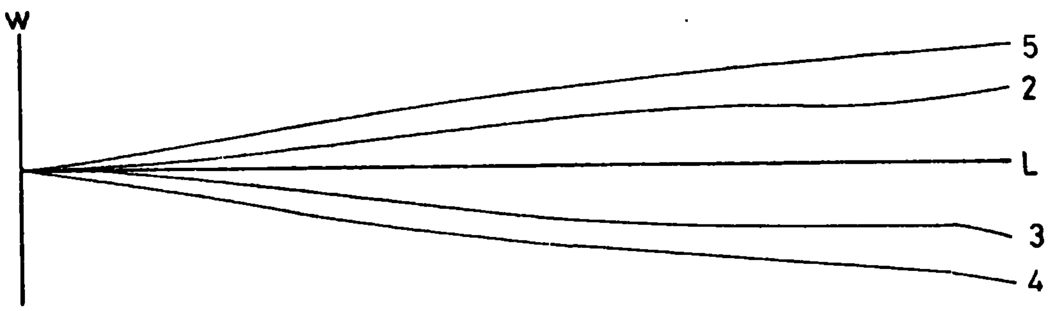

Figure A.3.14: Mode 15, (S), f = 1419 Hz.

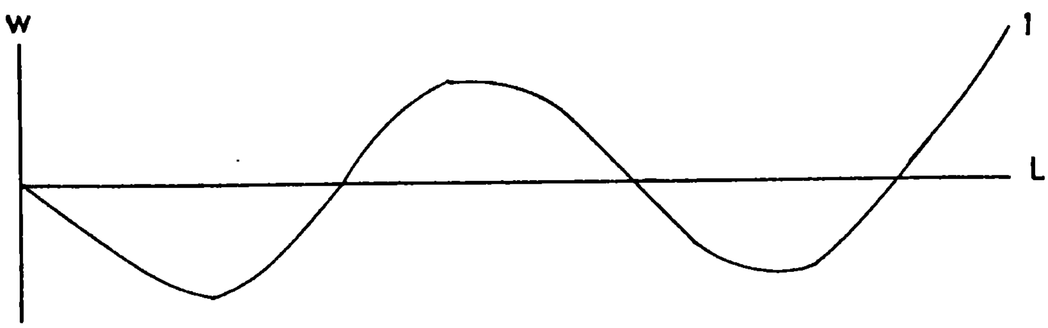

Figure A.3.15: Mode 16, (MI), f = 1502 Hz.

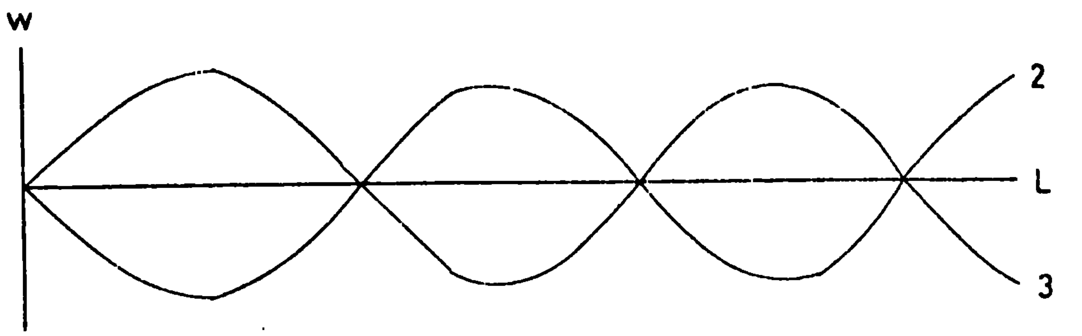

Figure A.3.16: Mode 17, (MI), f = 1583 Hz.

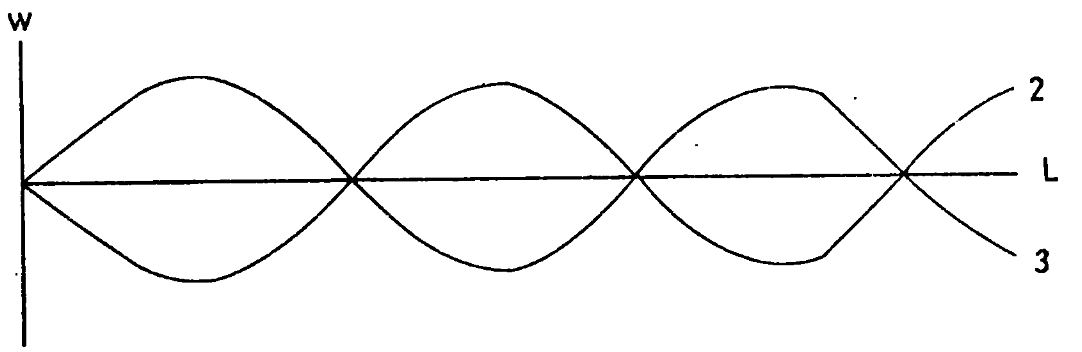

Figure A.3.17: Mode 18, (S), f = 1598 Hz.

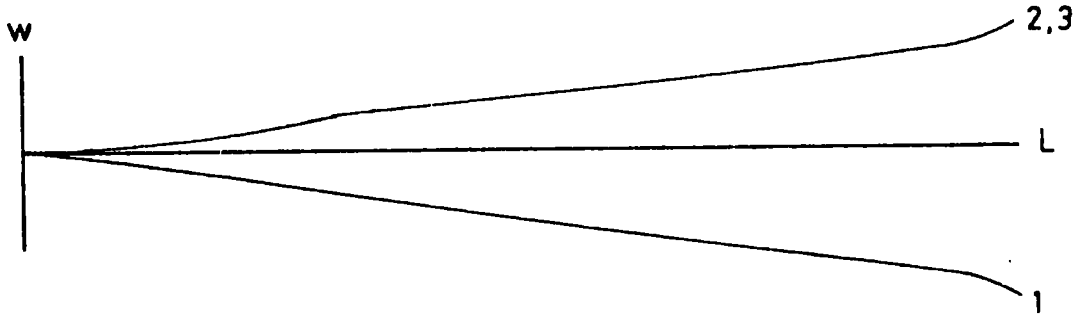

Figure A.3.18: Mode 19, (MI), f = 1733 Hz

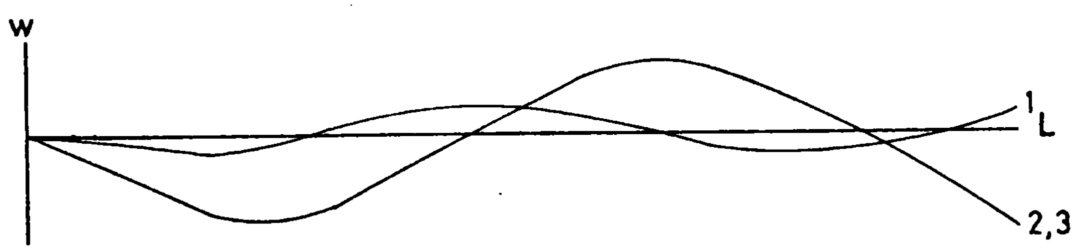

Figure A.3.19: Mode 20, (S), f = 1513 Hz.

Mod. No.	Top Face	Bottom Face	90 d.o.f.	146 d.o.f.	129 d.o.f.
1	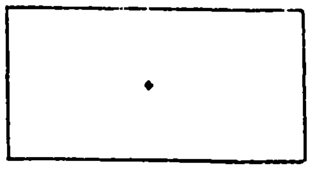	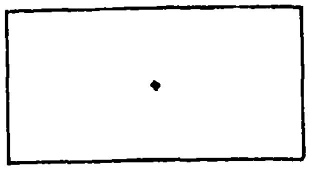	158	158	158
2	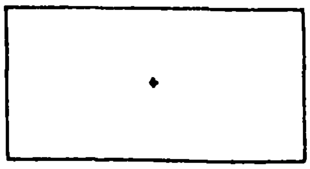	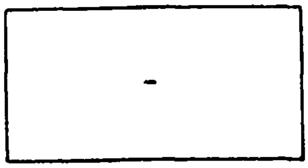	307	306.8	306.8
3	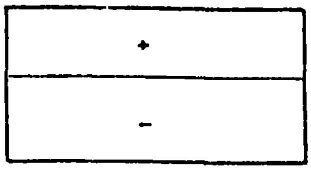	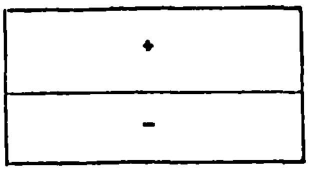	372	371.5	371.6
4	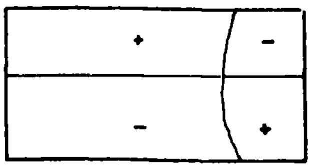	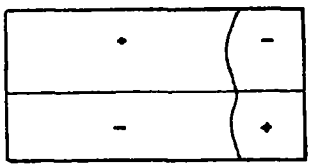	597	596	588.4
5	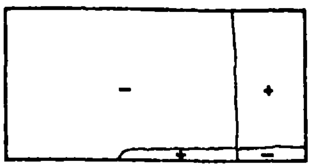	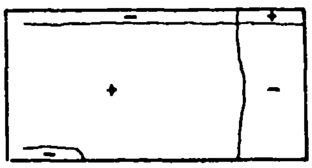	661	660	648
6	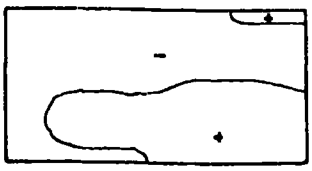	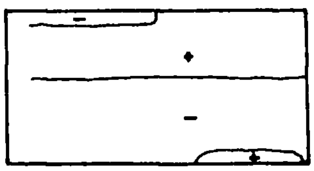	839	836	837
7	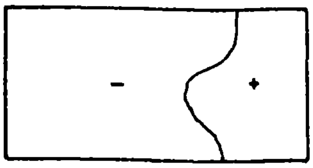	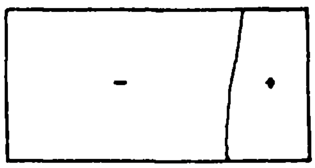	759	758	738
8	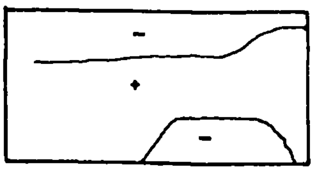	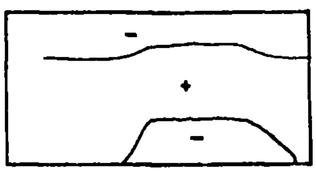	-	-	979

Figure A. 3.20 (a): Mode shapes obtained from the finite element analysis of the real geometry.

Mod. No.	Top Face	Bottom Face	90 d.o.f.	146 d.o.f.	129 d.o.f.
9	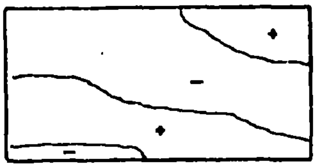	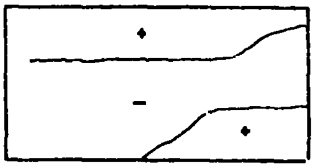	1043	1036	1027
10	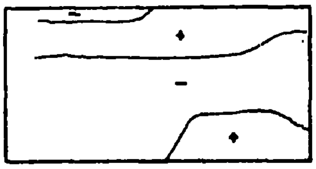	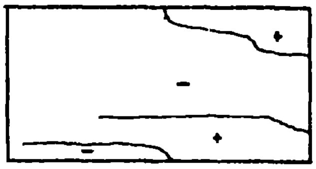	1016	1004	-
11	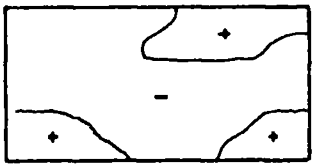	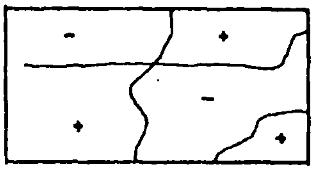	-	-	1052
12	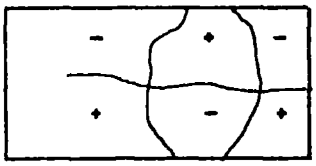	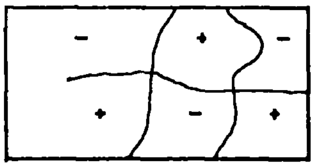	-	1109	-
13	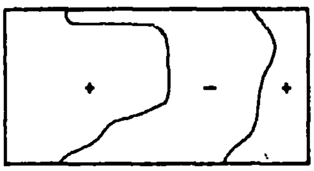	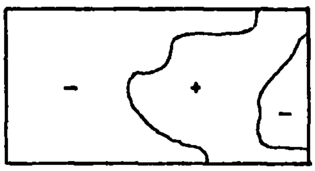	-	-	1155
14	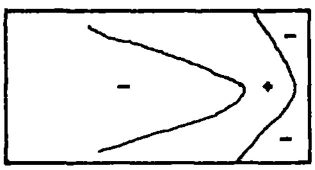	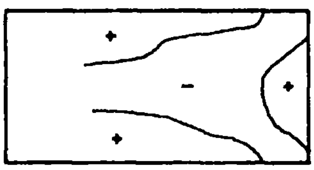	-	1249	-
15	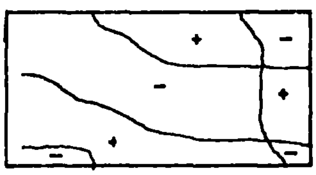	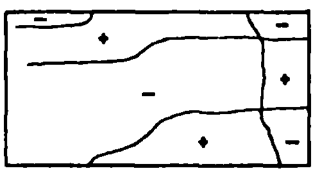	-	-	1299
16	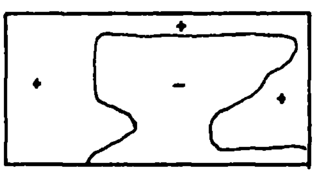	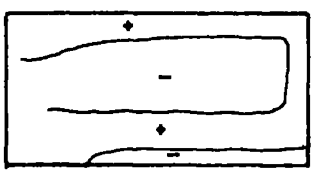	-	-	1456

Figure A.3.20 (b):

Mod. No.	Top Face	Bottom Face	129 d.o.f.
17	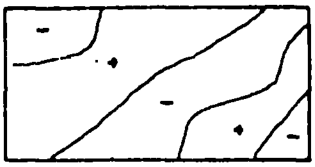	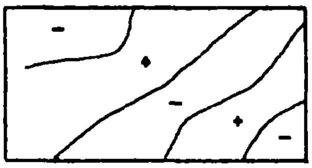	1541
18	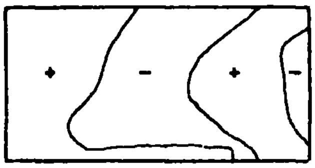	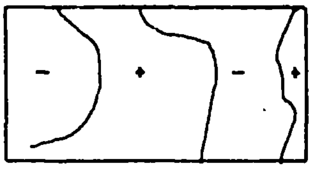	1638
19	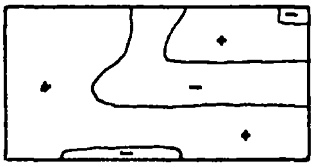	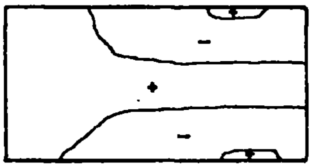	1818
20	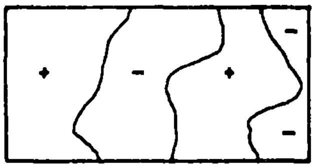	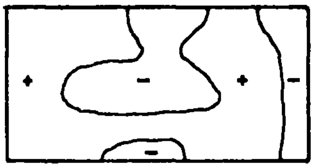	1876
21	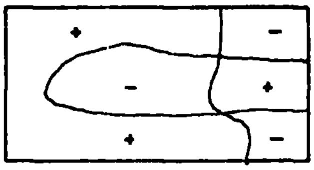	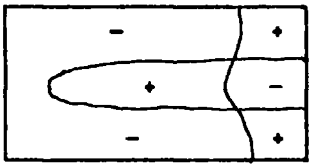	2005

Figure A.3.20 (c):

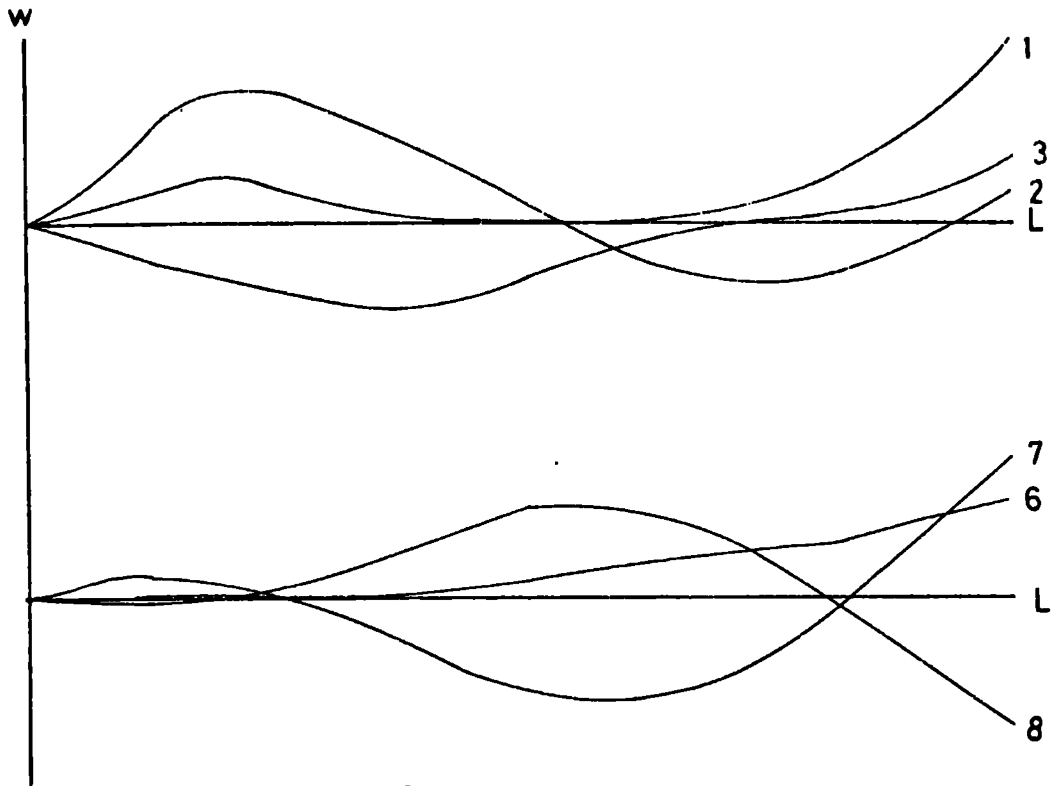

Figure A.3.21: Mode 8, f = 979 Hz.

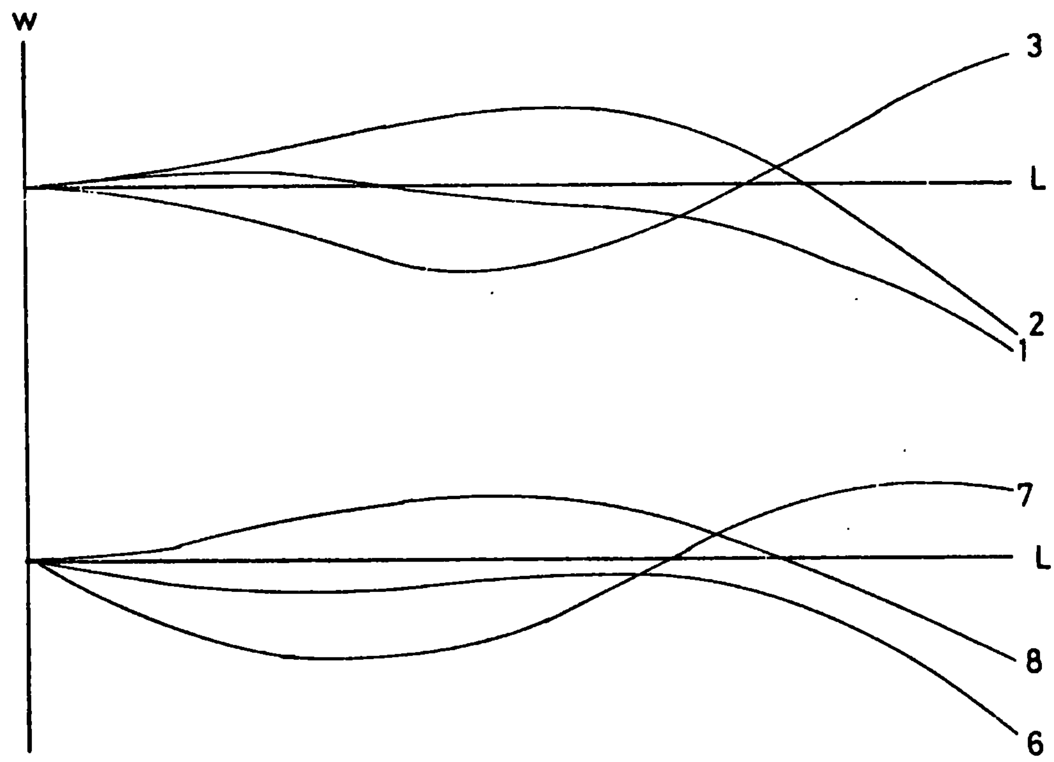

Figure A.3.22: Mode 9, f = 1027 Hz.

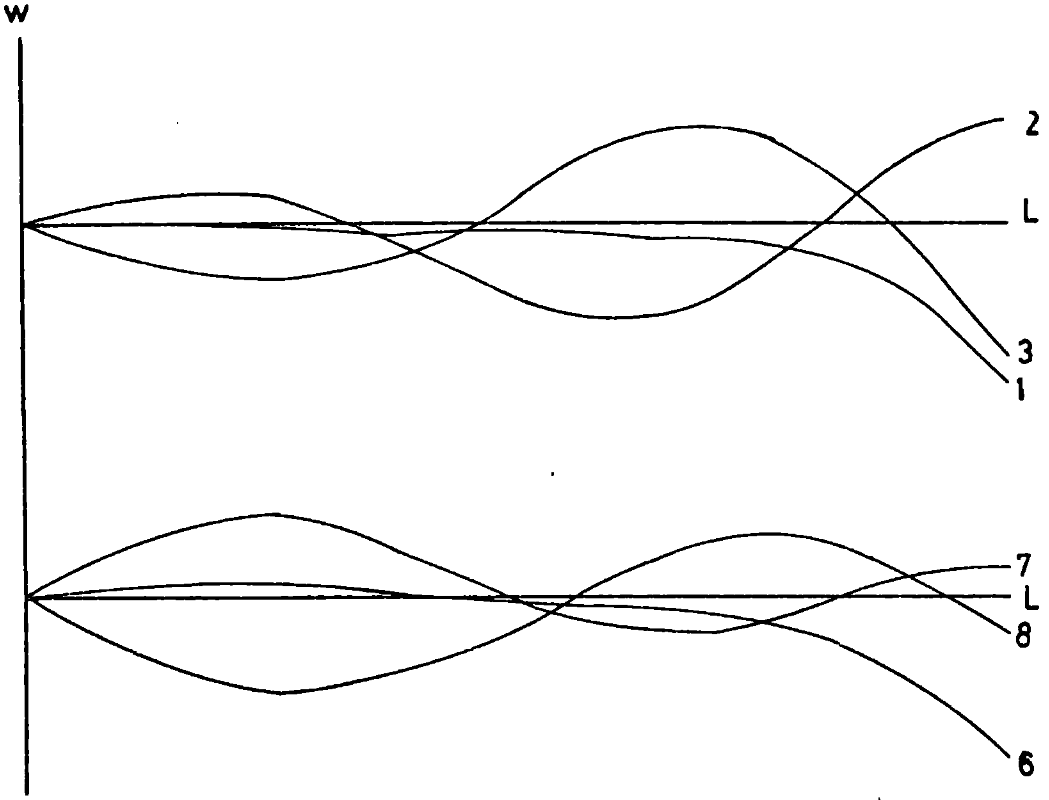

Figure A.3.23: Mode 11, f = 1052 Hz.

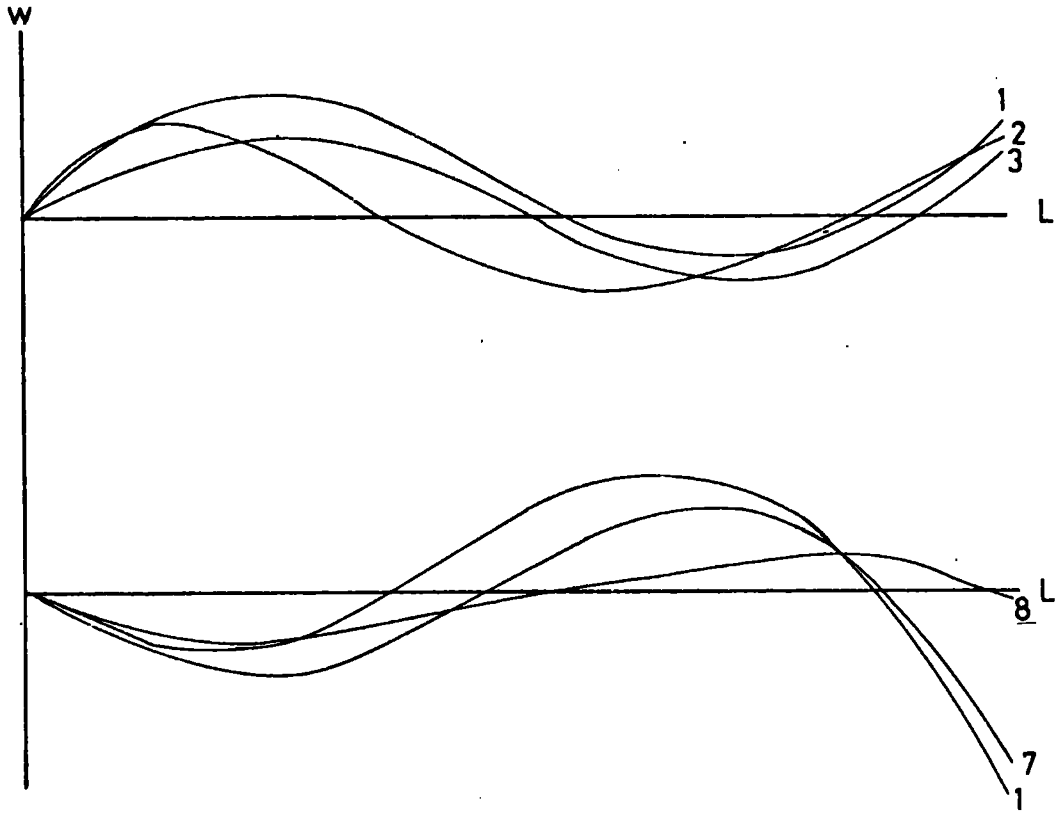

Figure A.3.24: Mode 13, f = 1155 Hz.

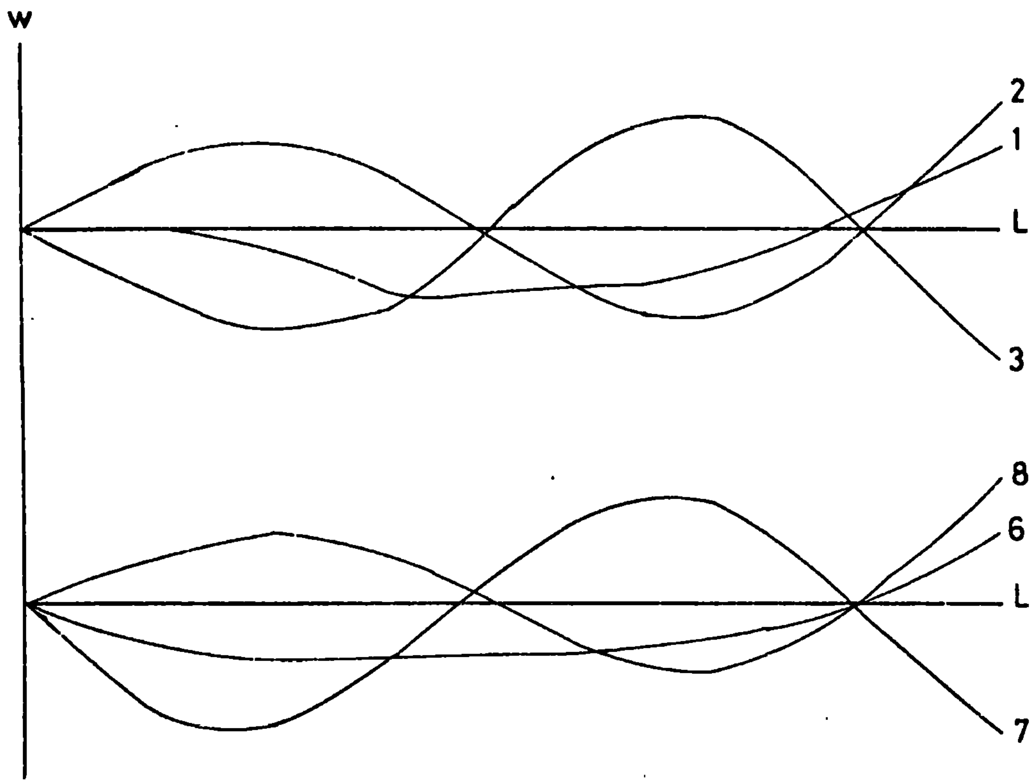

Figure A.3.25: Mode 15, f = 1299 Hz

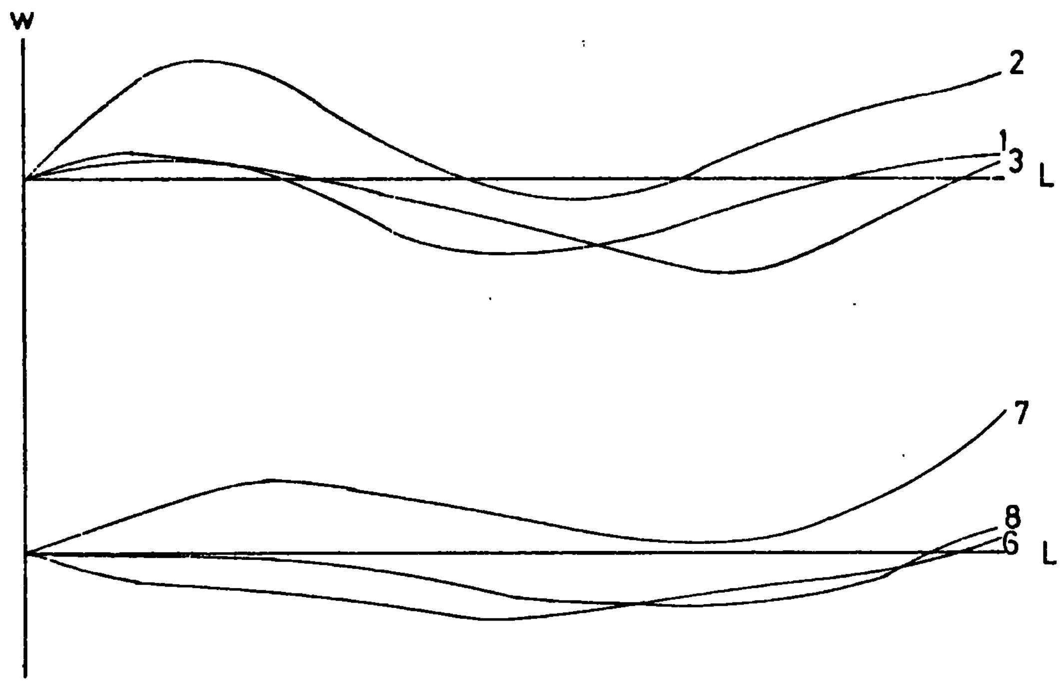

Figure A.3.26: Mode 16, f = 1456 Hz.

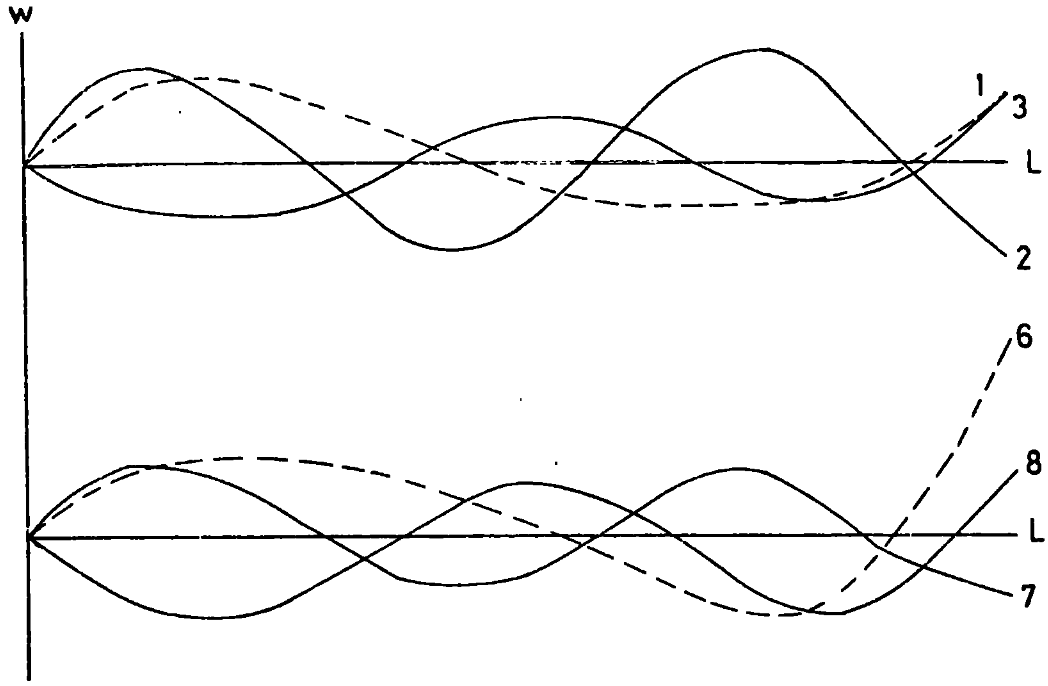

Figure: A.3.27: Mode 17, f = 1541 Hz.

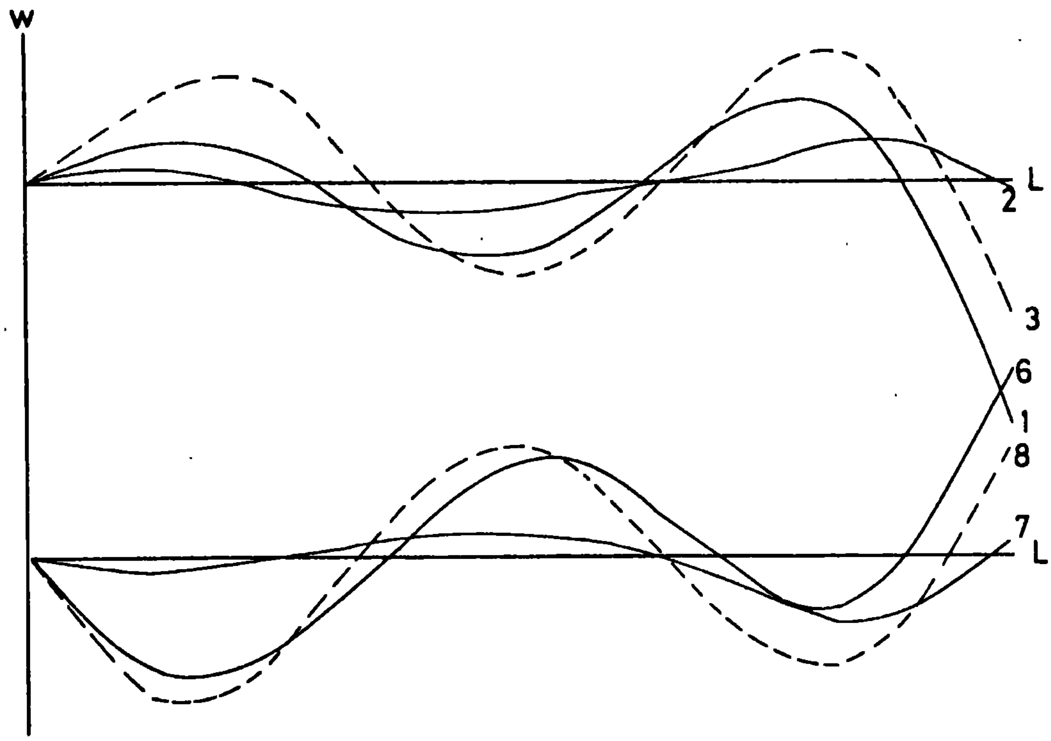

Figure A.3.28: Mode 18, f = 1638 Hz.

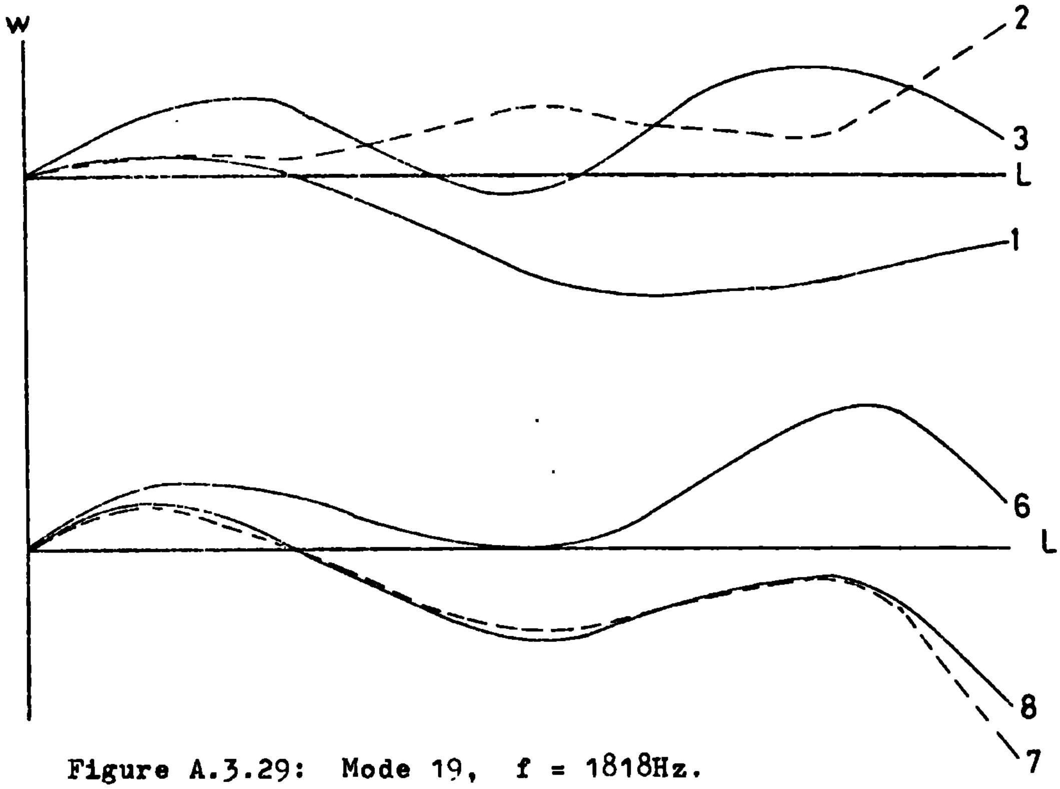

Figure A.3.29: Mode 19, f = 1818Hz.

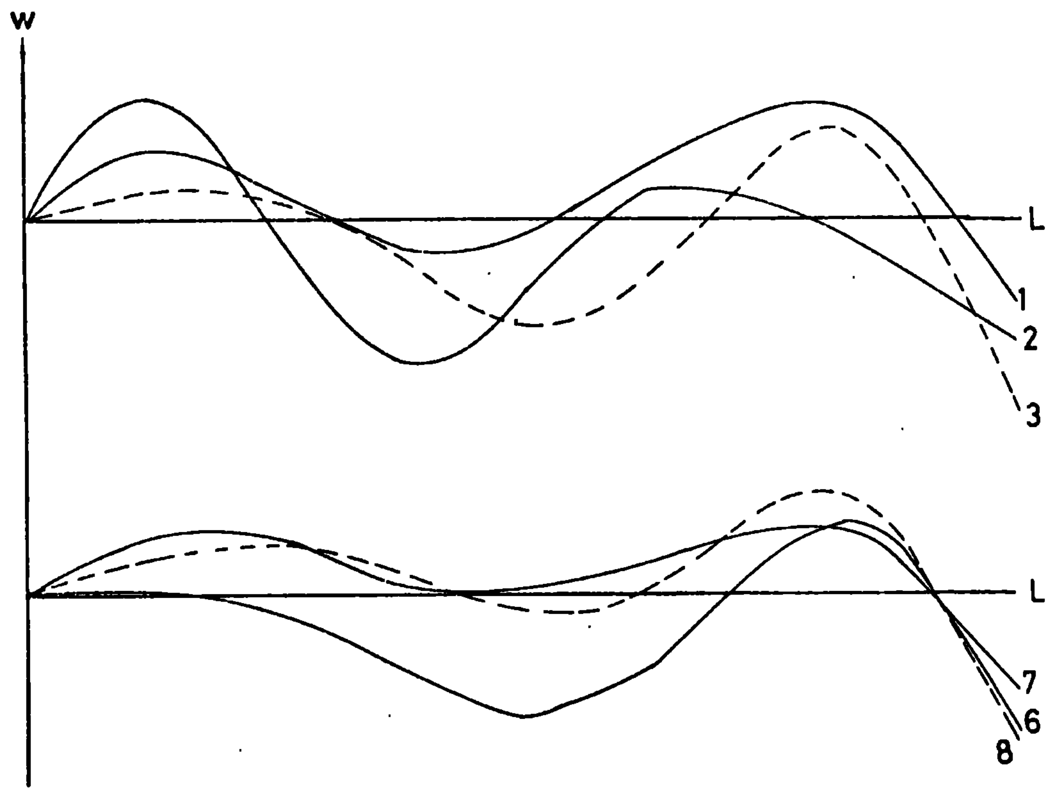

Figure A.3.30: Mode 20. f = 1876 Hz.

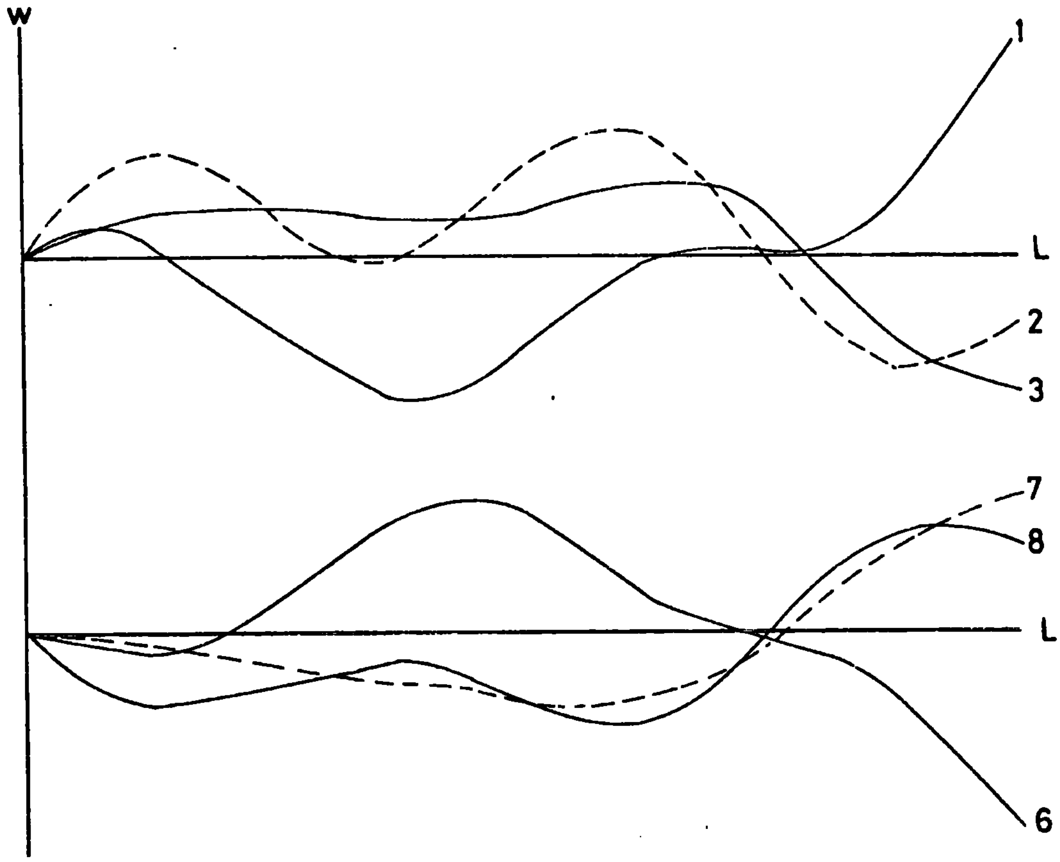

Figure A.3.31: Mode 21, f = 2005 Hz.

Mod. No.	Top Face	Bottom Face	Freq. Hz.
1	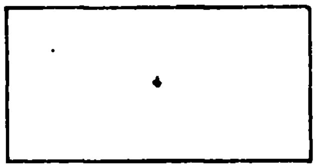	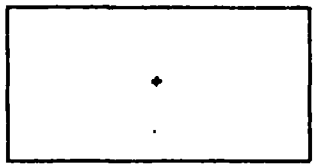	142
2	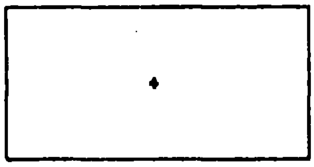	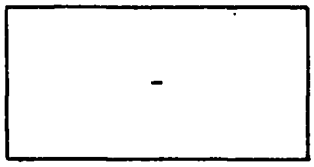	297
3	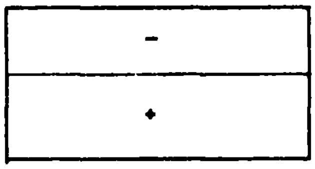	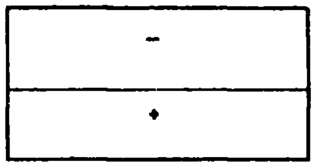	355
4	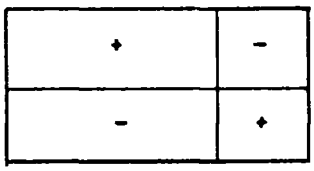	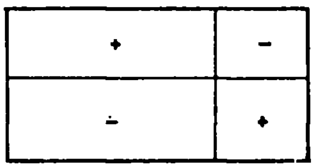	561.5
5	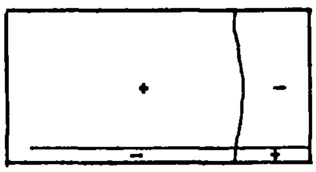	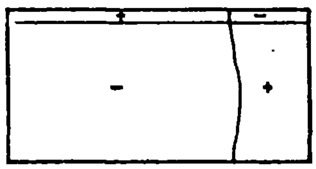	598
6	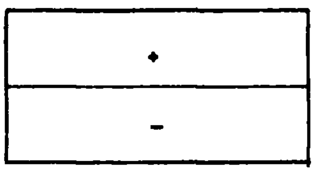	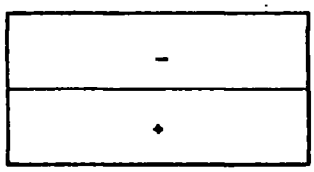	812
7	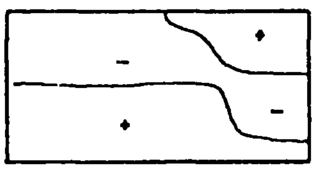	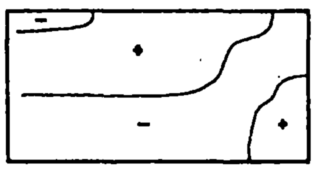	905
8	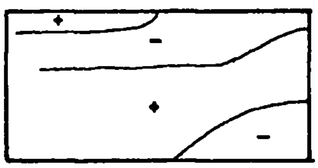	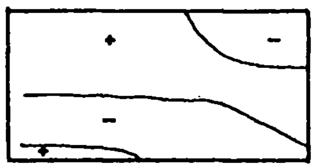	935

Figure A.3.32(a): Experimental mode shapes and natural frequencies.

Mod. No.	Top Face	Bottom Face	Freq. Hz.
9	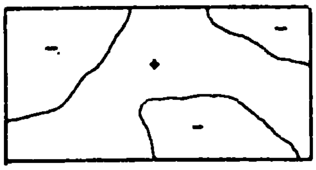	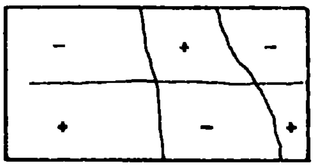	980
10	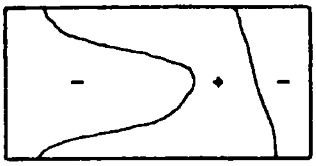	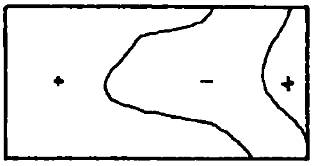	1096
11	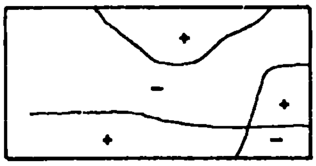	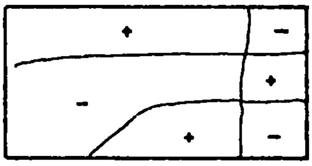	1136
12	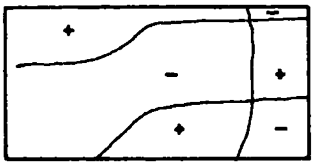	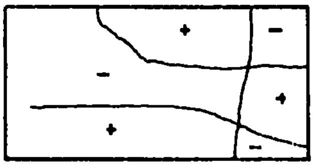	1157
13	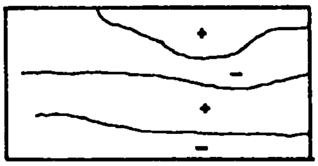	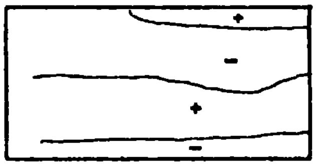	1314
14	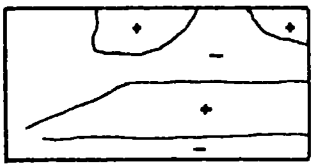	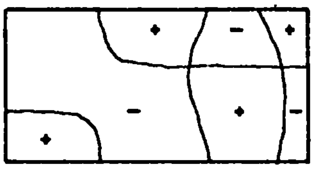	1387
15	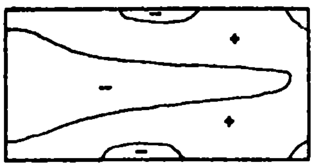	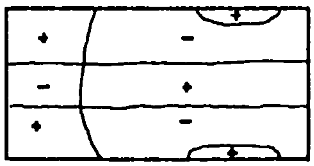	1633

Figure A.3.32 (b): Experimental mode shapes and natural frequencies.

APPENDIX 4

Deflection of the cross-section of the G.E.C. turbine blade analysed in Section 6.4.

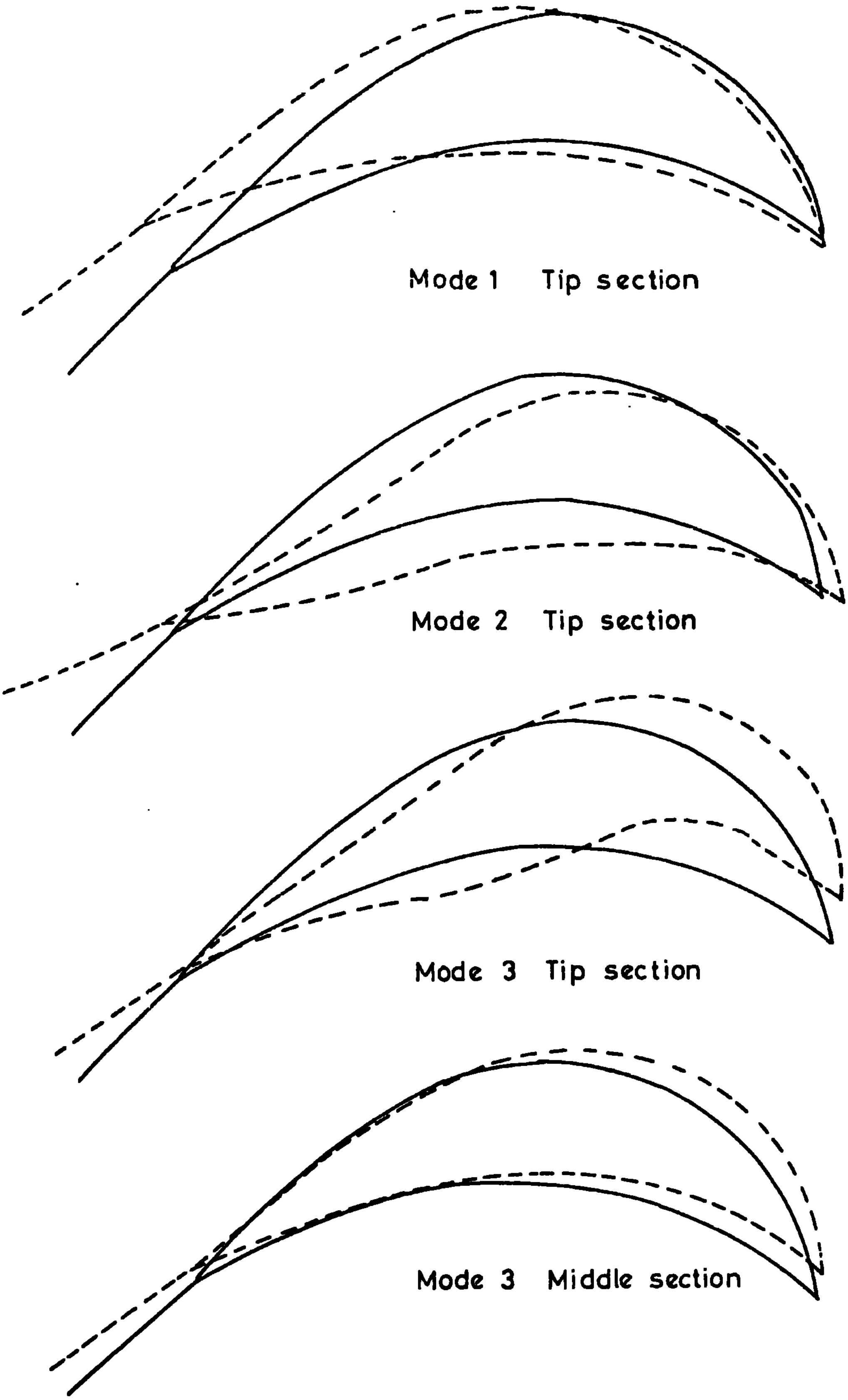
Mode 1 Tip section
Mode 2 Tip section
Mode 3 Tip section
Mode 3 Middle section

Figure A.4. 1(a).

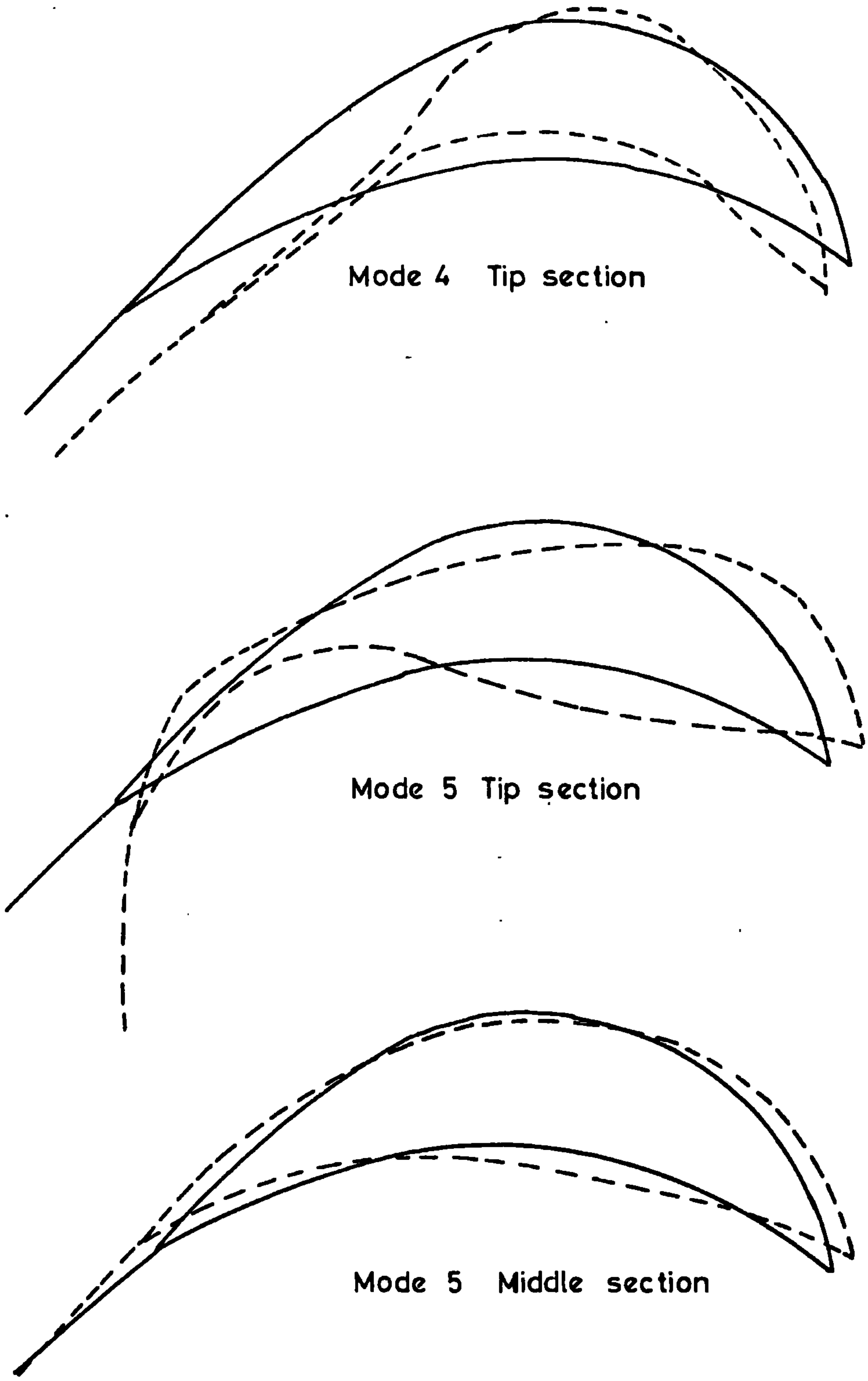

A.4.1. (b):

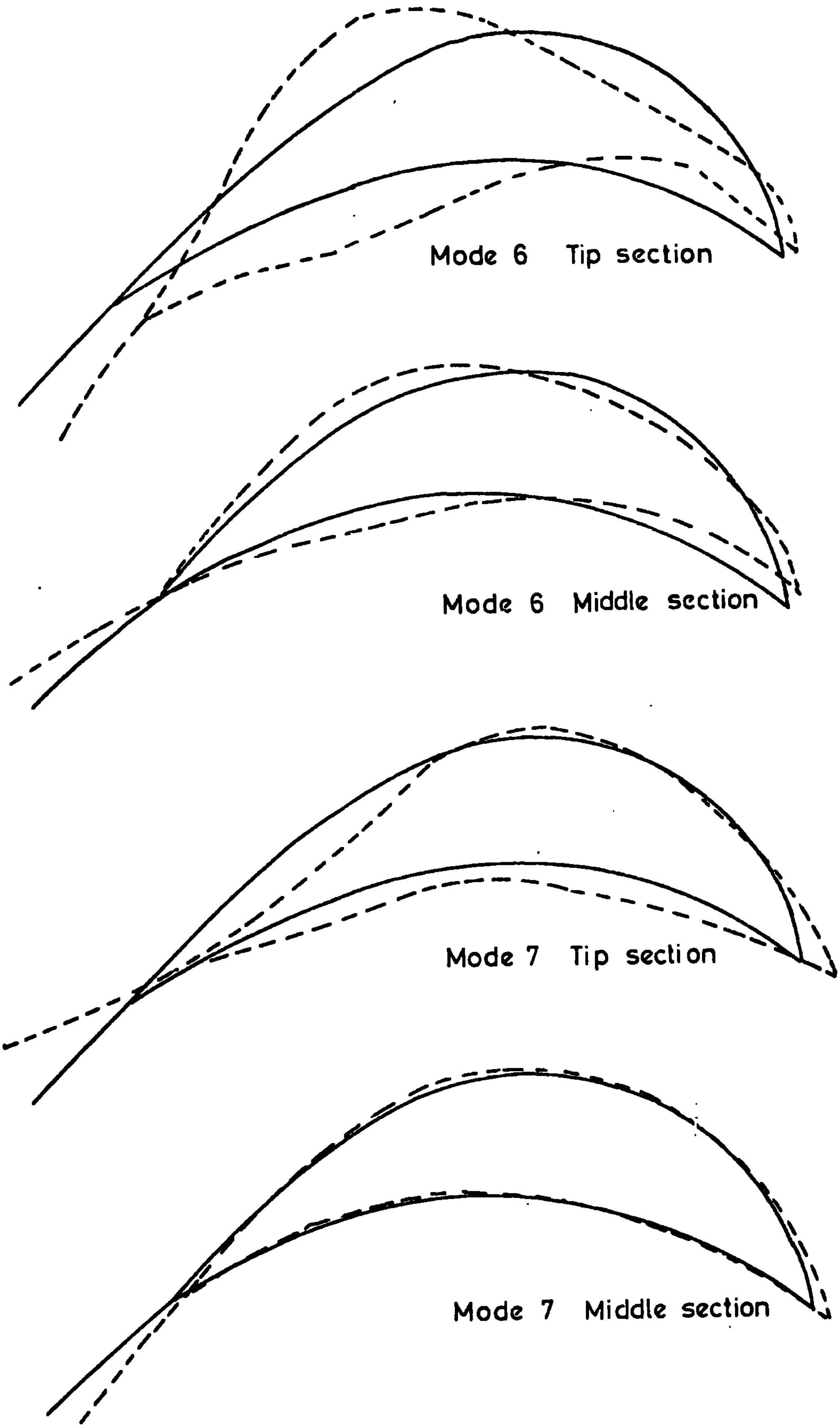
Mode 6 Tip section
Mode 6 Middle section
Mode 7 Tip section
Mode 7 Middle section

Figure A.4.1 (c):

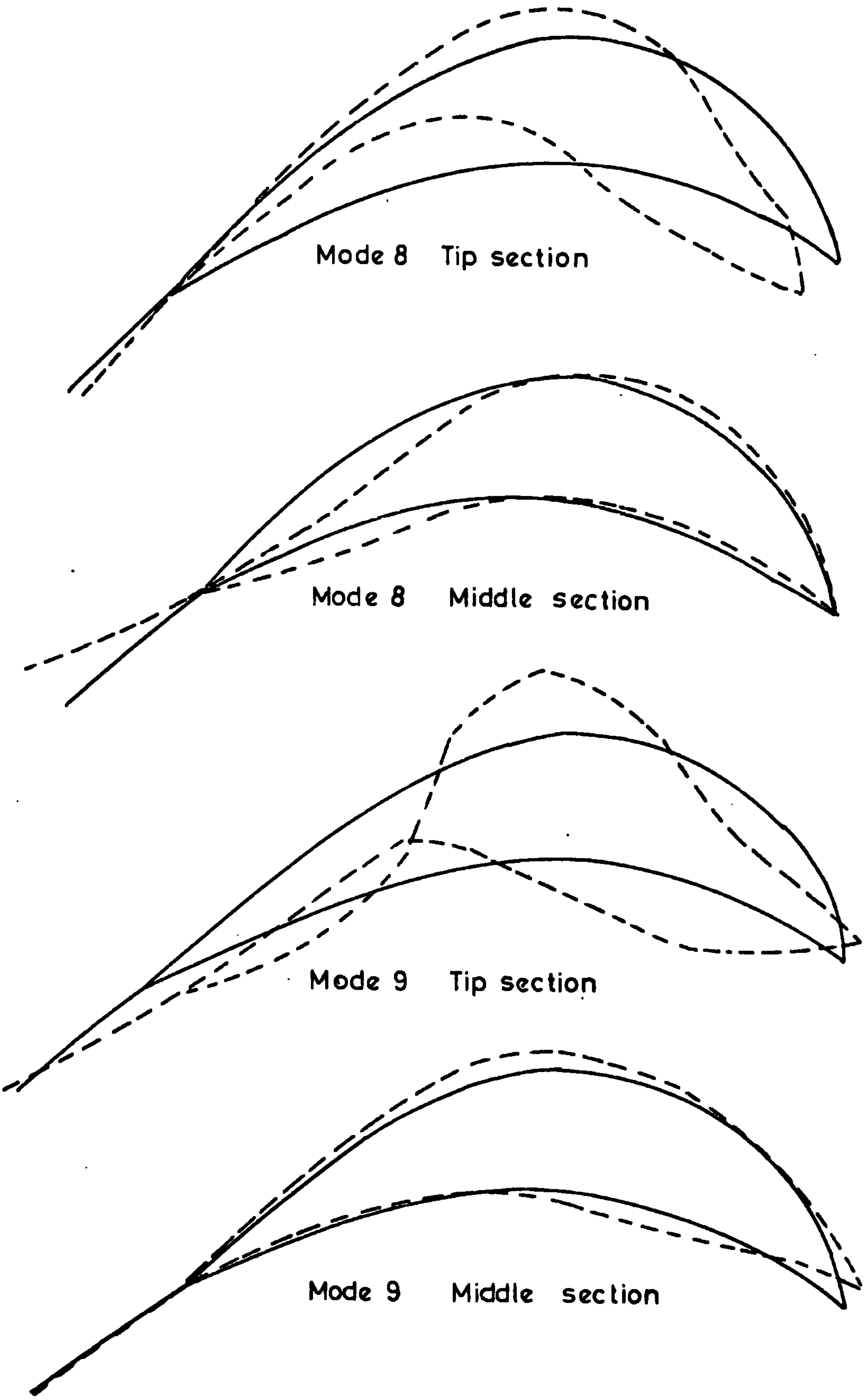
Mode 8 Tip section
Mode 8 Middle section
Mode 9 Tip section
Mode 9 Middle section

Figure A.4.1.(d):

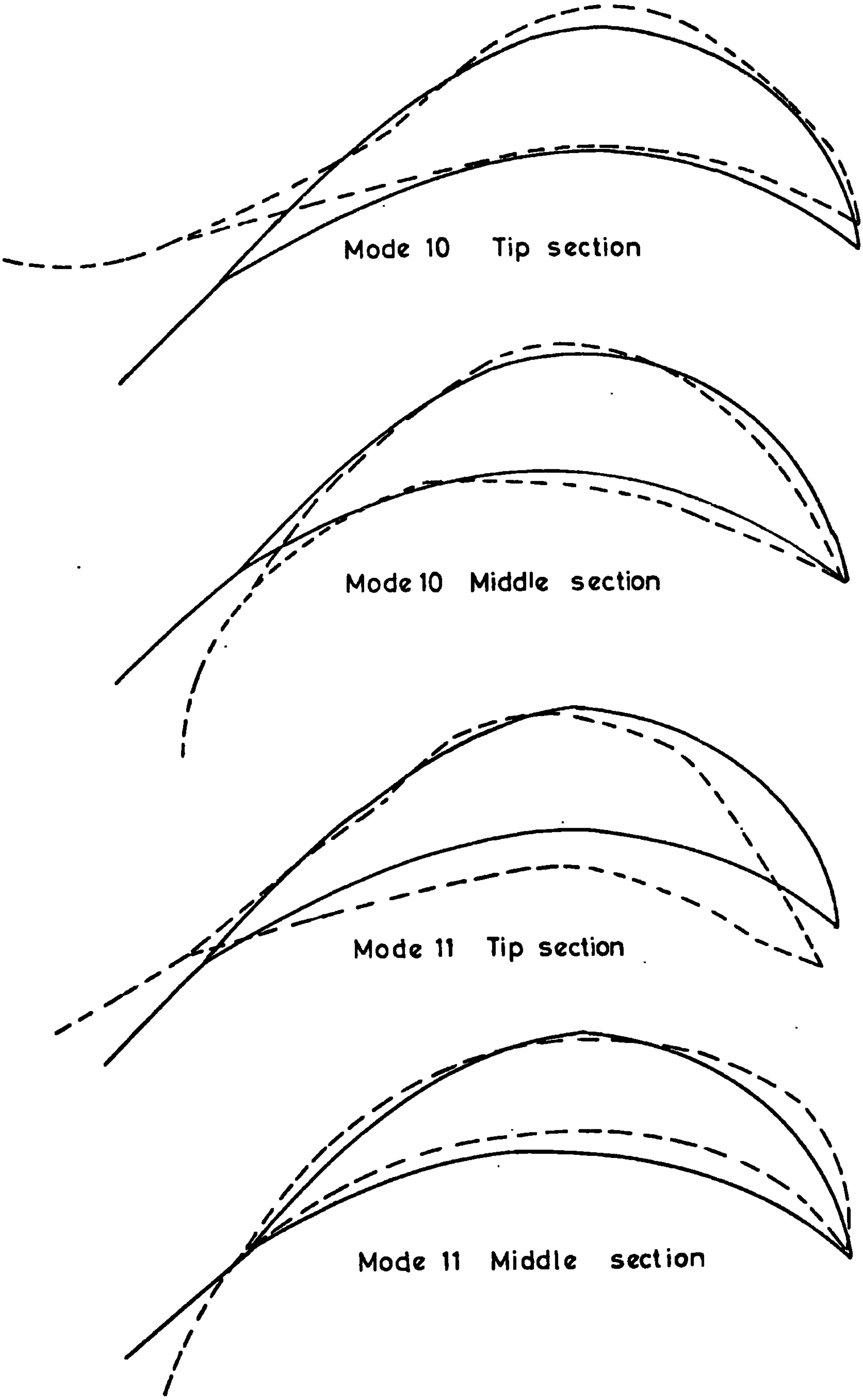
Mode 10 Tip section
Mode 10 Middle section
Mode 11 Tip section
Mode 11 Middle section

Figure A.4.1.(e):

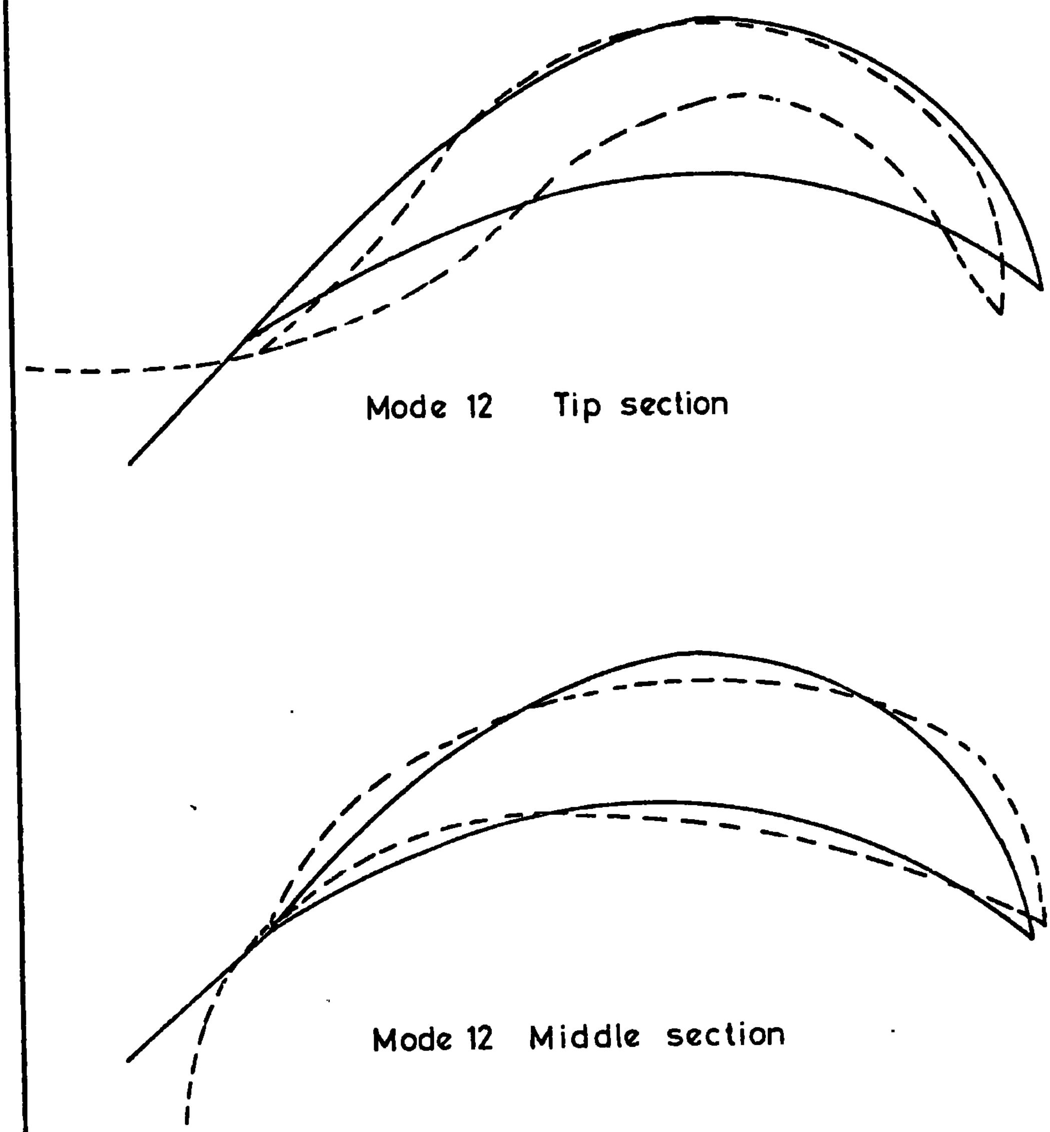

Figure A.4.1. (f):

APPENDIX 5

Listing of the computer program used in this thesis.

```
C      PLATE AND SHELL VIBRATION WITH FINITE ELEMENTS
C PSVFE
C
C
C   ##################################################################
C   #                                                                #
C   #    NATUREL FREQUENCY ANALYSIS OF ARBITRARY SHELL STRUCTURES    #
C   #    USING AHMAD'S THICK-SHELL ELEMENT                           #
C   #                                                                #
C   #                                                                #
C   #    MEHMET UCMAKLIOGLU                                          #
C   #                                                                #
C   #    DEPARTMENT OF ENGINEERING SCIENCE                           #
C   #    UNIVERSITY OF DURHAM                                        #
C   #                                                                #
C   #    1975-1978                                                   #
C   #                                                                #
C   #                                                                #
C   ##################################################################
C
C
C
      IMPLICIT REAL*8(A-H,O-Z)
      LOGICAL IFAIL
      COMMON/COR/XT(10),XB(10),YT(10),YB(10),ZT(10),ZB(10)
      COMMON/JAK/RJ3(3,3),RJ2(3,3),AINT(3)
      COMMON/INTG/PNT4(4),PNT3(3),PNT2(2),H4(4),H3(3)
      COMMON/STHE/V1(3),V2(3),V3(3)
      COMMON/UNI/UNIT(3)
      COMMON/GEN/WS(50),IPT(50),IBC1,IBC2,IS1,IS2,MIS1,MIS2
      COMMON/EPRO/E(5),RC(5),PR(5)
      COMMON/RED/SLAVES(300),SLAVEM(300),NODE(10,2),NDIS(10,5),
     &KAYVEC(500),ICOM(500)
C
      DIMENSION TITLE(20), RJI(3,3),RJ(3,3),
     &DUDG(3,50,3),DUDC(3,50,3),B(5,50),BT(50,5),S(50,50),Z(5),D(5,5),
     &UVW(3,50),UVWT(50,3),EFEM(50,50),SS(50,50),ELMAS(50,50)
     &,DCM(3,3),DCMT(3,3),PMM(45150),PSM(45150),
     &ROOT(50),VEC(7500),V1I(3),V2I(3),V3I(3),INVER(4)
C
```

```
      DIMENSION STF(10,10),TRAN(10,10),TRANT(10,10)                     MU C041
C                                                                       MU CC42
C                                                                       MU 0043
      READ(5,60) TITLE                                                  MU 0044
   60 FORMAT(20A4)                                                      MU 0045
      READ(5,66) NO,NONO,NNC,M1,M2,ISTEK,IPRINT,MAPRC,NEY               MU 0046
   66 FORMAT(9I5)                                                       MU 0047
      READ(5,99) (E(I),RC(I),PR(I),I=1,MAPRC)                           MU 0048
   99 FORMAT(3E10.5)                                                    MU 0049
      READ(5,91)RLEN,THIC                                               MU 0C50
   91 FORMAT(2F10.4)                                                    MU 0051
      READ(5,554)(IPT(I),I=1,NNC)                                       MU 0052
  554 FORMAT(16I5)                                                      MU 0053
C                                                                       MU 0054
C     PRINT THE TITLE & THE  MATERIAL PROPERTIES                        MU 0C55
C                                                                       MU 0056
      WRITE(6,61)TITLE                                                  MU C057
   61 FORMAT('1',20A4)                                                  MU 0058
      IF(IPRINT.LT.5) GC TO 700                                         MU 0059
      WRITE(6,800)                                                      MU 0060
  800 FORMAT(//20X,'PHYSICAL & GECMETRICAL PROPERTIES:'/)               MU 0061
      WRITE(6,801) (E(I),RO(I),PR(I),I=1,MAPRO)                         MU 0062
  801 FORMAT(/20X,'YOUNGS MODULUS  =',E15.5,/20X,'DENSITY          ='   MU 0063
     &     ,E15.5,/20X,'POISSONS RATIO  =',E 15.5)                      MU 0064
      WRITE(6,802) NC,NCNC,RLEN,THIC                                    MU 0C65
  802 FORMAT(/20X,'TOTAL NO CF ELEMENTS =',I5,/                         MU 0066
     &         20X,'TOTAL NC CF NODES    =',I5,//                       MU C067
     &         20X,'LENGTH OF THE PLT.  =',F10.3,/                      MU 0068
     &         20X,'THICNESS & REF. PNT.=',F10.3,//)                    MU 0069
  700 IF(IPRINT.LT.4) GC TO 701                                         MU 0070
      WRITE(6,803) NNC                                                  MU C071
  803 FORMAT(//20X,'TOTAL NO OF NCDES RESTRAINED=',I2/)                 MU 0072
      WRITE(6,804)(IPT(I),I=1,NNC)                                      MU 0073
  804 FORMAT(20X,'NCDES RESTRAINED:',10I5)                              MU 0074
      WRITE(6,850) M1,M2                                                MU 0075
  850 FORMAT(///20X,'ALL THE VECTORS BETWEEN',I3,                       MU 0076
     &'  AND',I3,'  ARE TO BE CALCULATED')                              MU C077
      WRITE(6,852)ISTEK,IPRINT,MAPRC,NEY                                MU 0078
  852 FORMAT(/10X,'ISTEK   IPRINT  MAPRC   NEY',/10X,4(I3,5X))          MU 0079
C                                                                       MU 0C80
```

```
C     READ THE TOPOLOGY AND THE CCORDINATES                        MU 0081
C     PERFORM FIRST CALCULATIONS                                   MU 0082
C     PRINT OUT THE RESULTS                                        MU 0083
C     COPY THEM ON DEVICE NO:7 AS FURTFER DATA                     MU 0084
C                                                                  MU 0085
  701 DO 311 I=1,NONO                                              MU 0086
      ICOM(I)=0                                                    MU 0087
  311 CONTINUE                                                     MU 0088
      IF(IPRINT.LT.2) GO TO 332                                    MU 0089
      WRITE(6,315)                                                 MU 0090
  315 FORMAT(1H1,///20X,'***TOPOLCGY OF THE ELEMENTS***'           MU 0091
     &,///20X,'ELEM. NO:',22X,'TCPOLOGY',40 X,'INT.PNTS.'/)        MU 0092
C                                                                  MU 0093
C     READ AND WRITE TCPCLOGY                                      MU 0094
C                                                                  MU 0095
  332 IF(ISTEK.LT.3) GO TO 702                                     MU 0096
       CALL GENTOP(NODE,ICCM,NO,NEY,ISTEK)                         MU 0097
      DO 350 I=1,NO                                                MU 0098
      LINE=I*1000                                                  MU 0099
      READ(7'LINE,313)(NCDE(J,1),J=1,10),INTEG,LTIP,ITYP,IPRO,INVER MU 0100
  350 WRITE(6,314)I,(NODE(J,1),J=1,10),INTEG,LTIF,ITYP,IPRO,INVER  MU 0101
      GO TO 334                                                    MU 0102
C                                                                  MU 0103
  702 DO 312 I=1,NO                                                MU 0104
      READ(5,313) (NCDE(J,1),J=1,10),INTEG,LTIP,ITYP,IPRC,INVER    MU 0105
      WRITE(7,313) (NCDE(J,1),J=1,10),INTEG,LTIP,ITYP,IPRO,INVER   MU 0106
      IF(IPRINT.LT.2) GO TO 703                                    MU 0107
      WRITE(6,314) I,(NODE(J,1),J=1,1C),INTEG,LTIP,ITYP,IPRO,INVER MU 0108
  703 DO 312 K=1,LTIP                                              MU 0109
      LOC=NODE(K,1)                                                MU 0110
      ICCM(LOC)=ICCM(LOC)+11                                       MU 0111
  312 CONTINUE                                                     MU 0112
  313 FORMAT(14I5,4I2)                                             MU 0113
  314 FORMAT(20X,I4,10X,10(2X,I4),5X,I3,5X,7I2)                    MU 0114
  334 WRITE(6,327)                                                 MU 0115
C                                                                  MU 0116
C     READ AND WRITE THE CCORDINATES                               MU 0117
C                                                                  MU 0118
      IF(ISTEK.LT.3) GO TO 333                                     MU 0119
      CALL GENOD(RLEN,NODE,NC,NNC,NEY)                             MU 0120
```

```
      DO 351 I=1,NONO                                              MU 0121
      LINE=(NO+I)*1000                                             MU 0122
      READ(7'LINE,325)NDOF,IDIS,XC,XXC,YC,YYC,ZC,ZZC               MU 0123
  351 WRITE(6,326)I,XC,XXC,YC,YYC,ZC,ZZC,ICOM(I),NDOF,IDIS         MU 0124
      GO TO 335                                                    MU 0125
C                                                                  MU 0126
  333 DO 321 I=1,NONO                                              MU 0127
      READ(5,324)XC,XXC,YC,YYC,ZC,ZZC,NDOF,IDIS                    MU 0128
      WRITE(7,325)NDOF,IDIS,XC,XXC,YC,YYC,ZC,ZZC                   MU 0129
      IF(IPRINT.LT.2) GO TO 321                                    MU 0130
      WRITE(6,326) I,XC,XXC,YC,YYC,ZC,ZZC,ICOM(I),NDOF,IDIS        MU 0131
  321 CONTINUE                                                     MU 0132
  324 FORMAT(6E10.4,2I5)                                           MU 0133
  325 FORMAT(2I5,6E17.9)                                           MU 0134
  326 FORMAT(6X,I4,4X,6(2X,F10.4),5X,I2,6X,I3,5X,I5)               MU 0135
  327 FORMAT(1H1,///20X,'***COORDINATES OF THE NODES***'           MU 0136
     &///4X,'NODE NO:',10X,'XT',10X,'XB',10X,'YT',10X,'YB',10X,'ZT' MU 0137
     &,10X,'ZB',7X,'NODE',5X,'B.C.',4X,'DOF'/)                      MU 0138
  335 CONTINUE                                                     MU 0139
      MAX=0                                                        MU 0140
      MBD=NONO*5                                                   MU 0141
C                                                                  MU 0142
C     INITIAL VALUES OF KAYVEC                                     MU 0143
      KAYMA=0                                                      MU 0144
      DO 400 I=1,NONO                                              MU 0145
      LINE=(NO+I)*1000                                             MU 0146
      READ(7'LINE,401) NDOF                                        MU 0147
      KAYMA=KAYMA+(5-NDOF)                                         MU 0148
      KAYVEC(I)=KAYMA                                              MU 0149
  400 CONTINUE                                                     MU 0150
  401 FORMAT(I5)                                                   MU 0151
C                                                                  MU 0152
      IF(MAPRO.EQ.1) CALL CONEL(D,1)                               MU 0153
C                                                                  MU 0154
      WRITE(6,805)                                                 MU 0155
  805 FORMAT(1H1,10X,'ELEMENT INFORMATION:')                       MU 0156
C                                                                  MU 0157
      DO 441 I=1,45150                                             MU 0158
      PMM(I)=0.0                                                   MU 0159
      PSM(I)=0.0                                                   MU 0160
```

```
  441 CONTINUE
      DO 2222 NOEL=1,NC
      WRITE(6,806) NOEL
  806 FORMAT(//5X,'ELEM. NO=',I2/)
      LINEN=NOEL*1000
      READ(7'LINEN,89) (NODE(I,1),I=1,10),INT1,INT2,INT3,LTIP,ITYP,IPRO
     &,INVER
   89 FORMAT(10I5,2X,3I1,3I5,4I2)
      DO 62 IM=1,LTIP
      LINE=(NODE(IM,1)+NO)*1000
      DO 50 ININ=1,4
      IF(IM.EQ.INVER(ININ)) GO TO 51
   50 CONTINUE
      READ(7'LINE,88) NODE(IM,2),(NDIS(IM,J),J=1,5)
     &, XT(IM),XB(IM),YT(IM),YB(IM),ZT(IM),ZB(IM)
      GO TO 52
   51 READ(7'LINE,88) NODE(IM,2),(NDIS(IM,J),J=1,5)
     &, XB(IM),XT(IM),YB(IM),YT(IM),ZB(IM),ZT(IM)
   88 FORMAT(I5,5I1,6E17.9)
   52 INDEX=0
      DO 63 MI=1,5
   63 IF(NDIS(IM,MI).EQ.3) INDEX=1
      LOC=NODE(IM,1)
      IF(INDEX.NE.0) GO TO 64
      ICOM(LOC)=ICOM(LOC)-1
      GO TO 62
   64 IC=ICOM(LOC)
      ICOM(LOC)=-(IABS(IC))+1
   62 CONTINUE
      LT5=5*LTIP
      IF(IPRINT.LT.7) GO TO 777
      WRITE(6,807)(XT(I),I=1,LTIP)
  807 FORMAT(2X,'XT:',10(2X,F10.5))
      WRITE(6,808)(XB(I),I=1,LTIP)
  808 FORMAT(2X,'XB:',10(2X,F10.5))
      WRITE(6,809)(YT(I),I=1,LTIP)
  809 FORMAT(2X,'YT:',10(2X,F10.5))
      WRITE(6,820)(YB(I),I=1,LTIP)
  820 FORMAT(2X,'YB:',10(2X,F10.5))
      WRITE(6,821)(ZT(I),I=1,LTIP)
```

```
  821 FORMAT(2X,'ZT:',10(2X,F10.5))                                          MU 0201
      WRITE(6,822)(ZB(I),I=1,LTIP)                                           MU 0202
  822 FORMAT(2X,'ZB:',10(2X,F10.5))                                          MU 0203
      WRITE(6,90) (NODE(I,1),I=1,LTIP)                                       MU 0204
   90 FORMAT(/4X,'TOPOLOGY:'/5X,10I12)                                       MU C205
      WRITE(6,92) (NODE(I,2),I=1,LTIP)                                       MU 0206
   92 FORMAT(4X,'NO. OF D.O.F.:',/5X,10I12)                                  MU 0207
      WRITE(6,67)((NDIS(I,J),J=1,5),I=1,LTIP)                                MU 0208
   67 FORMAT(/4X,'DEGREES OF FREEDOMS(1:MDF, 0:SLAVE, 2:REST., 3:HINGED      MU 0209
     &):'/ 5X,10(7X,5I1))                                                    MU 0210
C                                                                            MU 0211
C     ****************************************************************       MU 0212
C                                                                            MU 0213
  777 IF(LTIP.GT.2) GO TO 7777                                               MU 0214
      CALL MATNUL(STF,10,10,10,10)                                           MU 0215
      CALL MATNUL(ELMAS,10,10,50,50)                                         MU 0216
      AREA=PR(IPRO)                                                          MU 0217
      CALL THETA(DCM,DCMT,RJ,ELEN,2)                                         MU 0218
      IF(IPRINT.GE.7)WRITE(6,652)ELEN,PR(IPRO)                               MU 0219
  652 FORMAT(' LENGTH OF THE ELEMENT=',E16.6/                                MU 0220
     &       ' AREA OF THE ELEMENT  =',E16.6)                                MU 0221
      IF(IPRINT.GE.10)WRITE(6,653)((DCM(I,J),I=1,3),J=1,3)                   MU 0222
  653 FORMAT('  DCM-MATRIX',/,3(5X,E16.6))                                   MU 0223
      STF(3,3)=E(IPRO)*AREA/ELEN                                             MU 0224
      STF(8,8)=STF(3,3)                                                      MU 0225
      STF(3,8)=-STF(3,3)                                                     MU 0226
      STF(8,3)=STF(3,8)                                                      MU 0227
      IF(IPRINT.GE.10)WRITE(6,651)((STF(I,J),I=1,10),J=1,10)                 MU 0228
  651 FORMAT('  STF-MATRIX',/,10(1X,E10.4))                                  MU 0229
      CALL FORMT(TRAN,10,DCM,LTIP)                                           MU 0230
      CALL TRNPOZ(TRAN,TRANT,10,10,10,10)                                    MU 0231
      CALL F01CKF(STF,STF,TRAN,10,10,10,WS,50,2,0)                           MU 0232
      CALL F01CKF(STF,TRANT,STF,10,10,10,WS,50,3,0)                          MU 0233
      IF(IPRINT.GE.10)WRITE(6,654)((TRAN(I,J),I=1,10),J=1,10)                MU 0234
  654 FORMAT('  TRAN-MATRIX',/,10(1X,E10.4))                                 MU 0235
      IF(IPRINT.GE.10)WRITE(6,651)((STF(I,J),I=1,10),J=1,10)                 MU 0236
      DO 655 I=1,10                                                          MU 0237
      DO 655 J=1,10                                                          MU 0238
  655 SS(I,J)=STF(I,J)                                                       MU 0239
      CALL REDUCE(ELMAS,SS,PMM,PSM,NONC,MAX,LTIP)                            MU 0240
```

```
      GO TO 2222                                                        MU 0241
C                                                                       MU 0242
C     ***************************************************************** MU 0243
C                                                                       MU 0244
 7777   GO TO(707,166,165),ITYP                                         MU 0245
  707 CALL MATNUL(SS,50,50,50,50)                                       MU 0246
      CALL MATNUL(ELMAS,50,50,50,50)                                    MU 0247
      IF(MAPRO.GT.1) CALL CONEL(D,IPRO)                                 MU 0248
      VOLUM=0.0D0                                                       MU 0249
      DO 1111 I3=1,INT3                                                 MU 0250
      DO 1111 I2=1,INT2                                                 MU 0251
      DO 1111 I1=1,INT1                                                 MU 0252
      CALL INTEGR(XI,ETA,ZETA,HI,HJ,HM,INT1,INT2,INT3,I1,I2,I3)         MU 0253
      CALL MATNUL(B,5,50,5,50)                                          MU 0254
C                                                                       MU 0255
CONSTRUCTION OF DUDC(DERIV.OF DISP.W.R.T.CURVILINEAR COORDINATES)       MU 0256
C                                                                       MU 0257
  301 DO 1031 I=1,3                                                     MU 0258
      DO 1031 J=1,LT5                                                   MU 0259
      DO 1031 K=1,3                                                     MU 0260
      DUDC(I,J,K)=0.0                                                   MU 0261
 1031 CONTINUE                                                          MU 0262
      DO 107 K=1,2                                                      MU 0263
      DO 104 I=1,LT5,5                                                  MU 0264
      J=(I+4)/5                                                         MU 0265
      DUDC(1,I,K)=SHODEN(XI,ETA,J,2,K,LTIP)                             MU 0266
      DUDC(2,I+1,K)=DUDC(1,I,K)                                         MU 0267
      DUDC(3,I+2,K)=DUDC(1,I,K)                                         MU 0268
  104 CONTINUE                                                          MU 0269
      DO 105 I=4,LT5,5                                                  MU 0270
      J=(I+1)/5                                                         MU 0271
      CALL VECI(V1I,V2I,V3I,V3IL,J)                                     MU 0272
      PARA=SHODEN(XI,ETA,J,2,K,LTIP)*ZETA*V3IL/2.C                      MU 0273
      DUDC(1,I,K)=PARA*V1I(1)                                           MU 0274
      DUDC(2,I,K)=PARA*V1I(2)                                           MU 0275
      DUDC(3,I,K)=PARA*V1I(3)                                           MU 0276
      DUDC(1,I+1,K)=-(PARA*V2I(1))                                      MU 0277
      DUDC(2,I+1,K)=-(PARA*V2I(2))                                      MU 0278
      DUDC(3,I+1,K)=-(PARA*V2I(3))                                      MU 0279
  105 CONTINUE                                                          MU 0280
```

```
  107 CONTINUE
      DO 109 I=4,LT5,5
      J=(I+1)/5
      CALL VECI(V1I,V2I,V3I,V3IL,J)
      PARA=SHODEN(XI,ETA,J,1,1,LTIP)*V3IL/2.0
      DUDC(1,I,3)=PARA*V1I(1)
      DUDC(2,I,3)=PARA*V1I(2)
      DUDC(3,I,3)=PARA*V1I(3)
      DUDC(1,I+1,3)=-(PARA*V2I(1))
      DUDC(2,I+1,3)=-(PARA*V2I(2))
      DUDC(3,I+1,3)=-(PARA*V2I(3))
  109 CONTINUE
C
C     MULTIPLY RJI BY DUCC
C
      CALL JAKOB(RJ,RJI,V1I,V2I,V3I,DETJ,XI,ETA,ZETA,2,LTIP)
      DO 202 L=1,3
      DO 202 I=1,3
      DO 202 J=1,LT5
      DUDG(L,J,I)=0.0
      DO 202 K=1,3
      DUDG(L,J,I)=DUDG(L,J,I)+RJI(I,K)*DUDC(L,J,K)
C     DUDC BECAME DERIV.OF DISP.W.R.T. CARTESIAN COORDINATES
  202 CONTINUE
      CALL THETA(DCM,DCMT,RJ,V3L,1)
C     MULTIPLY DUDG BY DCM, STORE IN DUCC
      DO 226 L=1,3
      DO 226 I=1,3
      DO 226 J=1,LT5
      DUDC(I,J,L)=0.0
      DO 226 K=1,3
      DUDC(I,J,L)=DUDC(I,J,L)+DCM(K,I)*DUDG(K,J,L)
  226 CONTINUE
C     MULTIPLY DCMT BY DUDC, STORE IN DUDG
      DO 227 L=1,3
      DO 227 I=1,3
      DO 227 J=1,LT5
      DUDG(L,J,I)=0.0
      DO 227 K=1,3
      DUDG(L,J,I)=DUDG(L,J,I)+DUDC(L,J,K)*DCMT(I,K)
```

```
  227 CONTINUE
C
CCNSTRUCTION OF B MATRIX
C
      DO 204 I=1,LT5
      B(1,I)=DUDG(1,I,1)
      B(2,I)=DUDG(2,I,2)
      B(3,I)=DUDG(1,I,2)+DUDG(2,I,1)
      B(4,I)=DUDG(3,I,1)+DUDG(1,I,3)
      B(5,I)=DUDG(3,I,2)+DUDG(2,I,3)
  204 CONTINUE
C     TRANSPOSE THE B MATRIX, FIND BT
      CALL TRNPDZ(B,BT,5,50,5,50)
C
CCNSTRUCTION OF S MATRIX (S= BT*D*B )
C
      CALL F01CKF(B,D,B,5,50,5,Z,5,3,0)
      CALL F01CKF(S,BT,B,50,50,5,Z,5,1,C)
      VCLUM=VOLUM+HI*HJ*HM*DETJ
C
C     PERFORM THE INTEGRATIONS
C
      DO 1111 I=1,LT5
      DO 1111 J=1,LT5
      SS(I,J)=SS(I,J)+HI*HJ*HM*DETJ*S(I,J)
 1111 CONTINUE
      WRITE(6,1000) VCLUM
      VOL=0.0D0
C
CCNSTRUCTION OF THE MASS MATRIX
C
      DC 3333 K3=1,2
      DO 3333 K2=1,3
      DC 3333 K1=1,3
      CALL INTEGR(XI,ETA,ZETA,HI,HJ,HM,3,3,2,K1,K2,K3)
C
CCNSTRUCTION OF NBAR(UVW) FCR THE MASS MATRIX
C
      CALL MATNUL(UVW,3,50,3,50)
      DO 211 I=1,LT5,5
```

```
      J=(I+4)/5
      UVW(1,I)=SHODEN(XI,ETA,J,1,1,LTIP)
      UVW(2,I+1)=UVW(1,I)
      UVW(3,I+2)=UVW(1,I)
  211 CONTINUE
      DO 212 I=4,LT5,5
      J=(I+1)/5
      CALL VECI(V1I,V2I,V3I,V3IL,J)
      PARA=SHODEN(XI,ETA,J,1,1,LTIP)*ZETA*V3IL/2.C
      UVW(1,I)=PARA*V1I(1)
      UVW(2,I)=PARA*V1I(2)
      UVW(3,I)=PARA*V1I(3)
      UVW(1,I+1)=-(PARA*V2I(1))
      UVW(2,I+1)=-(PARA*V2I(2))
      UVW(3,I+1)=-(PARA*V2I(3))
  212 CONTINUE
      CALL JAKOB(RJ,RJI,V1I,V2I,V3I,DETJ,XI,ETA,ZETA,1,LTIP)
      CALL TRNPOZ(UVW,UVWT,3,50,3,50)
C
      VOL=VOL+HI*HJ*HM*DETJ
CONSTRUCTION OF EFEM MATRIX(EFEM=UVWT*UVW)
C
      CALL FO1CKF(EFEM,UVWT,UVW,50,50,3,Z,5,1,0)
C     PERFORM THE INTEGRATIONS
      DO 3333 I=1,LT5
      DO 3333 J=1,LT5
      ELMAS(I,J)=ELMAS(I,J)+HI*HJ*HM*DETJ*EFEM(I,J)*RC(IPRO)
 3333 CONTINUE
      WRITE(6,1000) VOL
 1000 FORMAT(5X,'VOLUME OF THE ELEMENT=',E16.6)
      IF(INVER(1).GT.0) CALL TRNSFR(ELMAS,SS,INVER,LTIP)
        GO TO 166
165     CALL MATCCP(DCM,RJ,3,3,3,3)
        CALL THETA(DCM,DCMT,RJI,V3L,2)
        CALL FO1CKF(RJ,RJ,DCMT,3,3,3,WS,50,2,0)
        CALL FORMT(S,50,RJ,LTIP)
        CALL TRNPOZ(S,EFEM,50,50,50,50)
        CALL FO1CKF(SS,SS,S,50,50,50,WS,50,2,C)
        CALL FO1CKF(ELMAS,ELMAS,S,50,50,50,WS,50,2,0)
        CALL FO1CKF(SS,EFEM,SS,50,50,50,WS,50,3,0)
```

```
      CALL FO1CKF(ELMAS,EFEM,ELMAS,50,50,50,WS,50,3,C)
  166   CONTINUE
      CALL REDUCE(ELMAS,SS,PMM,PSM,NONO,MAX,LTIP)
        IF(ITYP.NE.1) GO TO 2222
        CALL THETA(DCM,DCMT,RJ,V3L,2)
 2222 CONTINUE
C
C
C
      NON=MBD-KAYVEC(NONO)
      WRITE(6,1282) MBD,NON
 1282 FORMAT(///4X,'ORIGINAL NO OF DEGREES OF FREEDCMS  =',I5/
     &           4X,'NO OF DEGREES OF FREECOMS RETAINED  =',I5)
C
C EIGEN SOLUTION
C
      IF(IPRINT.GE.9) CALL MAPRIN(PSM,NON,6)
      CALL DEIGS(PSM,PMM,NON,M1,M2,ROOT,VEC,IFAIL)
      MDIM=NON+NON*(NON-1)/2
      IF(IFAIL) GO TO 199
C
C
      WRITE(6,1583)
 1583 FORMAT(1H1,///20X,'***SQUARES OF THE NATUREL FREQUENCIES***'///)
      GO TO 198
  199 CALL MAPRIN(PSM,NON,6)
      STOP
  198 NEV=M2-M1+1
      DO 1 I=1,NEV
      K=M2+1-I
      WRITE(6,608)K,ROOT(I)
    1 CONTINUE
  608 FORMAT(25X,'EIGEN VALUE NO:',I2,'=',E15.6)
C
      WRITE(6,17)
   17 FORMAT(///)
      PFR=E(1)*THIC**3/(12.0*(1.-PR(1)**2))
      DO 607 I=1,NEV
      ROOT(I)=DSQRT(DABS(ROOT(I)))
      FREQ=ROOT(I)/6.28318531
```

```
      PHI=ROCT(I)/DSQRT(PFR/(RO(1)*THIC*RLEN**4))                      MU 0441
      K=M2+1-I                                                          MU 0442
      WRITE(6,1975) K,ROCT(I),FREQ,PHI                                  MU 0443
 1975 FORMAT(/10X,'FREQ.NO:',I2,5X,'CMEGA=',E15.6,5X,'FREQLENCY=',      MU 0444
     &E15.6,5X,'PHI=',E15.6)                                            MU 0445
  6C7 CONTINUE                                                          MU 0446
      WRITE(6,812)                                                      MU C447
  812 FORMAT(1H1,///20X,'EIGEN VECTORS'//)                              MU 0448
      DO 810 I=1,NEV                                                    MU 0449
      IZA=NON*(I-1)+1                                                   MU 0450
      IZB=NJN*I                                                         MU 0451
      K=M2+1-I                                                          MU 0452
  810 WRITE(6,811) K,(VEC(J),J=IZA,IZB)                                 MU 0453
  811 FORMAT(5X,'VECTOR(',I2,')'/,5(8X,E14.5))                          MU 0454
      STOP                                                              MU 0455
      END                                                               MU 0456
C                                                                       MU 0457
C                                                                       MU 0458
C     FUNCTICN DEFINITICN                                               MU 0459
C                                                                       MU 0460
      FUNCTICN SHCDEN(XI,ETA,I,N,NN,LTIP)                               MU 0461
      IMPLICIT REAL*8(A-H,O-Z)                                          MU 0462
      IF(LTIP.EQ.10) GO TO(10,20,20,10,1,2,20,2,1,10),I                 MU 0463
      GO TO(10,20,20,10,30,20,30,10),I                                  MU 0464
   10 XII=-1.0                                                          MU 0465
      GO TO 40                                                          MU 0466
   20 XII=1.0                                                           MU 0467
      GO TO 40                                                          MU 0468
   30 XII=0.0                                                           MU 0469
           GO TO 40                                                     MU 0470
    1 XII=-1.0/3.0                                                      MU 0471
           GC TO 40                                                     MU 0472
    2    XII=1.0/3.0                                                    MU 0473
   40 IF(LTIP.EQ.10) GO TO(50,50,60,60,50,50,70,60,60,70),I             MU 0474
      GO TO (50,50,60,60,50,70,60,70),I                                 MU 0475
   50 ETAI=-1.0                                                         MU 0476
      GO TO 80                                                          MU 0477
   60 ETAI=1.0                                                          MU 0478
      GO TO 80                                                          MU 0479
   70 ETAI=0.0                                                          MU 048C
```

```
80 XIO=XI*XII
   ETAO=ETA*ETAI
   GO TO (85,95),N
85 IF(LTIP.EQ.10) GC TO(3,3,3,3,4,4,25,4,4,25),I
   GO TO(90,90,90,90,15,25,15,25),I
90 SHODEN=0.25*(1.+ETAO)*(1.+XIO)*(XIC+ETAO-1.0)
   RETURN
15 SHODEN=0.50*(1.0-XI**2)*(1.0+ETAO)
   RETURN
25 SHODEN= 0.5*(1.0+XIO)*(1.0-ETA**2)
   RETURN
 3 SHODEN=1.0/32.0*(1.0+XIC)*(1.0+ETAO)*(8.0*ETAC-9.0*
  &(1.0-XI**2))
   RETURN
 4 SHODEN=9.0/32.0*(1.0+ETAO)*(1.0-XI**2)*(1.0+9.0*XIO)
   RETURN
95 GO TO (96,11),NN
96 IF(LTIP.EQ.10) GO TO(5,5,5,5,6,6,55,6,6,55),I
   GC TO (35,35,35,35,45,55,45,55),I
35 SHODEN=0.25*(1.0+ETAO)*XII*(2.*XIC+ETAC)
   RETURN
45 SHODEN=-XI*(1.+ETAO)
   RETURN
55 SHODEN=0.5*XII*(1.C-ETA**2)
   RETURN
 5 SHODEN=1.0/32.0*(1.0+ETAO)*(XII*(8.0*ETAC-9.0*(1.0-XI**2))+
  &18.0*XI*(1.0+XIC))
   RETURN
 6 SHODEN=9.0/32.0*(1.0+ETAO)*((-2.0*XI)*(1.0+9.C*XIO)+9*XII*
  & (1.0-XI**2))
   RETURN
11 IF(LTIP.EQ.10) GO TO(7,7,7,7,8,8,41,8,8,41),I
   GO TO(21,21,21,21,31,41,31,41),I
21 SHODEN=0.25*(1.0+XIO)*ETAI*(2.*ETAC+XIC)
   RETURN
31 SHODEN=0.50*(1.0-XI**2)*ETAI
   RETURN
41 SHODEN=-ETA*(1.0+XIO)
   RETURN
 7 SHODEN=1.0/32.0*(1.0+XIO)*(ETAI*(8.0*ETAC-9.0*
```

```
      &(1.0-XI**2))+8.C*ETAI*(1.C+ETAC))
      RETURN
    8 SHODEN=9.0/32.0*(1.0-XI**2)*(1.0+9.0*XIO)*ETAI
      RETURN
      END
C
C
      SUBROUTINE JAKOB(RJ,RJI,V1I,V2I,V3I,DETJ,XI,ETA,ZETA,KAYI,LTIP)
      IMPLICIT REAL*8(A-H,O-Z)
      COMMON/JAK/RJ3(3,3),RJ2(3,3),AINT(3)
      COMMON/COR/XT(10),XB(10),YT(10),YB(10),ZT(10),ZB(10)
      DIMENSION RJI(3,3),RJ(3,3)
      DIMENSION V1I(3),V2I(3),V3I(3)
CCNSTRUCTION OF JACCBIAN (RJ)
      CALL MATNUL(RJ,3,3,3,3)
      DO 102 NN=1,2
      DO 102 I=1,LTIP
      CALL VECI(V1I,V2I,V3I,V3IL,I)
      SHDER=SHODEN(XI,ETA,I,2,NN,LTIP)
      PARSH=SHDER*ZETA/2.0*V3IL
      RJ(NN,1)=RJ(NN,1)+SHDER*(XT(I)+XB(I))/2.0+PARSH*V3I(1)
      RJ(NN,2)=RJ(NN,2)+SHDER*(YT(I)+YB(I))/2.0+PARSH*V3I(2)
      RJ(NN,3)=RJ(NN,3)+SHDER*(ZT(I)+ZB(I))/2.0+PARSH*V3I(3)
  102 CONTINUE
      DO 103 I=1,LTIP
      CALL VECI(V1I,V2I,V3I,V3IL,I)
      SHAPE=SHODEN(XI,ETA,I,1,1,LTIP)*0.5*V3IL
      RJ(3,1)=RJ(3,1)+SHAPE*V3I(1)
      RJ(3,2)=RJ(3,2)+SHAPE*V3I(2)
      RJ(3,3)=RJ(3,3)+SHAPE*V3I(3)
  103 CONTINUE
      DO 1032 I=1,3
      DO 1032 J=1,3
      RJ2(I,J)=RJ(I,J)
      RJ3(I,J)=RJ(I,J)
 1032 CONTINUE
      IF(KAYI .EQ. 1) GO TO 100
C     INVERSICN OF JACCBIAN (RJI)
      NFAIL=0
      CALL F01AAF(RJ2,3,3,RJI,3,AINT,NFAIL)
```

```
      C      DETERMINATICN OF THE DETERMINANT CF THE JACOBIAN(DETJ)
        100 DETJ=RJ3(1,1)*(RJ3(2,2)*RJ3(3,3)-RJ3(3,2)*RJ3(2,3))
           &    -RJ3(1,2)*(RJ3(2,1)*RJ3(3,3)-RJ3(3,1)*RJ3(2,3))
           &    +RJ3(1,3)*(RJ3(2,1)*RJ3(3,2)-RJ3(3,1)*RJ3(2,2))
             RETURN
             END
      C
      C
             BLOCK DATA
             IMPLICIT REAL*8(A-H,O-Z)
             COMMON/INTG/PNT4(4),PNT3(3),PNT2(2),H4(4),H3(3)
             COMMON/UNI/UNIT(3)
             DATA PNT4/-0.861136311594053,-C.339981043584856,
           &            0.339981043584856, 0.861136311594053/
             DATA PNT3/-0.774596669241483,0.0D0,0.774596669241483/
             DATA PNT2/-0.577350269189626,0.577350269189626/
             DATA H3 /C.555555555555556,0.888888888888889,C.555555555555556/
             DATA H4/0.347854845137454,0.652145154862546,
           &        0.652145154862546,0.347854845137454/
             DATA UNIT/0.0D00,1.0D00,0.0D00/
             END
      C
      C      SUBROUTINE FOR THE DIRECTICN CCSINES
      C
             SUBROUTINE THETA(DCM,DCMT,RJ,V3L,NE)
      C   NE=2 DIREC. COS. FOR ELEMENT
             IMPLICIT REAL*8(A-H,O-Z)
             COMMON/UNI/UNIT(3)
             COMMON/STHE/V1(3),V2(3),V3(3)
             COMMON/COR/XT(10),XB(10),YT(10),YB(10),ZT(10),ZB(10)
             DIMENSION RJ(3,3),DCM(3,3),DCMT(3,3)
      CCNSTRUCTION OF THE DIRECTICN CCSINE MATRIX
      CCNSTRUCTING THE VECTOR V3
               IF(NE.EQ.2) GO TC 1
             V3(1)=RJ(1,2)*RJ(2,3)-RJ(2,2)*RJ(1,3)
             V3(2)=RJ(2,1)*RJ(1,3)-RJ(1,1)*RJ(2,3)
             V3(3)=RJ(1,1)*RJ(2,2)-RJ(2,1)*RJ(1,2)
               GO TO 2
          1    V3(1)=(XT(2)+XB(2))/2.0-(XT(1)+XB(1))/2.0
               V3(2)=(YT(2)+YB(2))/2.0-(YT(1)+YB(1))/2.0
```

```
         V3(3)=(ZT(2)+ZB(2))/2.0-(ZT(1)+ZB(1))/2.0                    MU 0601
CONSTRUCT VECTOR V1                                                   MU 0602
    2 V1(1)=UNIT(2)*V3(3)-UNIT(3)*V3(2)                               MU 0603
      V1(2)=UNIT(3)*V3(1)-UNIT(1)*V3(3)                               MU 0604
      V1(3)=UNIT(1)*V3(2)-UNIT(2)*V3(1)                               MU 0605
CONSTRUCT V2 VECTOR                                                   MU 0606
      V2(1)=V3(2)*V1(3)-V3(3)*V1(2)                                   MU 0607
      V2(2)=V3(3)*V1(1)-V3(1)*V1(3)                                   MU 0608
      V2(3)=V3(1)*V1(2)-V3(2)*V1(1)                                   MU 0609
C     NORMALIZE THE VECTORS                                           MU 0610
      V3L=DSQRT(V3(1)**2+V3(2)**2+V3(3)**2)                           MU 0611
      V1L=DSQRT(V1(1)**2+V1(2)**2+V1(3)**2)                           MU 0612
      V2L=DSQRT(V2(1)**2+V2(2)**2+V2(3)**2)                           MU 0613
      DO 220 I=1,3                                                    MU 0614
      V1(I)=V1(I)/V1L                                                 MU 0615
      V2(I)=V2(I)/V2L                                                 MU 0616
      V3(I)=V3(I)/V3L                                                 MU 0617
  220 CONTINUE                                                        MU 0618
CONSTRUCT THE DIRECTION COSINE MATRIX                                 MU 0619
C                                                                     MU 0620
      DO 221 I=1,3                                                    MU 0621
      DCM(I,1)=V1(I)                                                  MU 0622
      DCM(I,2)=V2(I)                                                  MU 0623
      DCM(I,3)=V3(I)                                                  MU 0624
  221 CONTINUE                                                        MU 0625
C     TRANSPOSE DCM MATRIX FIND DCMT                                  MU 0626
      DO 225 I=1,3                                                    MU 0627
      DO 225 J=1,3                                                    MU 0628
      DCMT(I,J)=DCM(J,I)                                              MU 0629
  225 CONTINUE                                                        MU 0630
      RETURN                                                          MU 0631
      END                                                             MU 0632
C                                                                     MU 0633
C                                                                     MU 0634
      SUBROUTINE VEC1(V1I,V2I,V3I,V3IL,I)                             MU 0635
      IMPLICIT REAL*8(A-H,O-Z)                                        MU 0636
      COMMON/COR/XT(10),XB(10),YT(10),YB(10),ZT(10),ZB(10)            MU 0637
      COMMON /UNI/UNIT(3)                                             MU 0638
      DIMENSION V1I(3),V2I(3),V3I(3)                                  MU 0639
CONSTRUCT V3I VECTOR                                                  MU 0640
```

```
      V3I(1)=XT(I)-XB(I)                                                MU 0641
      V3I(2)=YT(I)-YB(I)                                                MU 0642
      V3I(3)=ZT(I)-ZB(I)                                                MU 0643
 CCNSTRUCT VECTOR V1I                                                   MU 0644
      V1I(1)=UNIT(2)*V3I(3)-UNIT(3)*V3I(2)                              MU 0645
      V1I(2)=UNIT(3)*V3I(1)-UNIT(1)*V3I(3)                              MU 0646
      V1I(3)=UNIT(1)*V3I(2)-UNIT(2)*V3I(1)                              MU 0647
 CCNSTRUCT V2I VECTOR                                                   MU 0648
      V2I(1)=V3I(2)*V1I(3)-V3I(3)*V1I(2)                                MU 0649
      V2I(2)=V3I(3)*V1I(1)-V3I(1)*V1I(3)                                MU 0650
      V2I(3)=V3I(1)*V1I(2)-V3I(2)*V1I(1)                                MU 0651
C     NCRMALIZE THE VECTCRS                                             MU 0652
      V3IL=DSQRT(V3I(1)**2+V3I(2)**2+V3I(3)**2)                         MU 0653
      V1IL=DSQRT(V1I(1)**2+V1I(2)**2+V1I(3)**2)                         MU 0654
      V2IL=DSQRT(V2I(1)**2+V2I(2)**2+V2I(3)**2)                         MU 0655
      DO 1 K=1,3                                                        MU 0656
      V1I(K)=V1I(K)/V1IL                                                MU 0657
      V2I(K)=V2I(K)/V2IL                                                MU 0658
      V3I(K)=V3I(K)/V3IL                                                MU 0659
    1 CONTINUE                                                          MU 0660
      RETURN                                                            MU 0661
      END                                                               MU 0662
C                                                                       MU 0663
C     MATRIX PRINT SUBROUTINE                                           MU 0664
      SUBROUTINE MAPRIN(A,N,NPRIN)                                      MU 0665
      IMPLICIT REAL*8(A-H,O-Z)                                          MU 0666
      DIMENSION A(1)                                                    MU 0667
          IF(NPRIN.EQ.3) GO TC 2                                        MU 0668
      WRITE(NPRIN,1) N                                                  MU 0669
    1 FCRMAT(//'MATRIX-DIMENSICN=',I3//)                                MU 0670
    2 M=1                                                               MU 0671
      DO 3 I=1,N                                                        MU 0672
      M=M+I-1                                                           MU 0673
      MM=M+I-1                                                          MU 0674
      WRITE(NPRIN,5) I,(A(J),J=M,MM)                                    MU 0675
    3 CONTINUE                                                          MU 0676
    5 FORMAT(2X,'ROW NG:',I3/(9(2X,E12.5)))                             MU 0677
      RETURN                                                            MU 0678
      END                                                               MU 0679
C     SUBROUTINE TO NULL A MATRIX                                       MU 0680
```

```
C                                                                       MU 0681
      SUBROUTINE MATNUL(A,M,N,MM,NN)                                    MU 0682
      IMPLICIT REAL*8(A-H,O-Z)                                          MU 0683
      DIMENSION A(MM,NN)                                                MU 0684
      DO 1 I=1,M                                                        MU 0685
      DO 1 J=1,N                                                        MU 0686
    1 A(I,J)=0.0D0                                                      MU 0687
      RETURN                                                            MU 0688
      END                                                               MU 0689
C                                                                       MU 0690
C SUB. TO PUT ZERO MATRIX INTO UNIT FORM                                MU 0691
C                                                                       MU 0692
      SUBROUTINE MATUNI(A,M,N)                                          MU 0693
      IMPLICIT REAL*8(A-H,O-Z)                                          MU 0694
      DIMENSION A(N,N)                                                  MU 0695
      DO 1 I=1,M                                                        MU 0696
    1 A(I,I)=1.0D0                                                      MU 0697
      RETURN                                                            MU 0698
      END                                                               MU 0699
C                                                                       MU 0700
C SUB. TO FORM TRANSFORMATION MATRIX                                    MU 0701
C                                                                       MU 0702
      SUBROUTINE FORMT(T,M,DCM,LTIP)                                    MU 0703
      IMPLICIT REAL*8(A-H,O-Z)                                          MU 0704
      DIMENSION T(M,M),DCM(3,3)                                         MU 0705
      CALL MATNUL(T,M,M,M,M)                                            MU 0706
      CALL MATUNI(T,M,M)                                                MU 0707
      DO 1 I=1,LTIP                                                     MU 0708
      DO 1 J=1,3                                                        MU 0709
      K=(I-1)*5+J                                                       MU 0710
      DO 1 L=1,3                                                        MU 0711
      LL=(I-1)*5+L                                                      MU 0712
    1 T(K,LL)=DCM(J,L)                                                  MU 0713
      RETURN                                                            MU 0714
      END                                                               MU 0715
C                                                                       MU 0716
C  SUB. TO TRANSPOSE A MATRIX                                           MU 0717
C                                                                       MU 0718
      SUBROUTINE TRNPOZ(A,B,M,N,MM,NN)                                  MU 0719
      IMPLICIT REAL*8(A-H,O-Z)                                          MU 0720
```

```
      DIMENSION A(MM,NN),B(NN,MM)                                       MU 0721
      DO 1 I=1,M                                                        MU 0722
      DO 1 J=1,N                                                        MU 0723
    1 B(J,I)=A(I,J)                                                     MU 0724
      RETURN                                                            MU 0725
      END                                                               MU 0726
C                                                                       MU 0727
C SUB. TO COPY A MATRIX                                                 MU 0728
      SUBROUTINE MATCOP(A,B,M,N,MM,NN)                                  MU 0729
      IMPLICIT REAL*8(A-H,O-Z)                                          MU 0730
      DIMENSION A(MM,NN), B(MM,NN)                                      MU 0731
      DO 1 I=1,M                                                        MU 0732
      DO 1 J=1,N                                                        MU 0733
    1 B(I,J)=A(I,J)                                                     MU 0734
      RETURN                                                            MU 0735
      END                                                               MU 0736
C                                                                       MU 0737
C     SUBROUTINE FOR INTEGRATION POINTS                                 MU 0738
C                                                                       MU 0739
      SUBROUTINE INTEGR(XI,ETA,ZETA,HI,HJ,HM,INT1,INT2,INT3,I1,I2,I3)   MU 0740
      IMPLICIT REAL*8(A-H,O-Z)                                          MU 0741
      COMMON/INTG/PNT4(4),PNT3(3),PNT2(2),H4(4),H3(3)                   MU 0742
      GO TO(1,2,3,40),INT1                                              MU 0743
    1 XI=0.0D0                                                          MU 0744
      HI=2.0D0                                                          MU 0745
      GO TO 4                                                           MU 0746
    2 XI=PNT2(I1)                                                       MU 0747
      HI=1.00D0                                                         MU 0748
      GO TO 4                                                           MU 0749
    3 XI=PNT3(I1)                                                       MU 0750
      HI=H3(I1)                                                         MU 0751
      GO TO 4                                                           MU 0752
   40 XI=PNT4(I1)                                                       MU 0753
      HI=H4(I1)                                                         MU 0754
    4 GO TO (11,12,13),INT2                                             MU 0755
   11 ETA=0.0D0                                                         MU 0756
      HJ=2.00D0                                                         MU 0757
      GO TO 14                                                          MU 0758
   12 ETA=PNT2(I2)                                                      MU 0759
      HJ=1.00D0                                                         MU 0760
```

```
      GO TO 14                                                   MU 0761
   13 ETA=PNT3(I2)                                               MU 0762
      HJ=H3(I2)                                                  MU 0763
   14 GO TO(21,22,23),INT3                                       MU 0764
   21 ZETA=0.0D0                                                 MU 0765
      HM=2.0D0                                                   MU 0766
      RETURN                                                     MU 0767
   22 ZETA=PNT2(I3)                                              MU 0768
      HM=1.00D0                                                  MU 0769
      RETURN                                                     MU 0770
   23 ZETA=PNT3(I3)                                              MU 0771
      HM=H3(I3)                                                  MU 0772
      RETURN                                                     MU 0773
      END                                                        MU 0774
C                                                                MU 0775
C     SUBROUTINE FOR D MATRIX                                    MU 0776
C                                                                MU 0777
      SUBROUTINE CONEL(D,I)                                      MU 0778
      IMPLICIT REAL*8(A-H,O-Z)                                   MU 0779
      COMMON/EPRO/E(5),RO(5),PR(5)                               MU 0780
      DIMENSION D(5,5)                                           MU 0781
CONSTRUCTION OF ELASTICITY MATRIX (D)                            MU 0782
      CALL MATNUL(D,5,5,5,5)                                     MU 0783
      C=E(I)/(1.0-PR(I)**2)                                      MU 0784
      D(1,1)=C                                                   MU 0785
      D(2,2)=C                                                   MU 0786
      D(3,3)=(1.0-PR(I))/2.0*C                                   MU 0787
      D(4,4)=(1.0-PR(I))/2.4*C                                   MU 0788
      D(5,5)=D(4,4)                                              MU 0789
      D(1,2)=C*PR(I)                                             MU 0790
      D(2,1)=C*PR(I)                                             MU 0791
      RETURN                                                     MU 0792
      END                                                        MU 0793
C     SUBROUTINE FOR ASSEMBLY & REDUCTION                        MU 0794
C                                                                MU 0795
      SUBROUTINE REDUCE(ELMAS,SS,PMM,PSM,NCNC,MAX,LTIP)          MU 0796
      IMPLICIT REAL*8(A-H,O-Z)                                   MU 0797
      COMMON/RED/SLAVES(300),SLAVEM(300),NODE(10,2),NDIS(10,5),  MU 0798
     &KAYVEC(500),ICCM(500)                                      MU 0799
      DIMENSION ELMAS(50,50), SS(50,50), PMM(45150),PSM(45150)   MU 0800
```

```
C     ASSEMBLE THE SYSTEM MATRICES, INSERT THE BOUNDARY CONDITIONS          MU 0801
      DO 403 I=1,LTIP                                                       MU 0802
      IF(NODE(I,2).EQ.0)GO TO 403                                           MU 0803
      LOC1=NODE(I,1)                                                        MU 0804
      ILCP=LOC1*5-KAYVEC(LOC1)-NODE(I,2)                                    MU 0805
      ILCE=I*5-5                                                            MU 0806
      DO 404 J=1,LTIP                                                       MU 0807
      IF(NODE(J,2).EQ.0) GO TO 404                                          MU 0808
      IF(NODE(J,1).LT.LOC1) GO TO 404                                       MU 0809
      LOC2=NODE(J,1)                                                        MU 0810
      ILRP=LOC2*5-KAYVEC(LOC2)-NODE(J,2)                                    MU 0811
      ILRE=J*5-5                                                            MU 0812
      KS=NODE(J,2)                                                          MU 0813
      LS=NODE(I,2)                                                          MU 0814
      MK=0                                                                  MU 0815
      DO 402 K=1,KS                                                         MU 0816
      IF(I.EQ.J) LS=K                                                       MU 0817
      MKF=MK+1                                                              MU 0818
      DO 8 MK=MKF,5                                                         MU 0819
      IF(NDIS(J,MK).NE.2) GO TO 9                                           MU 0820
    8 CONTINUE                                                              MU 0821
      GO TO 404                                                             MU 0822
    9 ML=0                                                                  MU 0823
      DO 402 L=1,LS                                                         MU 0824
      LCPM=ILCP+L                                                           MU 0825
      LRPM=ILRP+K                                                           MU 0826
      LIVE=LCPM+LRPM*(LRPM-1)/2                                             MU 0827
      MLF=ML+1                                                              MU 0828
      DO 5 ML=MLF,5                                                         MU 0829
      IF(NDIS(I,ML).NE.2) GO TO 6                                           MU 0830
    5 CONTINUE                                                              MU 0831
      GO TO 403                                                             MU 0832
    6 LCEM=ILCE+ML                                                          MU 0833
      LREM=ILRE+MK                                                          MU 0834
      PMM(LIVE)=PMM(LIVE)+ELMAS(LREM,LCEM)                                  MU 0835
      PSM(LIVE)=PSM(LIVE)+SS(LREM,LCEM)                                     MU 0836
  402 CONTINUE                                                              MU 0837
  404 CONTINUE                                                              MU 0838
  403 CONTINUE                                                              MU 0839
C     DETERMINE THE INSTATANEOUS SIZE OF SYSTEM MATRICES                    MU 0840
```

```
      CO 100 IL=1,LTIP                                                  MU 0841
      IF(NODE(IL,2).EQ.0) GO TO 100                                     MU 0842
      IF(NODE(IL,1).GT.MAX) MAX=NODE(IL,1)                              MU 0843
  100 CONTINUE                                                          MU 0844
      LIM1=5*MAX-KAYVEC(MAX)                                            MU 0845
C                                                                       MU 0846
C     REDUCTION OF SCME VARIABLES                                       MU 0847
C                                                                       MU 0848
      DO 10 I=1,LTIP                                                    MU 0849
      LIM=5*MAX-KAYVEC(MAX)                                             MU 0850
      IF(NODE(I,2).EQ.0) GC TO 10                                       MU C851
      LOC=NUDE(I,1)                                                     MU 0852
      IN1=ICCM(LOC)/10                                                  MU C853
      IN2=ICCM(LCC)-10*IN1                                              MU 0854
      IF(IN2) 19,17,10                                                  MU 0855
   19 IF(IN2+2) 10,21,22                                                MU 0856
   22 IF(IN1.NE.-2)GC TO 10                                             MU 0857
   21 CO 18 MEM=1,5                                                     MU 0858
      IF(NDIS(I,MEM).EQ.0)NDIS(I,MEM)=1                                 MU C859
   18 CONTINUE                                                          MU 0860
   17 IKCL=LOC*5-KAYVEC(LOC)                                            MU 0861
      IND=0                                                             MU 0862
      JSON=NODE(I,2)                                                    MU 0863
          JAN=0                                                         MU 0864
      DO 20 J=1,JSON                                                    MU 0865
      JAN=JAN+1                                                         MU 0866
   16 IF(NDIS(I,JAN).EQ.1)GC TO 20                                      MU 0867
      IF(NDIS(I,JAN).NE.2) GO TC 15                                     MU 0868
      JAN=JAN+1                                                         MU 0869
      GO TO 16                                                          MU C870
   15 KCLE=IKOL-JSON+J-IND                                              MU 0871
      ISAV=KOLE*(KCLE-1)/2                                              MU 0872
      PIVCT=PSM(KOLE+ISAV)                                              MU 0873
      IF(PIVOT.EQ.0) GO TO 32                                           MU 0874
      GO TO 31                                                          MU 0875
   32 WRITE(6,30) KCLE,NODE(I,1),KAYVEC(LOC),I,J                        MU 0876
   30 FORMAT(/5X,'PIVOT FGR THE SLAVE',I5,'IS ZERC',5X,'NODE=',I5,      MU 0877
     &'KAYMA=',I5,'I=',I5,3X,'J=',I5)                                   MU 0878
      STOP                                                              MU 0C79
   31 IF(LIM-KOLE) 101,101,102                                          MU 0880
```

```
  102 LSON=KCLE
      GC TO 103
  101 LSON=LIM
  103 DC 1 L=1,LSCN
      LIVE=L+ISAV
      SLAVES(L)=PSM(LIVE)
      SLAVEM(L)=PMM(LIVE)
      PSM(LIVE)=0.0D0
      PMM(LIVE)=0.0D0
    1 CONTINUE
      IF(LSON.EQ.LIM) GO TO 104
      ILK=LSCN+1
      DO 4 L=ILK,LIM
      LIVE=KOLE+L*(L-1)/2
      SLAVES(L)=PSM(LIVE)
      SLAVEM(L)=PMM(LIVE)
      PSM(LIVE)=0.0D0
      PMM(LIVE)=0.0D0
    4 CONTINUE
  104 IF(LIM-KOLE) 105,1C6,106
  106 KSCN=KOLE-1
      GO TO 107
  105 KSON=LIM
  1C7 DO 2 K=1,KSON
      IPK=K*(K-1)/2
      PARI=SLAVES(K)/PIVCT
      DO 3 L=1,K
      LIVE=L+IPK
      PARA=SLAVES(L)*PARI
      PMM(LIVE)=PMM(LIVE)-(SLAVEM(K)*SLAVES(L)
     &             +SLAVEM(L)*SLAVES(K)-SLAVEM(KCLE)*PARA)/PIVCT
      PSM(LIVE)=PSM(LIVE)-PARA
    3 CONTINUE
    2 CONTINUE
      IF(LIM-KOLE) 108,1C8,201
  201 KILK=KCLE+1
      KSON=LIM
      IF(IN2.EQ.0) GO TO 202
      DO 212 K=KILK,KSCN
      IPK=K*(K-1)/2
```

```
      PARI=SLAVES(K)/PIVCT                                      MU 0921
      LSON=KOLE-1                                               MU 0922
      DO 213 L=1,LSON                                           MU 0923
      LIVE=L+IPK                                                MU 0924
      PARA=SLAVES(L)*PARI                                       MU 0925
      PMM(LIVE)=PMM(LIVE)-(SLAVEM(K)*SLAVES(L)                  MU 0926
     &           +SLAVEM(L)*SLAVES(K)-SLAVEM(KCLE)*PARA)/PIVOT  MU 0927
      PSM(LIVE)=PSM(LIVE)-PARA                                  MU 0928
  213 CONTINUE                                                  MU 0929
      DO 223 L=KILK,K                                           MU 0930
      LIVE=L+IPK                                                MU 0931
      PARA=SLAVES(L)*PARI                                       MU 0932
      PMM(LIVE)=PMM(LIVE)-(SLAVEM(K)*SLAVES(L)                  MU 0933
     &           +SLAVEM(L)*SLAVES(K)-SLAVEM(KOLE)*PARA)/PIVOT  MU 0934
      PSM(LIVE)=PSM(LIVE)-PARA                                  MU 0935
  223 CONTINUE                                                  MU 0936
  212 CONTINUE                                                  MU 0937
      GO TO 108                                                 MU 0938
  202 DO 112 K=KILK,KSON                                        MU 0939
      KK=K-1                                                    MU 0940
      IPK=K*(K-1)/2                                             MU 0941
      IPKK=KK*(KK-1)/2                                          MU 0942
      PARI=SLAVES(K)/PIVOT                                      MU 0943
      LSON=KOLE-1                                               MU 0944
      DO 113 L=1,LSON                                           MU 0945
      LIVE1=L+IPKK                                              MU 0946
      LIVE2=L+IPK                                               MU 0947
      PARA=SLAVES(L)*PARI                                       MU 0948
      PMM(LIVE1)=PMM(LIVE2)-(SLAVEM(K)*SLAVES(L)                MU 0949
     &           +SLAVEM(L)*SLAVES(K)-SLAVEM(KCLE)*PARA)/PIVOT  MU 0950
      PSM(LIVE1)=PSM(LIVE2)-PARA                                MU 0951
  113 CONTINUE                                                  MU 0952
      DO 123 L=KILK,K                                           MU 0953
      LL=L-1                                                    MU 0954
      LIVE1=LL+IPKK                                             MU 0955
      LIVE2=L+IPK                                               MU 0956
      PARA=SLAVES(L)*PARI                                       MU 0957
      PMM(LIVE1)=PMM(LIVE2)-(SLAVEM(K)*SLAVES(L)                MU 0958
     &           +SLAVEM(L)*SLAVES(K)-SLAVEM(KOLE)*PARA)/PIVOT  MU 0959
      PSM(LIVE1)=PSM(LIVE2)-PARA                                MU 0960
```

```
123 CONTINUE                                                              MU 0961
112 CONTINUE                                                              MU 0962
108     IF(IN2.NE.0) GC TO 20                                             MU 0963
    IND=IND+1                                                             MU 0964
    LIM=LIM-1                                                             MU 0965
 20 CCNTINUE                                                              MU 0966
    DO 11 M=1,NONC                                                        MU 0967
    IF(M.LT.NCDE(I,1)) GO TC 11                                           MU 0968
    KAYVEC(M)=KAYVEC(M)+IND                                               MU 0969
 11 CONTINUE                                                              MU 0970
 10 CONTINUE                                                              MU 0971
    WRITE(6,50) LIM1,LIM                                                  MU 0972
 50 FORMAT(//5X,'INSTANTANEOUS SIZE OF THE SYSTEM MATRICES  =',           MU 0973
   &     I5,/5X,'SIZE OF THE SYSTEM MATRICES AFTER REDUCTICN=',I5//)      MU 0974
    LIM=LIM+1                                                             MU 0975
    IF(LIM.GT.LIM1) GO TO 52                                              MU 0976
    DO 51 MM=LIM,LIM1                                                     MU 0977
    DO 51 MN=1,MM                                                         MU 0978
    LIVE3=MN+MM*(MM-1)/2                                                  MU 0979
    PMM(LIVE3)=0.0                                                        MU 0980
    PSM(LIVE3)=0.0                                                        MU 0981
 51 CONTINUE                                                              MU 0982
 52 CONTINUE                                                              MU 0983
    RETURN                                                                MU 0984
    END                                                                   MU 0985
C                                                                         MU 0986
C     DATA GENERATICN SUBROUTINE                                          MU 0987
C                                                                         MU 0988
C   MAIN GENDAT                                                           MU 0989
    SUBROUTINE GENOD(UZUN,NODE,NC,NNC,NEY)                                MU 0990
    IMPLICIT REAL*8(A-H,O-Z)                                              MU 0991
    COMMON/GEN/ WS(50),IPT(50),IBC1,IBC2,IS1,IS2,MIS1,MIS2                MU 0992
    DIMENSION NODE(10,2),ISAR(4)                                          MU 0993
    READ(5,3) NOPAR,INC,ID,IR,IBC1,IBC2,IS2,MIS1,MIS2,ISAR                MU 0994
    READ(5,35) TOTAN, (WS(I),I=1,ID)                                      MU 0995
    PI=3.141592653589793                                                  MU 0996
    TANIN=TOTAN/(NEY*180)*PI                                              MU 0997
    IS1=0                                                                 MU 0998
    ZINC=UZUN/NEY                                                         MU 0999
    LEVEL=NEY+1                                                           MU 1000
```

```
      L=LEVEL+NEY                                                     MU 1001
      DO 1 J=1,NCPAR                                                  MU 1002
      READ(5,7) INDE                                                  MU 1003
    7 FORMAT(I5)                                                      MU 1004
      GO TO (51,52,53),INDE                                           MU 1005
   51 READ(5,56) XTI,YTI,XBI,YBI,XTF,YTF,XBF,YBF,NOPT,NTERS           MU 1006
   56 FORMAT(8E10.4,/2I5)                                             MU 1007
      M1=0                                                            MU 1008
      M2=NOPT-1                                                       MU 1009
      GO TO 55                                                        MU 1010
   52 READ(5,4) XC,YC,RAD,THIC,AINI,AFIN,NOPT,NTERS                   MU 1011
      AINI=AINI/180.0*PI                                              MU 1012
      AFIN=AFIN/180.0*PI                                              MU 1013
      AINC=(AFIN-AINI)/(NOPT-1)                                       MU 1014
      A=AINI                                                          MU 1015
      GO TO 55                                                        MU 1016
   53 READ(5,58)NOPT,NTERS                                            MU 1017
   58 FORMAT(2I5)                                                     MU 1018
   55 READ(5,5) NODE                                                  MU 1019
      DO 1 I=1,NOPT                                                   MU 1020
      GO TO (61,62,63) ,INDE                                          MU 1021
   61 XATI=(M1*XTF+M2*XTI)/FLOAT(M1+M2)                               MU 1022
      XABI=(M1*XBF+M2*XBI)/FLOAT(M1+M2)                               MU 1023
      YATI=(M1*YTF+M2*YTI)/FLCAT(M1+M2)                               MU 1024
      YABI=(M1*YBF+M2*YBI)/FLCAT(M1+M2)                               MU 1025
      GO TO 66                                                        MU 1026
   62 XATI=XC+RAD*DCOS(A)                                             MU 1027
      XABI=XC+(RAD-THIC)*DCOS(A)                                      MU 1028
      YATI=YC+RAD*DSIN(A)                                             MU 1029
      YABI=YC+(RAD-THIC)*DSIN(A)                                      MU 1030
      GO TO 66                                                        MU 1031
   63 READ(5,67)XATI,XABI,YATI,YABI                                   MU 1032
   67 FORMAT(4E10.4)                                                  MU 1033
   66 DO 41 N=1,4                                                     MU 1034
      IF(ISAR(N).EQ.NODE(I,1)) GO TO 43                               MU 1035
   41 CONTINUE                                                        MU 1036
      GO TO 42                                                        MU 1037
   43 XATI=(XATI+XABI)/2.0                                            MU 1038
      XABI=XATI                                                       MU 1039
   42 IF(NODE(I,2)) 10,20,30                                          MU 1040
```

```
10 IF(NODE(I,2).LT. -1) GC TC 3C                                     MU 1041
   IF(NTERS.LT.O) WRITE(6,11)NODE(I,1),XABI,XATI,YABI,YATI            MU 1042
   IF(NTERS.GE.O) WRITE(6,11) NCDE(I,1),XATI,XABI,YATI,YABI           MU 1043
   GC TO 2                                                            MU 1044
20 DO 21 K=1,LEVEL                                                    MU 1045
   Z=ZINC*(K-1)                                                       MU 1046
   NODNO=NODE(I,1)+(K-1)*INC                                          MU 1047
   CALL DOF(Z,NODNC,NNC,ID,IR,NDOF,IDIS)                              MU 1048
   TANG=(K-1)*TANIN                                                   MU 1049
   XAT=XATI*DCOS(TANG)-YATI*DSIN(TANG)                                MU 1050
   XAB=XABI*DCOS(TANG)-YABI*DSIN(TANG)                                MU 1051
   YAT=XATI*DSIN(TANG)+YATI*DCOS(TANG)                                MU 1052
   YAB=XABI*DSIN(TANG)+YABI*DCOS(TANG)                                MU 1053
   LINE=(NODNO+NG)*1000                                               MU 1054
   IF(NTERS.LT.O)WRITE(7'LINE,22)NDOF,IDIS,XAB,XAT,Z,Z,YAB,YAT        MU 1055
   IF(NTERS.GE.O) WRITE(7'LINE,22) NDOF,IDIS, XAT,XAB,Z,Z,YAT,YAB     MU 1056
21 CONTINUE                                                           MU 1057
   GO TO 2                                                            MU 1058
30 DO 31 K=1,L                                                        MU 1059
   Z=ZINC/2.00*(K-1)                                                  MU 1060
   KK=2                                                               MU 1061
   IF(K/2*2 .NE. K) KK=1                                              MU 1062
   NODNO=IABS(NODE(I,KK))+(K-KK)*INC/2                                MU 1063
   IF(INC.NE.1) GO TO 40                                              MU 1064
   NCDNO=NODE(I,1)+K-1                                                MU 1065
40 IF(NODE(I,2).LT.-1)IS1=99                                          MU 1066
   CALL DOF(Z,NODNO,NNC,ID,IR,NDCF,IDIS)                              MU 1067
   TANG=(K-1)*TANIN/2.0                                               MU 1068
   XAT=XATI*DCOS(TANG)-YATI*DSIN(TANG)                                MU 1069
   XAB=XABI*DCOS(TANG)-YABI*DSIN(TANG)                                MU 1070
   YAT=XATI*DSIN(TANG)+YATI*DCOS(TANG)                                MU 1071
   YAB=XABI*DSIN(TANG)+YABI*DCOS(TANG)                                MU 1072
   LINE=(NODNO+NG)*1000                                               MU 1073
   IF(NTERS.LT.O)WRITE(7'LINE,22)NDOF,IDIS,XAB,XAT,Z,Z,YAB,YAT        MU 1074
   IF(NTERS.GE.O) WRITE(7'LINE,22) NDOF,IDIS, XAT,XAB,Z,Z,YAT,YAB     MU 1075
31 CONTINUE                                                           MU 1076
 2 GO TO(71,72,1),INDE                                                MU 1077
71 M1=M1+1                                                            MU 1078
   M2=M2-1                                                            MU 1079
   GO TO 1                                                            MU 1080
```

```
  72 A=A+AINC                                                          MU 1081
   1 CONTINUE                                                          MU 1082
   3 FORMAT(13I5)                                                      MU 1083
   4 FORMAT(6E10.4,2I5)                                                MU 1084
   5 FORMAT(10I5)                                                      MU 1085
  11 FORMAT(5X,'NODE:',I3,3X,'CO-OR.=',4E12.4)                         MU 1086
  22 FORMAT(2I5,6E17.9)                                                MU 1087
  35 FORMAT(8E10.4)                                                    MU 1088
     RETURN                                                            MU 1089
     END                                                               MU 1090
C                                                                      MU 1091
C                                                                      MU 1092
     SUBROUTINE DOF(Z,NODNO,NNC,ID,IR,NDOF,IDIS)                       MU 1093
     IMPLICIT REAL*8(A-H,O-Z)                                          MU 1094
     COMMON/GEN/ WS(50),IPT(50),IBC1,IBC2,IS1,IS2,MIS1,MIS2            MU 1095
     IDIS=0                                                            MU 1096
     NDOF=5                                                            MU 1097
     DO 1 I=1,NNC                                                      MU 1098
     IF(IPT(I).EQ.NODNO) GO TO 3                                       MU 1099
   1 CONTINUE                                                          MU 1100
     IF(IS1.NE.99) GO TO 4                                             MU 1101
     IS1=0                                                             MU 1102
     IF(MIS1.NE.0) GO TO 7                                             MU 1103
     IDIS=IS2                                                          MU 1104
   4 DO 2 I=1,ID                                                       MU 1105
     IF(DABS(WS(I)-Z).LE.0.01) GO TO 5                                 MU 1106
   2 CONTINUE                                                          MU 1107
     RETURN                                                            MU 1108
   3 NDOF=IBC1                                                         MU 1109
     IDIS=IBC2                                                         MU 1110
     RETURN                                                            MU 1111
   5 IF(NDOF.EQ.MIS1) GO TO 8                                          MU 1112
     IF(IDIS.EQ.IS2) GO TO 6                                           MU 1113
     IDIS=IR                                                           MU 1114
     RETURN                                                            MU 1115
   6 IDIS=IS2+IR                                                       MU 1116
     RETURN                                                            MU 1117
   7 NDOF=MIS1                                                         MU 1118
     IDIS=MIS2                                                         MU 1119
     GO TO 4                                                           MU 1120
```

```
    8 IDIS=IDIS+IR
      IF(IDIS/10000.EQ.3)IDIS=IDIS-10000
      IF((IDIS/1000-IDIS/10000*10).EQ.3)IDIS=IDIS-1000
      IF((IDIS/100-IDIS/1000*10).EQ.3)IDIS=IDIS-100
      IF((IDIS/10-IDIS/100*10).EQ.3) IDIS=IDIS-10
      IF((IDIS-IDIS/10*10) .EQ.3) IDIS=IDIS-1
      RETURN
      END
C
C
      SUBROUTINE GENTOP(NODE,ICOM,NC,NEY,ISTEK)
      IMPLICIT REAL*8(A-H,O-Z)
      DIMENSION NODE(10,2),ICOM(500),INVER(4)
      DO 4 I=1,NO
      READ(5,5) (NODE(J,1),J=1,10),INTEG,LTIP,ITYP,IPRC,INVER
      INC1=0
      INC2=0
      DO 4 K=1,NEY
      NODE(1,1)=NODE(1,1)+INC1
      NODE(2,1)=NODE(2,1)+INC1
C
      IF(LTIP.EQ.2) GO TO 2
C
      NODE(3,1)=NODE(3,1)+INC1
      NODE(4,1)=NODE(4,1)+INC1
      NODE(5,1)=NODE(5,1)+INC2
      IF(LTIP.EQ.10) GO TO 1
      NODE(6,1)=NODE(6,1)+INC1
      NODE(7,1)=NODE(7,1)+INC2
      NODE(8,1)=NODE(8,1)+INC1
      GO TO 2
    1 NODE(6,1)=NODE(6,1)+INC2
      NODE(7,1)=NODE(7,1)+INC1
      NODE(8,1)=NODE(8,1)+INC2
      NODE(9,1)=NODE(9,1)+INC2
      NODE(10,1)=NODE(10,1)+INC1
    2 DO 3 M=1,LTIP
      LOC=NODE(M,1)
    3 ICOM(LOC)=ICOM(LOC)+11
C
```

```
C
      IF(LTIP.NE.2) GO TO 20
      INC1=INTEG
      IF(INC1.LE.2) GO TO 6
      GO TO 21
C
C
   20 INC1=NODE(4,1)-NODE(1,1)
      INC2=NODE(7,1)-NODE(5,1)
      IF(LTIP.EQ.10) INC2=NODE(9,1)-NODE(5,1)
      IF(INC1.NE.INC2) GOTO 6
   21 LINE=(I+(K-1)*NO)*1000
C
      IF(LTIP.EQ.2) GO TO 4
C
      IF (K.GT.1) GO TO 11
      GO TO 4
   11 IF(ISTEK-5) 4,13,14
   13 ITYP=2
      GO TO 4
   14 ITYP=3
      GO TO 4
    6 LINE=(K+(I-1)*NEY)*1000
      IF(K.GT.1) ITYP=2
    4 WRITE(7'LINE,5)(NODE(J,1),J=1,10),INTEG,LTIP,ITYP,IPRO,INVER
    5 FORMAT(14I5,4I2)
      NO=NO*NEY
      RETURN
      END
C
C
C       SUBROUTINE TO ADJUST THE MATRICES WHEN TOP AND BOTTOM
C       OF THE THICKNESS VECTOR IS DEFINED DIFFERENTLY
C
C
      SUBROUTINE TRNSFR(ELMAS,SS,INVER,LTIP)
      IMPLICIT REAL*8(A-H,O-Z)
      DIMENSION ELMAS(50,50),SS(50,50),INVER(4)
      LT5=5*LTIP
      DO 1 I=1,LTIP
```

LINE NUMBER TEXT PAGE

```
      DO 2 K=1,4                                                    MU 1201
      IF(I.EQ.INVER(K)) GO TO 3                                     MU 1202
    2 CONTINUE                                                      MU 1203
      GO TO 1                                                       MU 1204
    3 I5=I+5                                                        MU 1205
      DO 4 J=1,LT5                                                  MU 1206
      ELMAS(I5,J)=-ELMAS(I5,J)                                      MU 1207
      ELMAS(J,I5)=-ELMAS(J,I5)                                      MU 1208
      SS(I5,J)=-SS(I5,J)                                            MU 1209
      SS(J,I5)=-SS(J,I5)                                            MU 1210
    4 CONTINUE                                                      MU 1211
    1 CONTINUE                                                      MU 1212
      RETURN                                                        MU 1213
      END                                                           MU 1214
```